

University of Louisville

## ThinkIR: The University of Louisville's Institutional Repository

---

Electronic Theses and Dissertations

---

5-2021

### Thermo-hydro-mechanical characterization of Ottawa sand and Kaolin clay through experimental models.

Mohammad Joshaghani  
*University of Louisville*

Follow this and additional works at: <https://ir.library.louisville.edu/etd>



Part of the [Geotechnical Engineering Commons](#)

---

#### Recommended Citation

Joshaghani, Mohammad, "Thermo-hydro-mechanical characterization of Ottawa sand and Kaolin clay through experimental models." (2021). *Electronic Theses and Dissertations*. Paper 3666.  
<https://doi.org/10.18297/etd/3666>

This Doctoral Dissertation is brought to you for free and open access by ThinkIR: The University of Louisville's Institutional Repository. It has been accepted for inclusion in Electronic Theses and Dissertations by an authorized administrator of ThinkIR: The University of Louisville's Institutional Repository. This title appears here courtesy of the author, who has retained all other copyrights. For more information, please contact [thinkir@louisville.edu](mailto:thinkir@louisville.edu).

THERMO-HYDRO-MECHANICAL CHARACTERIZATION OF OTTAWA SAND  
AND KAOLIN CLAY THROUGH EXPERIMENTAL MODELS

By

Mohammad Joshaghani

B.S. Civil Engineering, Sharif University of Technology, 2010  
M. S. Civil Engineering, Sharif University of Technology, 2013

A Dissertation  
Submitted to the Faculty of the  
University of Louisville  
J.B. Speed School of Engineering  
as Partial Fulfillment of the Requirements  
for the Degree of

Doctor of Philosophy  
in Civil Engineering

Department of Civil & Environmental Engineering  
University of Louisville  
Louisville, Kentucky

May 2021

Copyright 2021 by Mohammad Joshaghani

All rights reserved



THERMO-HYDRO-MECHANICAL CHARACTERIZATION OF OTTAWA SAND  
AND KAOLIN CLAY THROUGH EXPERIMENTAL MODELS

By

Mohammad Joshaghani  
B.S. Civil Engineering, Sharif University of Technology, 2010  
M. S. Civil Engineering, Sharif University of Technology, 2013

A Dissertation Approved on

April 21, 2021

by the following Dissertation Committee:

---

Dr. Omid Ghasemi Fare, Dissertation Director

---

Dr. J.P. Mohsen

---

Dr. Thomas D. Rockaway

---

Dr. Ellen Brehob

*To my beloved parents, for their relentless support  
and my wife for her patience and support*

## ACKNOWLEDGEMENTS

I would like to extend my most sincere gratitude to all the people that contributed to my academic and professional endeavors. My first thanks go to my adviser Dr. Omid Ghasemi-Fare for his continuous support during the completion of this dissertation. Your insight and guidance have helped me grow as both a researcher and a writer.

I want to thank all my committee members, Dr. Mohsen, Dr. Rockaway, and Dr. Brehob, for your comments and support during this project. I have great respect and admiration for each one of you.

I would also like to acknowledge the financial support by National Science Foundation under Grant CMMI#1804822 and Kentucky Transportation Cabinet.

I want to acknowledge and thank my wife, Niloofar Sheikhan. Your unconditional support, encouragement, and love have helped me more than I could ever express with words. The completion of this work would not have been possible without you.

## ABSTRACT

### THERMO-HYDRO-MECHANICAL CHARACTERIZATION OF OTTAWA SAND AND KAOLIN CLAY THROUGH EXPERIMENTAL MODELS

Mohammad Joshaghani

April 21, 2021

Recent advances in energy geotechnics and increased utilization of ground source heat pump systems (e.g., geothermal boreholes and energy y piles) and energy geo-structures require improving the understanding of the thermo-hydro-mechanical behavior of soil. Energy geo-structures consist of above-ground facilities, buried structures, and the soil surrounding the buried structure. A buried structure transfers the energy between the ground and above-ground facilities. Energy transfer between above-ground facilities and the soil will cause temperature changes in soil and this will affect soil hydro-mechanical properties. The changes in soil temperature can also significantly alter the soil-structure interaction and its mechanical strength. Soil temperature change is not limited to the energy geo-structures. There are other sources of soil temperature changes in geotechnical engineering. Transferring samples from the field to the lab, daily and seasonal variations of the shallow subsurface soil, chemical reactions in landfills, buried high voltage cables and buried waste disposals change soil temperatures.

This study aims at gaining a better understanding of changes in soil properties under variable temperatures, including soil hydraulic conductivity and intrinsic permeability (as

hydraulic parameters that control seepage and fluid flow), thermal volume change (as a mechanical parameter to estimate soil deformation and settlement), and thermal pressurization (that is the reason of pore pressure generation and thermal fluid flow). The mentioned parameters are used in numerical modeling, and the outcome of this research can help to elaborate the accuracy of the numerical models by considering variations with temperature and also verifying those numerical models. In addition, the results of the volumetric changes with thermal load will affect foundation desing and required standards of the soil in the vicinity of foundations in buildings with geothermal energy.

To study the mentioned parameters, a novel method was engaged to modify the present triaxial cell in the geomechanics lab at the Civil and Environmental Engineering Department at the University of Louisville. Compared to the similar modification by other researchers, this cell with minimal expense was adjusted and modified to a temperature-controlled triaxial cell which can provide a uniform temperature around the soil sample using a novel approach, and has the flexibility to host different thermal tests by a simple change in the internal setup. Tests were conducted on Ottawa sand and Kaolin clay which are examples of coarse and fine-grained soils and are common soils in practice.

A series of hydraulic conductivity tests were conducted to study the effect of temperature on intrinsic permeability. Results showed a reduction in both hydraulic conductivity and intrinsic permeability of Ottawa sand (35% reduction in H.C of and 50% reduction in I.P) . In Kaolin clay, hydraulic conductivity showed an average of 150% increase and intrinsic permeability showed an average of 5% reduction most cases and a slight increase in confining pressure of 690 kPa. This increase could be because of the

degeneration of the immobile water into the free water. For both sand and clay, void ratio showed a reduction in the average range of 5 %.

The effects of temperature on volume change of Kaolin clay was studied. For this purpose, normally consolidated (NC) kaolin clay was tested under different cycles of heating/cooling and different confinement pressure. Besides, overconsolidated (OC) samples with  $OCR=6.5$  and  $OCR=1.6$  were also tested. The experimental results showed about 1 % irreversible thermal volume contraction which is known as thermal consolidation for normally consolidated Kaolin clay while 1 % thermal expansion was observed for highly overconsolidated Kaolin clay ( $OCR=6.5$ ) and almost no change for slightly OC sample ( $OCR=1.6$ ).

Based on the finding of thermal volume change, further investigation of permeability variations on NC Kaolin clay with temperature demonstrated that the changes in intrinsic permeability by temperature change are time-dependent. This confirms that thermal consolidation which results in void ratio reduction with time reduces the Kaolin clay absolute permeability. Results showed a reduction of 8% for both H.C and I.P at two different confining pressure of 345 kPa and 690 kPa at different temperature when time of measurement was increased from 1 hour to 48 hours.

## TABLE OF CONTENTS

ACKNOWLEDGEMENTS .....	iv
ABSTRACT .....	v
LIST OF TABLES .....	xii
LIST OF FIGURES .....	xiii
CHAPTER 1 FTER INTRODUCTIONFINISH WRITING .....	1
1.1. Motivation.....	1
1.2. Objectives .....	4
1.3. Research Phases .....	4
1.3.1. Hydraulic Conductivity and Intrinsic Permeability .....	4
1.3.2. Thermal Volume Changes in Different Soils.....	5
1.3.3. Hydraulic Conductivity a Time-Dependent Parameter-A New Perspective .	6
1.4. Dissertation Overview .....	7
CHAPTER 2 MODIFIED APPARATUS.....	8
2.1. Background .....	8
2.1.1. Internal heat source .....	8
2.1.2. External Heat Source.....	9
2.2. Modifying Cell- Approach and Details .....	9
2.2.1. Modified Cell Using Immersion Heater .....	10

2.2.2. Modified Cell Using Metal Heat Exchanger ..... 14

CHAPTER 3 HYDRAULIC CONDUCTIVITY AND INTRINSIC PERMEABILITY

19

3.1. Background ..... 19

3.2. Experimental Setup ..... 23

3.3. Sample Preparation..... 26

3.4. Test Procedure..... 29

3.5. Test Program ..... 32

3.6. Results..... 33

    3.6.1. Effect of temperature on H.C. of Ottawa sand..... 33

    3.6.2. Effect of temperature on intrinsic permeability of Ottawa sand ..... 36

    3.6.3. Effect of temperature on H.C. of Kaolin clay ..... 37

    3.6.4. Effect of temperature on the intrinsic permeability of Kaolin clay..... 40

    3.6.5. Discussion ..... 40

    3.6.6. Summary ..... 46

CHAPTER 4 THERMAL VOLUMETRIC CHANGES ..... 47

4.1. Background ..... 47

4.2. Experimental Setup ..... 51

4.3. Sample Preparation..... 54

4.4. Test Procedure and Calibration Test ..... 54

4.5. Test Program .....	56
4.6. Results and Discussion .....	58
4.7. Semi Experimental-Analytical Relation .....	69
4.8. Summary .....	74
CHAPTER 5.....	76
HYDRAULIC CONDUCTIVITY A TIME DEPENDENT PARAMETER- A NEW PERSPECTIVE.....	76
5.1. Sample Preparation.....	77
5.2. Test procedure.....	78
5.3. Test Results .....	79
5.3.1. Hydraulic Conductivity .....	79
5.3.2. Intrinsic Permeability .....	81
5.3.3. Cyclic tests .....	85
5.3.4. Void ratio change .....	88
5.4. Summary .....	89
CHAPTER 6 DISCUSSION, CONCLUSION AND RECOMMENDATIONS.....	90
6.1. Discussion and Conclusion .....	90
6.2. Recommendations .....	94
REFERENCES.....	96
CURRICULUM VITA .....	108

## LIST OF TABLES

Table 3-1 Geotechnical and thermal properties of Illinois Ottawa silica sand .....	27
Table 3-2 Geotechnical and thermal properties of Columbus Kaolin clay.....	28
Table 3-3 Dynamic viscosity measurements by the Rheometer .....	31
Table 3-4 Hydraulic conductivity test program .....	32
Table 3-5 Comparison of measured and calculated intrinsic permeability of Ottawa sand using Kozeny-Carman equation at different temperatures and confinement stresses .....	45
Table 4-1 Columbus Kaolin Clay Geotechnical Properties.....	54
Table 4-2 Test program and samples properties .....	58
Table 4-3 Calculated confinement coefficients using experimental observations.....	73

## LIST OF FIGURES

Figure 1-1 Bridge deck de-icing project, using geothermal energy .....	2
Figure 1-2 Geothermal piles and heat transfer loop .....	3
Figure 1-3 Landfill profile and Temperature change .....	3
Figure 2-1 Early Modified triaxial cell (a),Thermocontroller (b), Data Acquisition (c)...	11
Figure 2-2 Thermocouple and Immersion heater From Omega Co. ....	11
Figure 2-3 Magnet Stirrer and the schematic metal bar .....	13
Figure 2-4 Modified triaxial cell and different parts and the temperature changes in cell and sample.....	14
Figure 2-5 (a) Copper coil (b) Modified cell with copper coil temperature exchange method .....	15
Figure 2-6 (a) Copper coil attached mounted under the top cap, (b) Modified cell with aluminum chamber .....	16
Figure 2-7 Different parts of the designed circulation system.....	17
Figure 2-8 Data acquisition system .....	18
Figure 2-9 Rotary motor with attached magnets and adjustable clamp .....	18
Figure 2-10 Schematic of the modified cell.....	18
Figure 3-1 schematic view of the complete modified temperature-controlled permeameter to perform hydraulic conductivity tests .....	24
Figure 3-2 soil sample inside the latex membrane sitting on the base plate of the cell ...	25
Figure 3-3 water bath used to change the temperature of the permeant water, before injecting to the sample.....	26

Figure 3-4 Samples used for H.C test covered by latex membrane .....	27
Figure 3-5 Particle size distribution for Illinois Ottawa sand .....	29
Figure 3-6 Rheometer used to measure the dynamic viscosity of water at different temperatures .....	31
Figure 3-7 Variations of hydraulic conductivity of uniform Ottawa sand with the temperature at different confinement stresses.....	35
Figure 3-8 Variations of hydraulic conductivity of uniform Ottawa sand with the temperature at different confinement stresses.....	35
Figure 3-9 Variations of intrinsic permeability of Ottawa sand with the temperature at different confinement stresses.....	37
Figure 3-10 Changes in hydraulic conductivity of Kaolin clay with the temperature at different confinement stresses.....	38
Figure 3-11 Changes in hydraulic conductivity of Kaolin clay with the temperature at different confinement stresses.....	39
Figure 3-12 Variations of intrinsic permeability of Kaolin clay during heating and cooling at different confinement stresses.....	39
Figure 3-13 Void ratio alterations with the temperature at different confinement stresses .....	41
<i>Figure 4-1 Different parts of the triaxial insert consolidometer disassembled (a) and assembled (b) .....</i>	<i>52</i>
Figure 4-2 (a) Triaxial-insert consolidometer installed on the base cap of a triaxial cell (b) Complete setup of thermal consolidation test including water bath, loading frame, triaxial cell .....	53

Figure 4-3 Consolidometer and the sample inside it on the base plate .....	53
Figure 4-4 Calibration test result.....	56
Figure 4-5 Thermal loading and void ratio variations for NC Kaolin clay .....	60
Figure 4-6 Thermal loading and void ratio variations for NC Kaolin clay (10 kPa) .....	61
Figure 4-7 Thermal consolidations of NC Kaolin clay under different thermal loading (10 kPa).....	62
Figure 4-8 Thermal loading and void ratio variations for NC Kaolin clay .....	64
Figure 4-9 Thermal consolidations of NC Kaolin clay with different confinement stresses .....	65
Figure 4-10 Volumetric changes of OC sample with OCR=6.5, and $e_0 = 1.120$ (Test 10) .....	66
<i>Figure 4-11 Volumetric changes of OC sample with OCR=1.6, and <math>e_0 = 1.008</math> (Test 11)</i> .....	67
Figure 4-12 Volumetric strain for Thermal consolidation tests .....	68
Figure 4-13 Measured thermal volumetric strains in MC clay (Abuel-Naga et al. (2007a)) .....	69
Figure 4-14 Changes in thermal compression index for different sample 1-D consolidation pressures.....	71
Figure 4-15 Changes in the coefficient of confinement for different 1-D consolidation pressure .....	73
Figure 0-1 Kalin sample placed on the base plate and covered by a latex membrane .....	77
Figure 0-2 View of the setup test for the hydraulic conductivity test .....	78

Figure 0-3 Hydraulic Conductivity versus Temp at different measurement time-345 kPa Confining Pressure .....	80
Figure 0-4 Hydraulic Conductivity versus Temp at different measurement time, 690 kPa Confining Pressure .....	81
Figure 0-5 Intrinsic Permeability versus Temp. at different measurement time, 345 kPa Confining Pressure .....	82
Figure 0-6 Intrinsic Permeability versus Temp at different measurement time, 690 kPa Confining Pressure .....	83
Figure 0-7 Hydraulic Conductivity changes versus measurement time, heating at 50°C, different Confining Pressure .....	84
Figure 0-8 Hydraulic Conductivity changes versus measurement time, heating at 80°C, different Confining Pressure .....	84
Figure 0-9 Intrinsic Permeability changes versus measurement time, heating at 50°C, different Confining Pressure .....	84
Figure 0-10 Intrinsic Permeability changes versus measurement time, heating at 80°C, different Confining Pressure .....	84
Figure 0-11 Cyclic Hydraulic Conductivity test at 345kPa .....	86
Figure 0-12 Cyclic Hydraulic Conductivity test at 690kPa .....	86
Figure 0-13 Cyclic Intrinsic Permeability test at 345kPa .....	87
Figure 0-14 Cyclic Intrinsic Permeability test at 690 kPa .....	87
Figure 0-15 Void ratio changes at different measurement time in heating .....	88

# CHAPTER 1

## INTRODUCTION

### 1.1. Motivation

Recently, there has been growing attention around the world on the utilization of geothermal energy and geo-structures. In ongoing research by the geotechnical group of the Civil and Environmental Engineering Department at the University of Louisville, harvesting heat from the ground is employed to defrost the snow and ice formation on the concrete slabs with the application of concrete bridge deck de-icing in cold weather. Figure 1-1 presents the results from his project, by comparing two concrete slabs, one heated with geothermal energy and one without that. The test was performed in severe cold weather on February 2021 which was lasted for 2 weeks.

Energy geo-structures (e.g., energy piles, and energy walls), and underground heat storage systems can significantly change soil temperature (Figure 1-2). Temperature alterations in the soil cause two important changes: thermal volume change (e.g., thermal consolidation), and permeability variations. Temperature increment near the heat source induces excessive pore water pressure due to the difference in thermal expansion coefficients of the pore fluid and pore volume. Thermally-induced pore pressure and dissipation in clay soil create volumetric changes with time which is known as thermal consolidation. In sandy soil, however, permeability is much higher, excessive pore water pressure dissipates quickly, and thermal loading may change the soil fabric and particles

rearrangement during expansion and contraction of the fluid phase, but this volumetric change is negligible.



*Figure 1-1 Bridge deck de-icing project, using geothermal energy*

Another important parameter that changes with temperature is soil hydraulic conductivity. Changes in hydraulic conductivity happen not only because of fluid density and viscosity variations with the temperature; thermal loading alters the soil fabric and porosity in both sand and clay formations and as a result, intrinsic permeability will change. Change in hydraulic conductivity directly affects the current water flow regime in the ground, seepage rate in impermeable soil layers, and also initiates fluid flow due to the pore pressure generated in porous media.

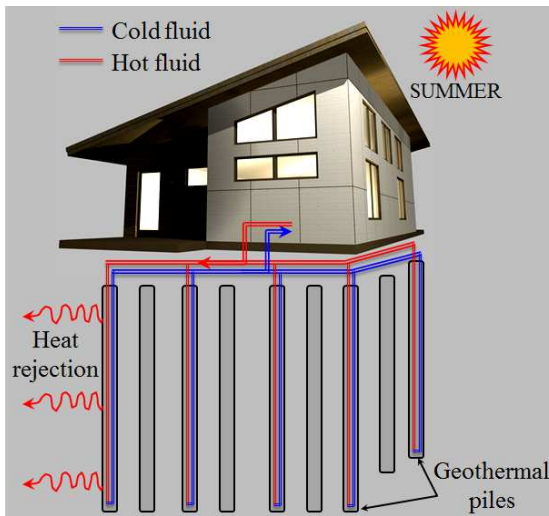


Figure 1-2 Geothermal piles and heat transfer loop

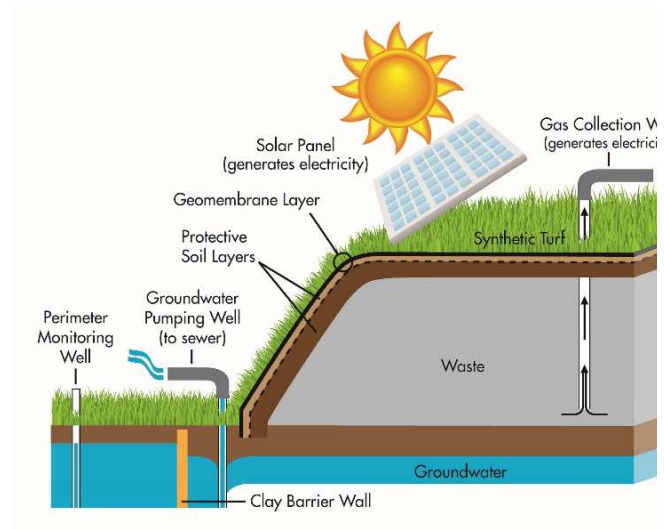


Figure 1-3 Landfill profile and Temperature change

[http://www.crra.org/pages/2015\\_Hartford\\_Landfill\\_Closing.htm](http://www.crra.org/pages/2015_Hartford_Landfill_Closing.htm)

It has been shown in the literature that hydraulic conductivity, strength, volumetric change, moisture content, and pore water pressure are temperature-dependent (Baldi et al. 1988; Campanella and Mitchell 1968; Cekerevac et al. 2004; Garakani et al. 2015; Ghasemi-Fare and Basu 2018; Joshaghani and Ghasemi-Fare 2019). To properly understand the thermo-hydro-mechanical (THM) response of the geotechnical infrastructures and to

accurately design ground storage of hazardous wastes the variations of all the aforementioned parameters with temperature must be investigated (Chen et al. 2017; François et al. 2009; Ghasemi-Fare and Basu 2019; Tamizdoust and Ghasemi-Fare 2020). Therefore in this study, the effects of temperature changes on soil hydro-thermo-mechanical properties are investigated.

## 1.2. Objectives

The overall research goal in this study is to study temperature effects on hydro-mechanical behavior of coarse and fine-grained soils and the objectives of this study are: (1) evaluating the effects of thermal loading on soil volumetric changes under variable confining pressures, and (2) measuring the changes in soil hydraulic conductivity and intrinsic permeability with temperature under different initial conditions (e.g., void ratios). To meet the overall goal and objectives of this research three different phases are outlined.

## 1.3. Research Phases

### 1.3.1. Hydraulic Conductivity and Intrinsic Permeability

An increase in temperature changes the groundwater density and viscosity, therefore, it is expected that the soil hydraulic conductivity varies with temperature. In addition, thermal loading may alter soil fabric and induces volumetric changes for both sand and clay. These variations might increase or decrease the absolute permeability of the soil. In this study, the hydraulic conductivity of both Ottawa sand and Kaolin clay under

different confinement stresses (69 kPa to 690 kPa) was measured. Then, absolute permeability was calculated considering water property variation with temperature. The results determined that, although hydraulic conductivity increases with temperature for both Ottawa sand and Kaolin clay, the absolute permeability of Ottawa sand reduces while in Kaolin clay it slightly increases. Nonetheless, analyzing volumetric changes and void ratio variations for both selected soil types shows a reduction in void ratio with temperature. Therefore, it can be concluded that the degeneration of a part of the immobile water within the structure into the mobile water causes an increase in the absolute permeability of Kaolin clay.

### 1.3.2. Thermal Volume Changes in Different Soils

Thermal loading changes pore water pressure. Generation and dissipation of the thermal excess pore water pressure result in alteration of void ratio and volumetric changes in the soil. Understanding the relationship between temperature and excess pore pressure variations with temperature for different soils is necessary to understand the mechanism of change in different parameters. In this study thermal pressurization is studied through a series of fully undrained tests. Different sandy soil samples are fabricated and tested by applying cyclic thermal loadings. Results showed a significant increase in excess pore water pressure at higher effective stress and when the effective stress approaches zero thermal pressurization is negligible. Thermal loading results in thermal volumetric contraction in normally consolidated (NC) clays while it may induce thermal volumetric expansion in overconsolidated (OC) clays. In this study thermal volumetric changes of Kaolin clay are carefully evaluated through 1-D Thermal Consolidation (TC) tests for both

normally consolidated and overconsolidated samples. Void ratio is measured at different temperatures during heating/cooling cycles and thermal volumetric changes are calculated. Thermal consolidation curve which shows the void ratio against the logarithm of temperature is presented and the coefficient of “thermal compression index” is introduced, which is similar to the compression index in conventional mechanical consolidation. For NC soil, several TC tests were conducted on samples with different initial void ratios that had already been consolidated under different 1D normal effective stresses, and the amount of consolidation was measured. For OC soil, experimental results on samples with different OCR values show different behavior based on OCR values.

### 1.3.3. Hydraulic Conductivity a Time-Dependent Parameter-A New Perspective

During the hydraulic conductivity tests for Kaolin clay, a time-dependent trend in the results was observed while repeating the measurements at a specific temperature for one specific sample at different time steps. Since thermal consolidation is a time dependent process and during this process, the void ratio is changing, it was noticed that we should be able to track the void ratio as a function of time using the thermal-hydraulic conductivity tests, by repeating the test at specific intervals. Based on the known analytical relations, hydraulic conductivity ( $k$ ) and void ratio ( $e$ ) are proportional as shown in the Kozeny-Carman equation:

$$k = \frac{1}{C_s S_s \Gamma} \frac{\gamma_w}{\eta} \frac{e^3}{1+e} \quad \text{Equation 1-1}$$

#### 1.4. Dissertation Overview

In the following dissertation, Chapter 2 describes the details of the modified test apparatus, which includes a triaxial cell facilitated to a temperature control system, monitoring sensors, and data acquisition. As the background, similar modified apparatus used by other researchers are presented and the cons and pros of each one are briefly mentioned. Chapter 3 describes the methodology employed for hydraulic conductivity tests and the related results as well as discussion over void ratio changes compared to hydraulic conductivity changes. A background of similar studies is provided. In Chapter 4, the thermal consolidation test methodology and test results on different samples of normally consolidated and overconsolidated Kaolin clay are discussed. Background of similar studies is also provided. In addition, the thermal pressurization test and results for an undrained condition are discussed to have a better understanding of the main source of the changes in soil parameters that are affected by temperature. Chapter 5 describes the time dependency of hydraulic conductivity results after applying thermal load, and the related void ratio changes in specific time intervals. Chapter 6 is allocated to the discussion, conclusion, and recommendations.

## CHAPTER 2

### MODIFIED APPARATUS

This chapter presents the details of the development of the temperature-controlled Triaxial cell. In this chapter, different steps and methods that were considered in this study to modify the current triaxial apparatus at the Geomechanics Lab at the Civil and Environmental Engineering Department are discussed. Different pieces of the modified setup are introduced and then the best approach that can keep the soil and cell temperatures uniform is presented.

#### 2.1. Background

In order to characterize thermo-hydro-mechanical properties of soils, we need to have a temperature-controlled cell in which changes in temperature and confinement pressure are easy to achieve and parameters like volumetric changes, permeability, and pore pressure are monitored. The most viable test setup to study the representative volume (REV) of soil is to modify a triaxial cell to control the temperature of the specimen. The temperature of the soil sample can be adjusted by changing the temperature of the confining fluid temperature (fluid inside the cell) as is verified in this chapter. Changing the temperature of the confining fluid could be performed in two different ways:

##### 2.1.1. Internal heat source

The first method is to accommodate a heat source inside the cell and directly change the temperature in the cell using one of the three available techniques: immersion heater

(Alsherif et al. 2013; Joshaghani et al. 2018), metal heat exchanger with a circulating fluid inside it (Cekerevac and Laloui 2004; Coccia and McCartney 2016; Joshaghani and Ghasemi-Fare 2019), and electrical resistance heaters (Alsherif and McCartney 2015). Except for the metal heat exchange method, which can lower the temperature as well as increase by changing the fluid temperature inside it, the other two can only increase the temperature. However, to lower the temperature in those methods passive cooling is employed, which means waiting until the system gets to room temperature while the heater is turned off. Therefore, soil properties cannot be studied using those two methods for temperatures lower than room temperature or by controlling the cooling rate. Therefore, the metal heat exchanger method is a good candidate for cyclic thermal tests.

#### 2.1.2. External Heat Source

The second method is to control the temperature by an external heating source. The external surface of the chamber can be heated and thus indirectly increase the confining fluid temperature (Delage et al. 2011) or constantly circulating the confining fluid into an external heating source and increase or decrease its temperature (Hueckel and Pellegrini 1992; Savvidou et al. 1995).

#### 2.2. Modifying Cell- Approach and Details

In the early stage of this research, a triaxial cell that was available in the geomechanics lab was modified by the inside heating source method. The cell was manufactured by Trautwein Geotechnical Test Acquisition and Control (GeoTAC) which could accommodate soil specimens up to 75 mm in diameter with a maximum height-to-diameter

ratio of 2.5. This modification included adding an immersion-type heater and two T-type thermocouples in the cell. There are some negative aspects about this method of heating which outweigh the positive points. The most important one is lacking a cooling system that can reduce the temperature at a controlled rate and keep it lower than room temperature. The second one is the difficulty in controlling cell temperature and stabilizing it. The reason is that the heating source reaches a temperature higher than the desired temperature and stops working frequently and while it stops working it is still producing heat. The latter issue can be remedied by using a less powerful heater and more accurate thermocouple and thermocontroller, but a heating/cooling source with a uniform temperature that continuously provides energy to the system is more accurate and provides a stable temperature inside the cell. Therefore, in this study, cell modification was improved by replacing the heat source with a metal heat/cool exchanger. The details of both setups as well as gained experiences by each one are explained in the next section.

#### 2.2.1. Modified Cell Using Immersion Heater

As mentioned earlier, the early modified cell was based on an immersion heating method as a heating source and two thermocouples. All these three elements were inserted into the cell through its top cap using watertight fittings, while thermocouples fittings allow us to adjust the submerged depth. One of the thermocouples was connected to a thermocontroller to keep the temperature of the cell at the desired level with an accuracy of  $\pm 0.1$  °C. The second thermocouple was connected to data acquisition to reflect and record the temperature variation during the test. Figure 2-1 presents the modified cell and related elements. Figure 2-2 shows the thermocouple and heater including their specifications.

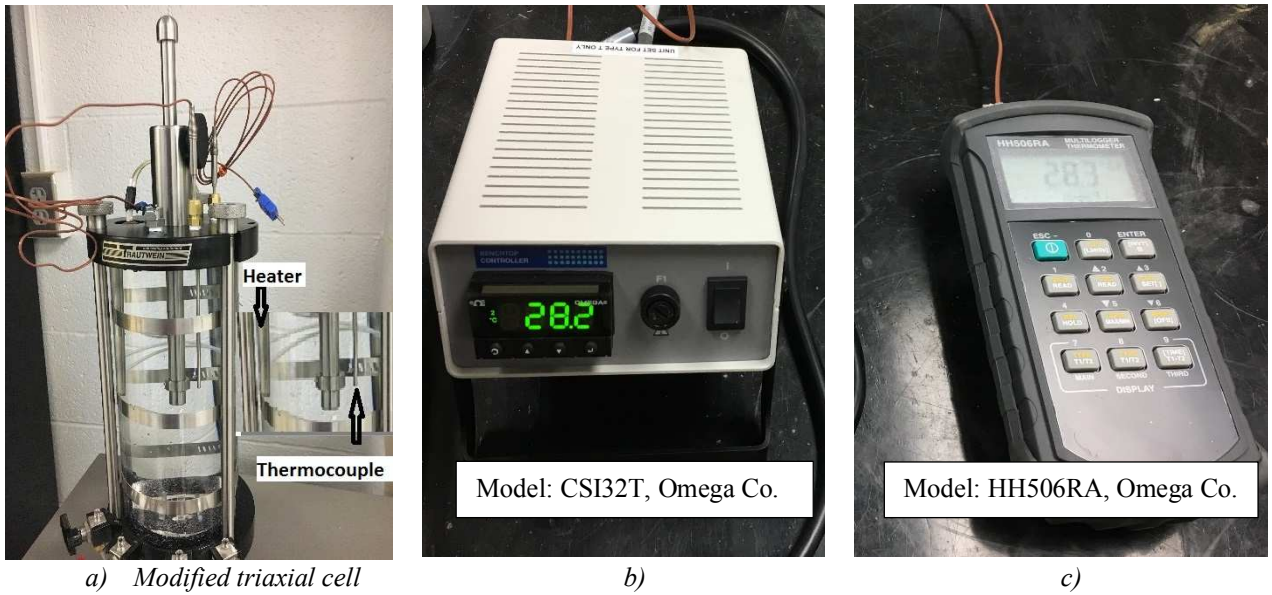


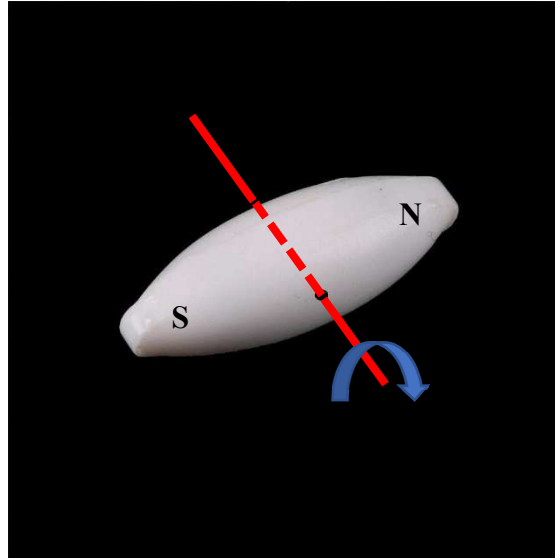
Figure 2-1 Early Modified triaxial cell (a), Thermocontroller (b), Data Acquisition (c)



Figure 2-2 Thermocouple and Immersion heater From Omega Co.

For a preliminary test, the cell was filled with water without any soil sample to measure the temperature of the water inside the cell. Results showed a significant temperature gradient along with the height of the cell, and the thermocontroller stopped the heater when

the temperature at the depth that the related thermocouple is located reached the target temperature. Temperature below that depth was less and above that depth was higher than the target temperature. This indicated the necessity of a circulation system inside the cell. Therefore, an innovative method was employed to circulate the water without affecting other part's functionality. In the literature, the proposed method to circulate the confining fluid is an internal solar pump which is dependent on charging the battery through continuous light. In addition, pumping the water out and in from opposite ends of the cell in a closed-loop brings limitation in providing confining pressure in the cell. The innovative method employed in this study is based on the magnet stirrer which is widely used in chemistry labs. Since the cell does not have room at the bottom to accommodate a magnet stirrer similar to the conventional way to employ it and on the other hand, the cell is tall (height of the cell is almost 3 times its diameter) thus fluid circulation at the bottom will not provide strong enough fluid movement in the cell to make the temperature uniform, the magnet stirrer was mounted on the inner surface of the cell using a small piece of metal bar glued to the surface which holds the magnet stirrer and also allowed the rotation of stirrer around it. The magnet stirrer was drilled at its center to let the metal bar go through it and at the end of the bar, a cap was glued to prevent the magnet stirrer from falling. Figure 2-3 shows a schematic of the magnet stirrer and the metal bar. The magnet stirrer is forced to rotate by two powerful magnets which are attached to a rotary motor and are placed in front of the stirrer from outside of the cell so that the outer magnets are in front of the magnets that the stirrer has inside it. The rotary motor position is adjusted using a clamp that holds the motor and attaches to the cell vertical rods.



*Figure 2-3 Magnet Stirrer and the schematic metal bar*

Results from measuring the temperature at different points in the cell, confirm that this circulation system will provide a uniform temperature inside it. To understand how soil temperature is affected by surrounding water temperature variation and determine the time needed to reach the desired temperature, several tests were conducted by passing a thin (0.5 mm diameter) T-type thermocouple through one of the drainage tubes and placing the tip of the thermocouple at the center of the soil specimens without using a top porous stone. The result of this test for target temperature of 80 °C as well as test setup and different parts are shown in Figure 2-4 and indicates that the temperature of the cell increases from room temperature to 80 °C in 40 minutes at the highest rate of heating, and the temperature inside the sample will finally reach to the cell temperature within 60 minutes of the beginning the test.

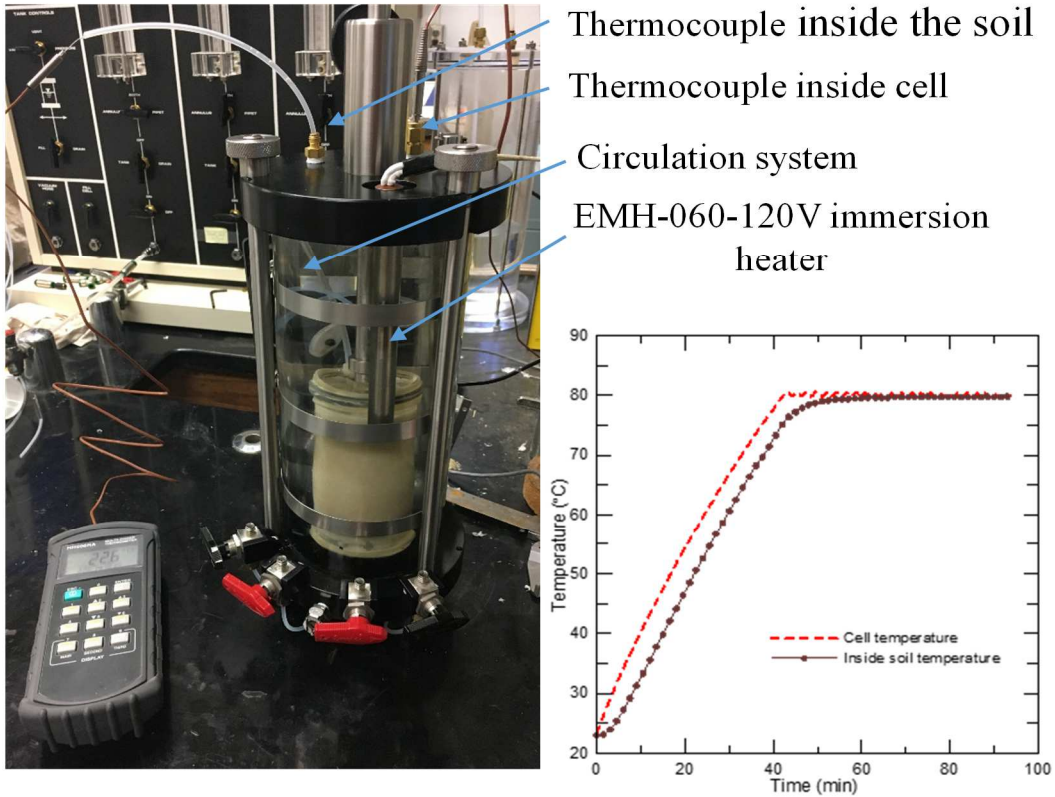


Figure 2-4 Modified triaxial cell and different parts and the temperature changes in cell and sample

As mentioned earlier this modified cell was performing well, except for having some temperature stability issues and also not having the ability to reduce the temperature. As a result, the immersion heater was replaced with a copper coil heat exchanger in which heat carrier fluid is circulated inside the tubes.

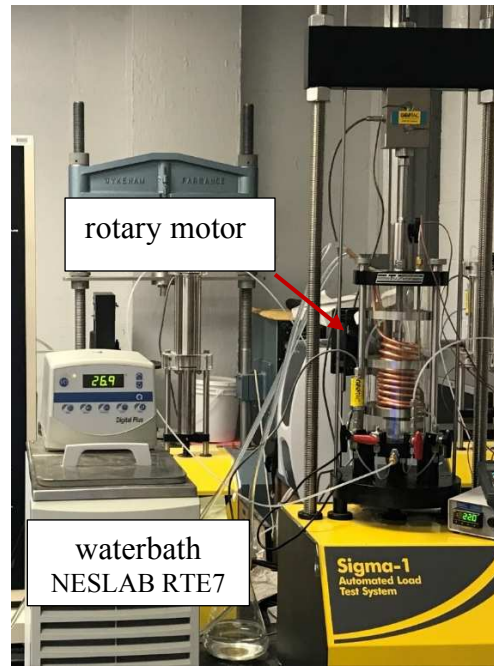
### 2.2.2. Modified Cell Using Metal Heat Exchanger

A spiral copper coil was mounted under the top cap of the cell as the heat exchanger (heating/cooling source) with both ends extruded out of the cell top cap. A water bath was

employed to pump the fluid to the copper coil while the temperature of the fluid could be adjusted and maintained at the water bath control panel. The temperature was controlled at the control panel at the desired rate. Two thermocouples were placed inside the cell to measure the water temperature at different depths of the cell and the results were continuously recorded using a data logger with an adjustable rate of recording. Figure 2-5 shows the modified cell with previous parts except for the heating source which is updated to the copper coil as the temperature exchanger. A constant temperature water bath facilitated with a built-in pump and related tubes that carry fluid to the copper coil.



(a)



(b)

Figure 2-5 (a) Copper coil (b) Modified cell with copper coil temperature exchange method

After several preliminary tests, it was noticed that some parts have resistibility issues. The main issue was with the Plexiglas cell that experienced deformation after some tests

with a temperature higher than 50 °C. Therefore, the cell could not fit properly in the bottom and top cap of the cell and the high viscose grease was not effective anymore to make the contact surfaces watertight. The second issue was with the metal bar which was glued to the inner surface of the cell and the glue failed after a couple of tests. Different glues were employed and the result was the same. Considering the two mentioned issues, the cell chamber was replaced with an aluminum one to prevent deformation and also providing the possibility to attach the metal bar in a more stable manner.

Figure 2-6 shows the modified cell with an aluminum chamber and also the copper coil which is attached to the top cap of the cell.



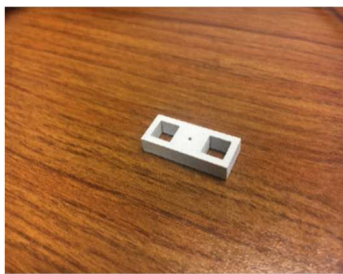
(a)



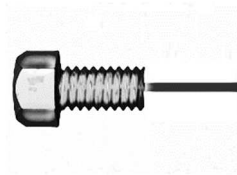
(b)

Figure 2-6 (a) Copper coil attached mounted under the top cap, (b) Modified cell with aluminum chamber

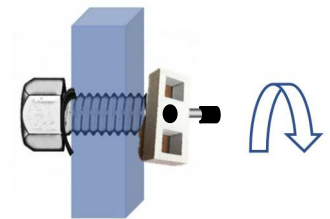
To improve the circulation system, a hole was made on the surface of the aluminum chamber and fine threads were created inside the hole to accommodate a bolt. Fine threads were selected to provide waterproof conditions. A bolt with matching threads was employed to screw into the hole and an O-ring was placed between the bolt head and outer surface of the chamber to waterproof the hole, in addition to covering the bolt with Teflon tape. That part of the bolt that stayed out of the inner surface of the aluminum chamber was shaved with a metal lathe machine to have a round surface and to hold the magnet stirrer. At the end of the shaved bolt, a cap was glued to prevent the stirrer from falling off. To have a stronger magnetic field between the magnets on the rotary motor and the magnets inside the stirrer by facing them accurately in front of each other, a custom-made magnet stirrer was designed and printed using 3-D printing techniques to accommodate two small but strong cubic shape magnets. Figure 2-7 presents the custom-made magnet stirrer, bolt, and the way these parts are assembled



*(a) Custom made magnet stirrer using 3-D printing technique*



*(b) Half-length shaved bolt using metal lathe machine*



*(c) Assembled parts of the circulation part*

*Figure 2-7 Different parts of the designed circulation system*

Figure 2-8 shows the data acquisition system with an adjustable rate of data recording, Figure 2-9 presents the rotary motor with attached magnets mounted on an adjustable clamp. Figure 2-10 presents the schematic of the modified cell and the placement of different parts.



Figure 2-8 Data acquisition system

Figure 2-9 Rotary motor with attached magnets and adjustable clamp

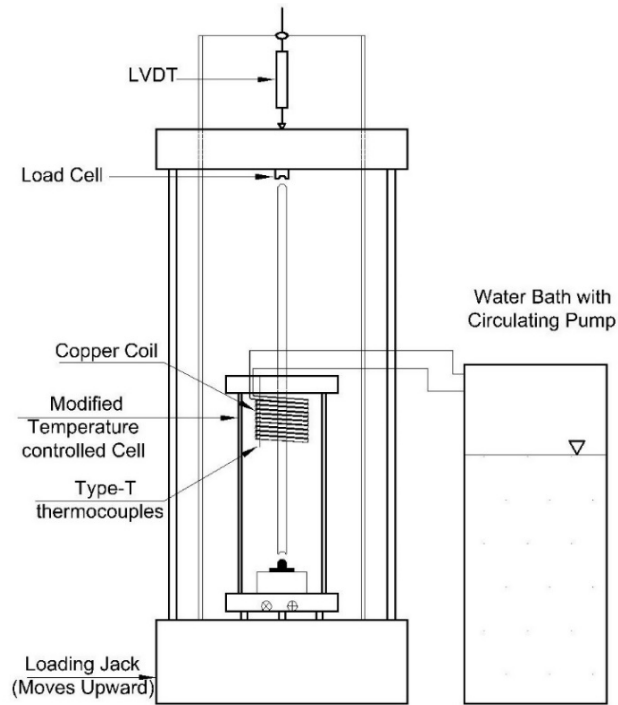


Figure 2-10 Schematic of the modified cell

## CHAPTER 3

### HYDRAULIC CONDUCTIVITY AND INTRINSIC PERMEABILITY

In this Chapter, the changes in hydraulic conductivity and intrinsic permeability of Ottawa sand and Kaolin clay versus temperature are studied. Different tests are conducted at different confinement stresses (60 kPa to 690 kPa) to study the effect of the initial condition of the soil. To conduct these tests, the modified temperature-controlled cell was used as a permeameter cell with connecting proper equipment. Then alterations in absolute permeability are also calculated by utilizing measured fluid properties (e.g., dynamic viscosity) at each temperature. In the second phase of this research, the changes in the void ratio are measured during the thermal loading for both Ottawa sand and Kaolin clay.

#### 3.1. Background

Permeability is one of the most important soil properties which controls the seepage and water movement in the ground and directly, or indirectly underpins many geotechnical problems such as slope stability analysis and landfill designs (Damiano et al. 2017; Dou et al. 2014; Jefferson and Rogers 1998; Ng and Leung 2012; Sadeghi and AliPanahi 2020). Accurate prediction of soil permeability and its variation with temperature is necessary to accurately model energy geo-structures, waste disposals, and landfill covers subjected to daily temperature variations (Monfared et al. 2014; Tamizdoust and Ghasemi-Fare 2020).

Thermal loading alters fluid properties (e.g., density, viscosity) in the soil skeleton. In most of the previous researches changes in hydraulic properties (e.g., hydraulic conductivity) of both coarse and fine-grained soils with temperature were mainly considered due to the fluid properties (density, and viscosity of the water) alteration (Cho et al. 1999; Delage et al. 2000; Gobran et al. 1987; Sageev 1980). Nevertheless, recently there have been studies that showed the measured hydraulic conductivity (H.C.) values at elevated temperatures are different from the calculated values by only using the updated viscosity and density of the water at the selected temperatures (Gao and Shao 2015; Ye et al. 2012; Ye et al. 2013a). Therefore, both hydraulic conductivity and absolute permeability are expected to change with temperature alterations.

There have been several attempts in the literature to predict the soil hydraulic conductivity and absolute permeability variations with temperature using indirect (Habibagahi 1977; Morin and Silva 1984; Towhata et al. 1993b) or direct measurements (Arihara 1974; Cho et al. 1999; Derjaguin et al. 1986; Gobran et al. 1987; Joshaghani and Ghasemi-Fare 2019; Joshaghani et al. 2018; McKay and Brigham 1984; Morin and Silva 1984; Potter 1981; Sydansk 1980). The indirect method is referred to as the back-calculation of hydraulic conductivity from consolidation tests at different temperatures. However, different behaviors (e.g., reduction, increase, and no changes in permeability) were reported in the literature for both sand and clays. Habibagahi (1977) performed isothermal consolidation on samples of slightly organic silty clay and observed an increase in derived hydraulic conductivity with temperature. Derjaguin et al. (1986) and Pusch (1992) reported that when the temperature increases, gaps in the soil can be filled more easily, and then water channels would form. Therefore, it could be concluded that in a more

condensed medium, these channels form readily and more changes in absolute permeability happen by an expansion of the soil skeleton. In another study, Towhata et al. (1993b) measured H.C. of MC clay (artificial Kaolin clay) and Bentonite at different temperatures and observed higher values for measured H.C. compared to the calculated values using only the updated fluid properties at elevated temperatures. They suggested that the degeneration of absorbed water into the free water accounts for this observation. In a recent study, Seiphoori (2015) reported higher hydraulic conductivity and absolute permeability for Bentonite when the temperature increased and indicated that the degeneration of a part of the immobile water within the structure into the mobile water causes the increase in absolute permeability. On the other hand, Romero et al. (2001) studied the thermal behavior of unsaturated Boom clay and reported that measured hydraulic conductivities at different temperatures are smaller than calculated values by only considering the changes in fluid properties and attributed this to clay fabric change and porosity redistribution by temperature. Villar and Lloret (2004) measured H.C. for Bentonite at different temperatures and reported that soil densification due to thermal consolidation causes a reduction in absolute permeability at elevated temperatures. In a recent study, Chen et al. (2017) studied alterations in H.C. of Boom clay with temperature and concluded the difference between measured and calculated values (considering only fluid properties variation) is related to the microstructure weakening effect by the thermal volume change. In contrast to the aforementioned studies, Delage et al. (2011) performed temperature-controlled constant head permeability tests on Boom clay and observed a 148% increase in hydraulic conductivity of the Boom clay when the temperature rises from 20 °C to 90 °C. While they reported no changes in absolute permeability of the Boom Clay in the selected

temperature range by considering the alteration in dynamic viscosity of the water according to the experimental measurements reported in the literature (Hillel 2013). In another study, Ren et al. (2014) performed a hydraulic conductivity test for a temperature range between 10 °C and 25 °C on silty clay specimens. They reported that for the selected range depending on the dry bulk density, absolute permeability can increase or decrease.

Similar to clayey soils, different behaviors were reported in the literature about the effect of temperature on the coarse-grained soil properties (e.g., void ratio changes and permeability). Several studies showed that the changes in absolute permeability are insignificant with temperature variations for cemented quartz samples and unconsolidated Ottawa sand at different confining pressures and indicated insignificant thermal volume change in sandy soils (Arihara 1974; Gobran et al. 1987; Greenberg et al. 1968; Sageev 1980). While a reduction (Aruna 1977; Weinbrandt et al. 1975) and an increase in soil permeability (Aktan and Ali 1975; Somerton and Gupta 1965) of coarse-grained soil with temperature were reported in other studies.

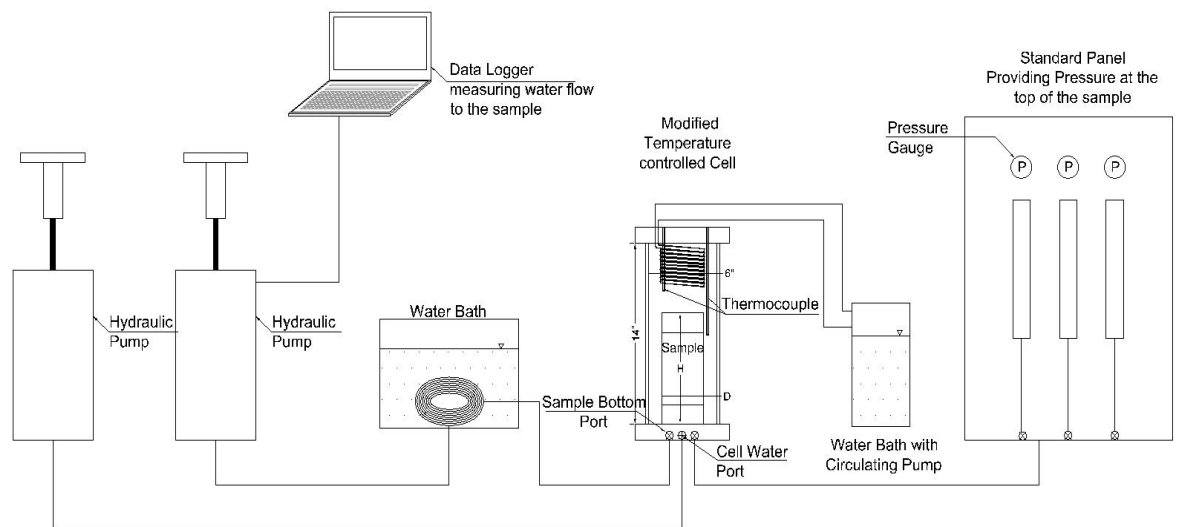
Although there is a consensus in the literature that temperature induces volume reduction in clayey soils, different observations on the amount of thermal volume change (or porosity change) and permeability values at elevated temperatures are reported in the literature. In addition, most of the previous researches indicated that the effect of temperature on sandy soil properties (e.g., permeability and volumetric strain) are minor. Besides, the effect of temperature on the absolute permeability of sand and clays with different initial conditions (initial confinement or initial void ratio) has not been completely studied in the literature. Therefore, to address these issues, and to compare the effect of fluid properties variations (dynamic viscosity and density) and other mechanisms (e.g.,

particle rearrangement in sandy soil and thermal volume reduction, or degeneration of adsorbed water in clayey soils) the changes in H.C. with temperature of Ottawa sand and Kaolin clay at different confinement stresses (60 kPa to 690 kPa) (or different initial void ratios) were measured using a modified temperature-controlled triaxial permeameter cell. Then alterations in absolute permeability were calculated by utilizing measured fluid properties (e.g., dynamic viscosity) at each temperature. In the second phase of this research, the changes in the void ratio were measured during the thermal loading for both Ottawa sand and Kaolin clay.

### 3.2. Experimental Setup

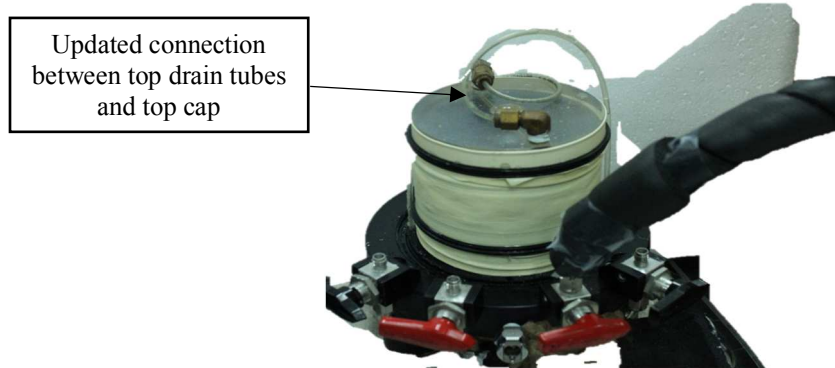
To prepare the setup and perform hydraulic conductivity tests at different temperatures using the modified cell, an acrylic bottom cap was mounted on the base plate of the modified cell. And the sample was placed between acrylic caps at the top and bottom, inside a latex membrane, similar to a regular triaxial test. The main difference compared to the conventional way to use a triaxial cell as a permeameter, except using the modified temperature control cell, is the modification to control the temperature of the inlet water and also employing the triaxial digitally-controlled pumps and controlling system to monitor the water passing through the sample, as well as controlling the pressure of the inlet and outlet water. With these modifications, the measurements of the passing water through the sample are more accurate and also we can calculate the changes in the volume of the sample and subsequently void ratio.

Figure 3-1 shows the full setup, including the standard panel; modified permeameter; and the secondary water bath, which controls the temperature of the injected water, and the two digital flow pumps which one of them provides confining pressure to the cell and the other one which provides pressure and measures the absorbed/expelled water to/from the sample. Please note, in the modified temperature-controlled permeameter, the temperature of the specimen and both the temperature and pressure of the permeant water can be controlled at the same time. Preliminary results and calibration tests determined that a reliable outcome highly depends on the controlled conditions (e.g., sample temperature at the core, uniform cell temperature, and most importantly, the temperature of the injected water). It is important to note that insufficient control in any of these mentioned parameters may lead to a wrong conclusion on the effect of temperature on the permeability of the soil.



*Figure 3-1 schematic view of the complete modified temperature-controlled permeameter to perform hydraulic conductivity tests*

Figure 3-2 shows the soil sample inside a latex membrane and between the Plexiglas top and bottom caps, on the base plate of the cell. Another update with the test setup was using fittings end at the end of the top drain tubes by making a proper hole and threads on the Plexiglas top cap to connect the tubes which is a more reliable method compared to the conventional one. In the conventional method, a combination of o-ring and high viscous grease is used at the tip of the tubes and they are pushed into the related holes in the top cap.



*Figure 3-2 soil sample inside the latex membrane sitting on the base plate of the cell*

In addition to the water bath which is used in the temperature control part of the cell, the second water bath (with no pump) is used to change the temperature of the water passing through the sample. For this purpose, a long tube is used between the hydraulic pump and sample, with placing a considerable length inside the water bath so the temperature of water change as desired (test temperature) before getting to the sample and to avoid causing temperature change to the sample. The tube between the water bath and the sample was

insulated and also a calibration test was conducted to correlate the temperature of the water bath and the temperature of the water in the tube where it reaches the cell.

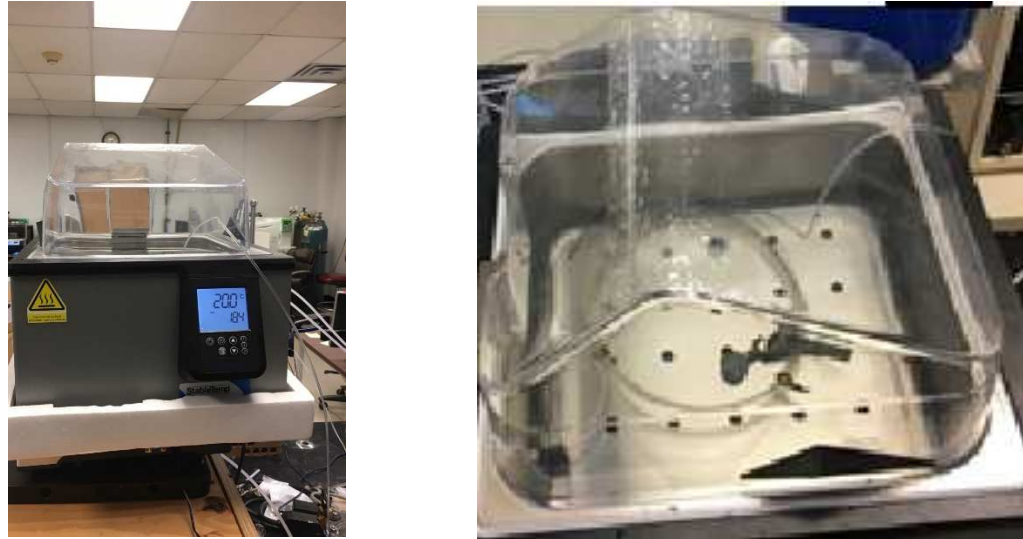


*Figure 3-3 water bath used to change the temperature of the permeant water, before injecting to the sample*

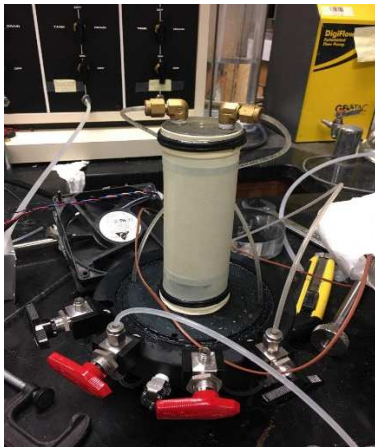
### 3.3. Sample Preparation

To compare the effects of temperature on permeability and void ratio of both fine and coarse-grained soils, uniform Ottawa sand (SP) and Kaolin clay were selected in this study. Kaolin clay and Ottawa sand have been widely studied in different geotechnical research as standard fine and granular soils (Darbari et al. 2017; Ghasemi-Fare and Basu 2018). After finalizing the setup, several permeability tests were performed using both selected soils, and changes in hydraulic conductivity and intrinsic permeability were analyzed. The properties of the Illinois Ottawa sand (washed silica sand) with a majority particle size of 0.425 mm (remained on sieve #40) are presented in Table 3-1. The particle size distribution of the selected sand is also shown in Figure 3-5. In addition, the geotechnical and thermal

properties of the Kaolin clay used in this research were measured and are presented in Table 3-2.

*Table 3-1 Geotechnical and thermal properties of Illinois Ottawa silica sand*

$G_s$	$e_{max}$	$e_{min}$	$D_{50}$	$C_c$	$C_u$	$\alpha_s [1/^\circ C]$
2.65	0.86	0.53	0.5 (mm)	0.92	1.02	$1.0 \times 10^{-5}$



*Ottawa sand sample*



*Kaolin clay sample*

*Figure 3-4 Samples used for H.C test covered by latex membrane*

Sandy soil was dried in the oven and then was used to fabricate the samples using the dry tamping method inside a latex membrane which was stretched using a two-part vacuum split former with 50.8 mm of diameter. The dry sand was compacted at 3 different layers using a plastic tamper. According to the sample dimensions and the weight of the soil, the initial void ratio was calculated. To prepare clay samples, a compaction mold with a diameter of 101.6 mm was filled with remolded Kaolin clay (compacted specimen), and then the soil was pushed out using a hydraulic jack. A thickness of 25.4 mm was cut using a trimming saw and was placed between the filter papers and porous stones. Please note,

since hydraulic conductivity was performed at higher confinement (stress) compared to the initial stress state, all clayey samples were considered as normally consolidated clays. The dimensions of the sample were measured, and the membrane was placed around it. Using the sample dimensions before the test and the dry weight of the soil specimen, the initial void ratio was calculated. After the specimen (Ottawa sand or Kaolin clay) was placed inside the cell, the de-aired water was used to fill the cell and its pressure was set to the target confinement stress. In the next step, the sample was saturated by passing de-aired water through the specimens by applying a pressure gradient between the bottom and the top of the sample. The saturation of the sample was verified before starting each test by measuring Skempton's coefficient B. To assure about reaching the fully saturated condition, cell pressure was increased (70 kPa) and then the changes in the sample pressure were measured to calculate Skempton's coefficient B. The measured B value was greater than 0.97. This value satisfies the saturation requirement which is at least 0.95. Figure 3-4 shows prepared samples of both Ottawa sand and Kaolin clay.

*Table 3-2 Geotechnical and thermal properties of Columbus Kaolin clay*

<b>Specific Gravity</b>	<b>Plasticity Index</b>	<b>Liquid Limit</b>	<b>VCL Slope (<math>\lambda</math>)</b>	<b>RCL Slope (<math>\kappa</math>)</b>	<b><math>\alpha_s</math>[1/°C]</b>
2.65	10	40 %	0.228	0.08	$2.0 \times 10^{-4}$

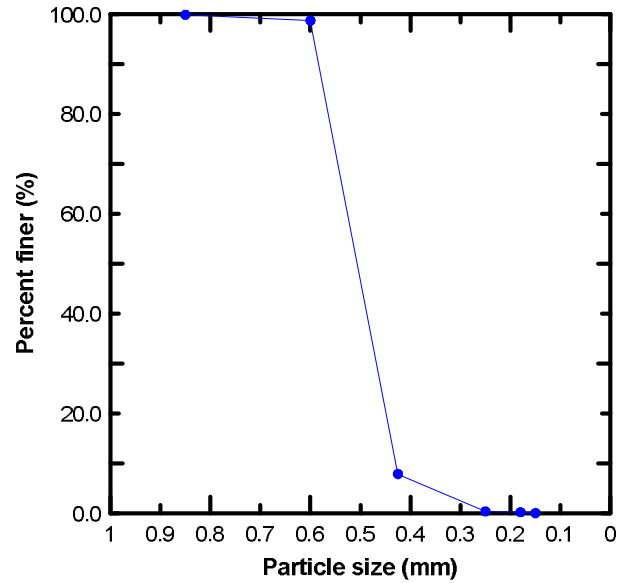


Figure 3-5 Particle size distribution for Illinois Ottawa sand

### 3.4. Test Procedure

After the sample was placed in the cell and the cell was filled with de-aired water, cell pressure was increased to the desired confining pressure. Cell pressure was adjusted and controlled by one of the digitally controlled flow pumps of the triaxial setup. After verifying that the saturation was achieved, the hydraulic conductivity test may be conducted at different temperatures by applying a pressure gradient from the bottom of the sample to the top. For this purpose, the pressure at the bottom of the sample is controlled by the second digitally controlled flow pump (range of 0 to 200 psi), and the pressure at the top of the sample is controlled by the standard panel in the lab with a range of pressure between 0 to 100 psi. The digital flow pump has the ability to measure the volume of the water as small as 0.001 ml. To perform a test at the desired temperature, the first step is to change the temperature of the cell (as discussed in chapter 2). In this step, the bottom drain

valve remains open to let the generated pore water pressure dissipates. The amount of dissipated water can be measured by the digital flow pump, but if we do not need to know this volume, the top drain valve can also remain open for expediting this process. The water in the second water bath (which includes the tube that connects the bottom drain valve to the digital flow pump) needs to change to the temperature that is determined from the calibration test to provide the test temperature at the bottom of the sample. As shown in chapter 2, sample temperature reaches the cell temperature within an hour. So after that hydraulic conductivity test can be started by applying a pressure gradient in the sample and measuring the volume of the passed water through it. It is assumed that during a hydraulic conductivity test, soil fabric changes are not considerable, therefore, the amount of water at the sample inlet (bottom) is equal to the amount of the water at the outlet (top) of the sample.

In the final step, the dynamic viscosity of the water (which was tap water in this study) was then measured at each thermal step to analyze the variation of soil intrinsic permeability. A temperature-controlled Rheometer testing device was used to quantify the dynamic viscosity at different temperatures (Please see Figure 3-6). The fluid properties at three different temperatures are presented in Table 3-3. Please note, the calibration of the used Rheometer was verified by comparing the measured dynamic viscosity of the distilled water with reported values in the literature and the difference was less than 6%. Then, the changes in intrinsic permeability of both Ottawa sand and Kaolin clay were investigated to explore if there were any changes in pore space and tortuosity (connectivity of the pores) that could be accounted as the soil fabric alterations (e.g., arrangement of particles, particle groups, and pore spaces) with temperature. The soil fabric alterations were not measured

directly in this study, however since soil fabric controls the intrinsic permeability, any changes in soil permeability can be interpreted as the result of soil fabric changes.



*Figure 3-6 Rheometer used to measure the dynamic viscosity of water at different temperatures*

*Table 3-3 Dynamic viscosity measurements by the Rheometer*

Temperature (°C)	Measurement from Rheometer (Pa.s)
20	0.001017
50	0.000615
80	0.000439

### 3.5. Test Program

In this research, hydraulic conductivity was initially measured at room temperature (20 °C). The cell temperature was then increased to 80 °C through four different steps ( $\Delta T= 15$  °C). At each step, the soil hydraulic conductivity was measured at least three times to ensure the repeatability of the tests, and the average value was considered as the hydraulic conductivity at that temperature. The same procedure was repeated at different confinement stresses (different initial void ratios) for both sand and clay. Please note that a higher pressure gradient was used to perform permeability tests with a higher hydraulic gradient ( $i=138$ ) for fine-grained soil (Kaolin clay).

To study hydraulic conductivity and intrinsic permeability of Ottawa sand (as granular material) and Kaolin clay (as fine-grain material), different tests were performed at different confinement pressure, which means different sample initial states (i.e. void ratio).

Table 3-4 presents the test program and the sample specifications used at each test.

*Table 3-4 Hydraulic conductivity test program*

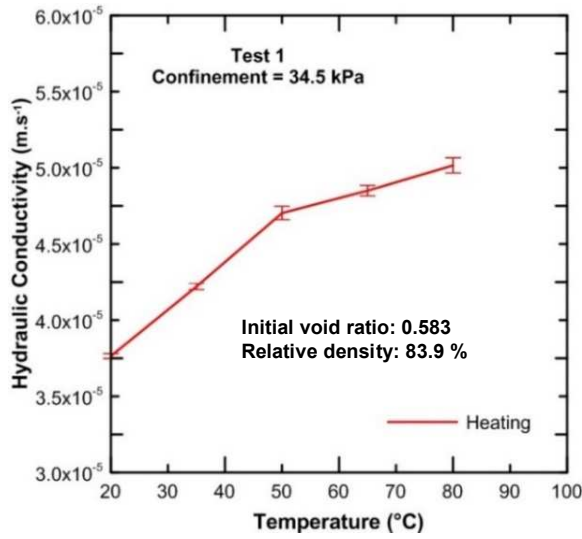
<b>Soil Type</b>	<b>Confinement Pressure (kPa)</b>	<b>Initial Void Ratio</b>	<b>Thermal Load Steps °C</b>
Ottawa Sand	34.5	0.583	20-35-50-65-80
	69	0.582	
	138	0.577	
	345	0.574	
	517	0.571	
Kaolin Clay	69	0.897	20-35-50-65-80
	207	0.838	
	414	0.775	
	690	0.728	

### 3.6. Results

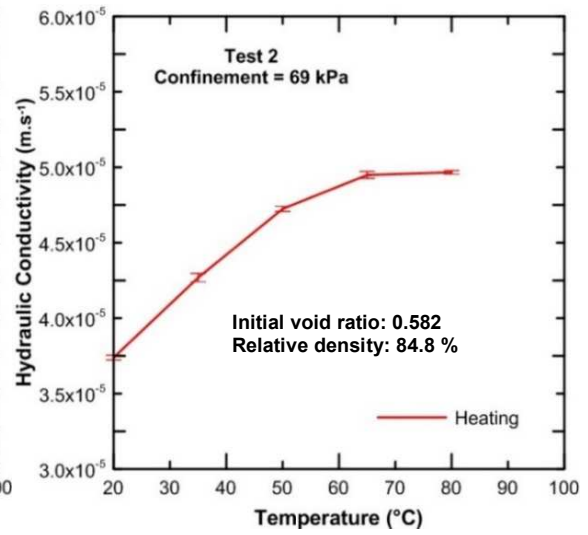
In the following sections, hydraulic conductivity and intrinsic permeability of the different samples (Ottawa sand and Kaolin clay) are provided, as well as changes in the volume and void ratio of the samples to have a better understanding of the changes in soil fabric by changing in temperature.

#### 3.6.1. Effect of temperature on H.C. of Ottawa sand

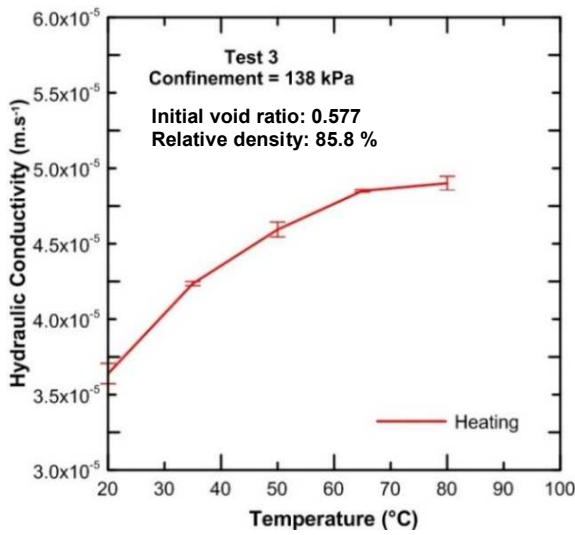
The results obtained from the hydraulic conductivity test on Ottawa sand at each thermal step are presented in Figure 3-7. Figure 3-7 presents the hydraulic conductivity variations for Ottawa sand with temperature for different confinement stresses and Figure 3-8 presents all those data in a single figure for a better comparison. The variation range of hydraulic conductivity at each temperature is presented using an error bar which are the results of the 3 repeated tests at each thermal step. The results confirm the repeatability of the experiment under thermal loading using the modified apparatus. Figure 3-7 shows that the hydraulic conductivity of Ottawa sand increases by 35% when the soil temperature is changed from 20 °C to 80 °C. The results which were obtained at different confinement stresses in this study show similar trends with an increase in temperature. Although hydraulic conductivity values were expected to increase at elevated temperatures for sandy soil, as mentioned earlier different rates of changes in hydraulic conductivity were reported in the literature, and consequently, contradictory observations were concluded for intrinsic permeability variations with an increase in temperature. Therefore, in the next step, the changes in density and dynamic viscosity of the water were measured at different temperatures and alterations in intrinsic permeability were analyzed.



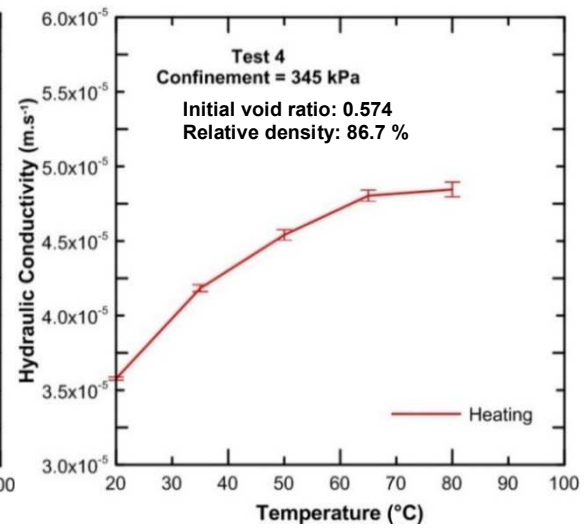
(a)



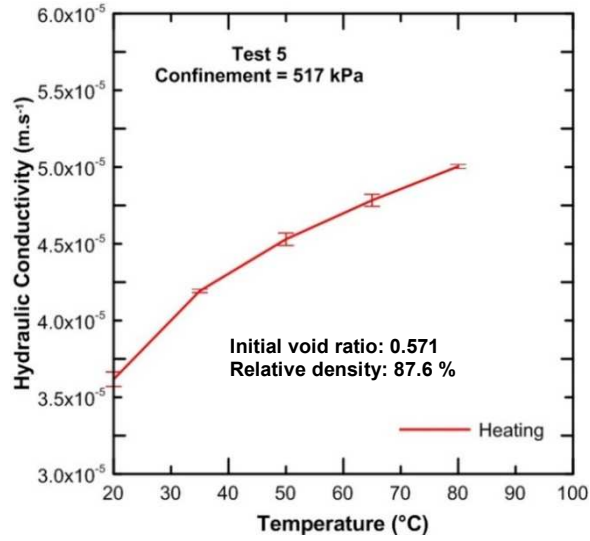
(b)



(c)



(d)



(e)

Figure 3-7 Variations of hydraulic conductivity of uniform Ottawa sand with the temperature at different confinement stresses

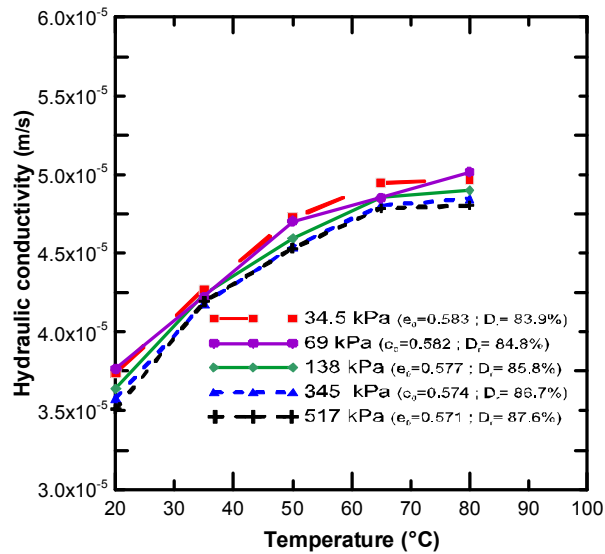


Figure 3-8 Variations of hydraulic conductivity of uniform Ottawa sand with the temperature at different confinement stresses

### 3.6.2. Effect of temperature on intrinsic permeability of Ottawa sand

Water density and viscosity are temperature dependent and thus to analyze how much of the change in hydraulic conductivity is due to the volume reduction, or degeneration of adsorbed water into free water (only in clays), the variation in intrinsic permeability of soil should be investigated.

Considering the changes in dynamic viscosity and density of the water, the intrinsic permeability ( $K$ ) variation with temperature can be calculated using the hydraulic conductivity results ( $\kappa = \frac{\gamma_w}{\eta} K$ ; where  $\eta$  is dynamic viscosity,  $\gamma_w$  is the unit weight of water and  $\kappa$  is hydraulic conductivity).

Figure 3-9 presents the changes in the intrinsic permeability of Ottawa sand at different temperatures for five different confinement stresses. By comparing Figure 3-7 and Figure 3-9, it is interesting to note that, although hydraulic conductivity increases, the intrinsic permeability is reduced by approximately 50% when the soil temperature is raised from 20 °C to 80 °C. Please note, any changes in intrinsic permeability or void ratio of sandy soil with thermal loading can confirm the soil fabric (arrangement of particles, and pore spaces) alterations in sandy soil. Figure 3-9 demonstrates almost a linear reduction of intrinsic permeability with temperature. The results show almost an identical reduction in the intrinsic permeability during heating phases for all cases. This reduction in the intrinsic permeability could be a result of void ratio reduction due to thermal loading, and soil densification which can be interpreted as soil fabric changes. Soil fabrics demonstrate the arrangement of particles, particle groups, and pore spaces and control the ability of the water to flow through the soil (e.g., permeability). Therefore, any changes in intrinsic

permeability can be claimed as soil fabric alterations. Although a wide temperature range (from 20 °C to 80 °C) is considered in this study, similar behavior can be concluded when soil temperature rises from 20 °C to 45 °C which can represent the ranges for ambient temperature fluctuations in summer and soil temperature variation close to geothermal piles. The presented results can be used for any desired temperature ranges from 20 °C to 80 °C depending on the geographical location or the nature of the problem.

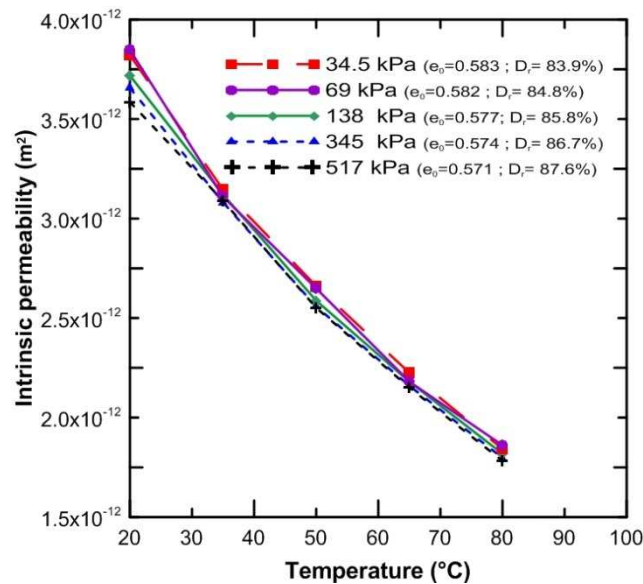


Figure 3-9 Variations of intrinsic permeability of Ottawa sand with the temperature at different confinement stresses

### 3.6.3. Effect of temperature on H.C. of Kaolin clay

For the second series of experiments, changes in the permeability of Kaolin clay were studied. Figure 3-10 presents the changes in the hydraulic conductivity of Kaolin clay with the temperature at four different confinement stresses and Figure 3-11 shows all those results in a single figure. The results show that the hydraulic conductivity of Kaolin clay increases by approximately 150% when the temperature increased from 20 °C to 80 °C.

Comparison of Figure 3-7 and Figure 3-10 demonstrates that the changes in the hydraulic conductivity of Kaolin clay with temperature are significantly higher than that of Ottawa sand. To better understand this comparison, the changes in the intrinsic permeability of Kaolin clay were analyzed.

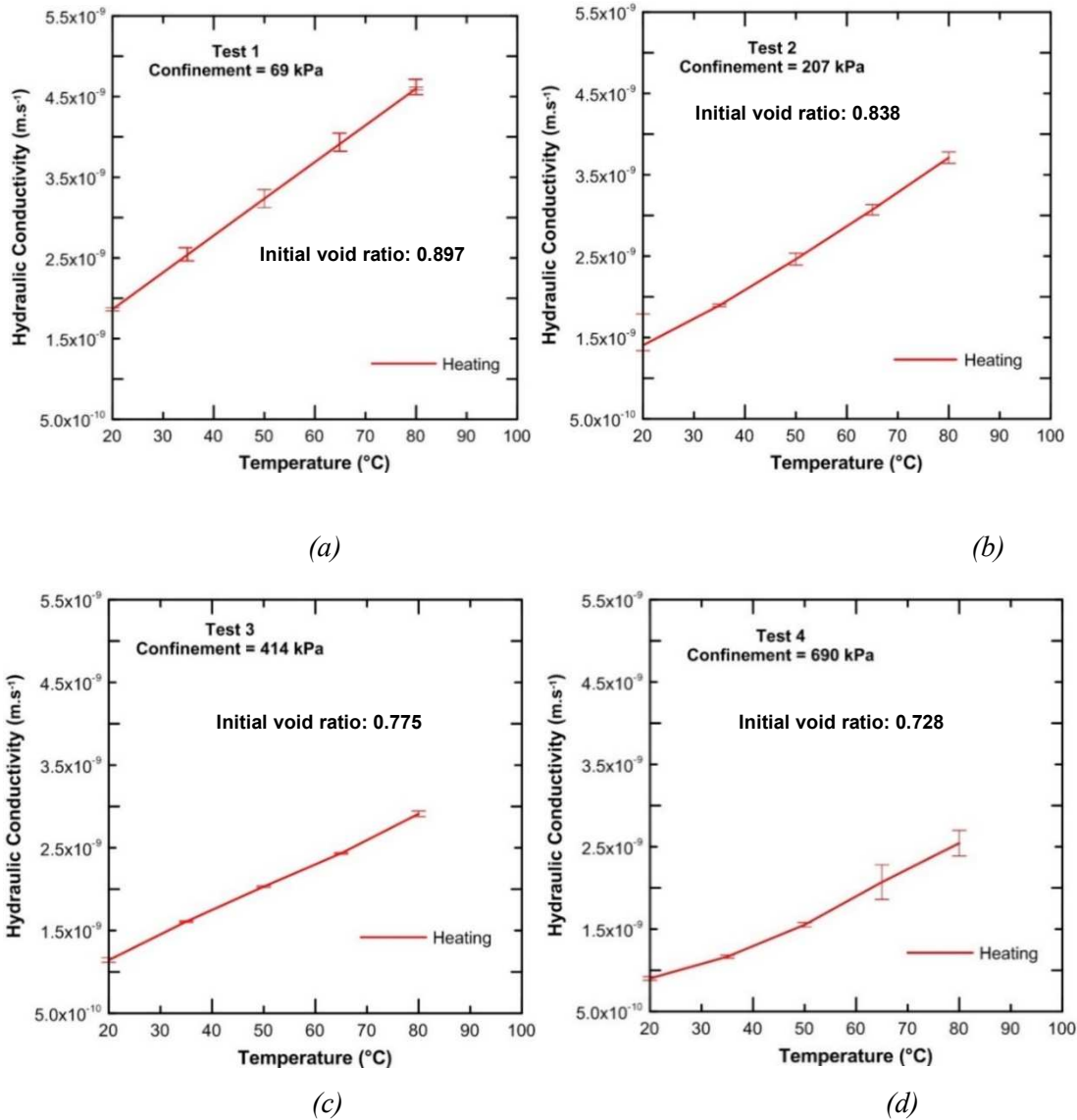


Figure 3-10 Changes in hydraulic conductivity of Kaolin clay with the temperature at different confinement stresses

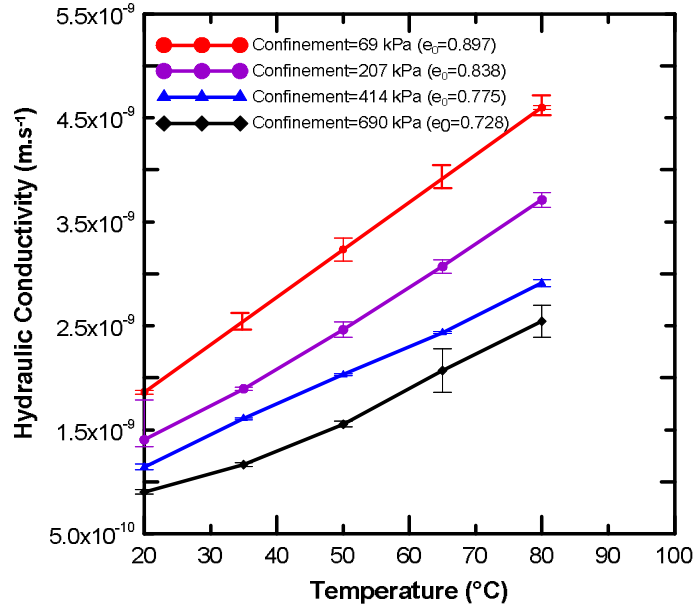


Figure 3-11 Changes in hydraulic conductivity of Kaolin clay with the temperature at different confinement stresses

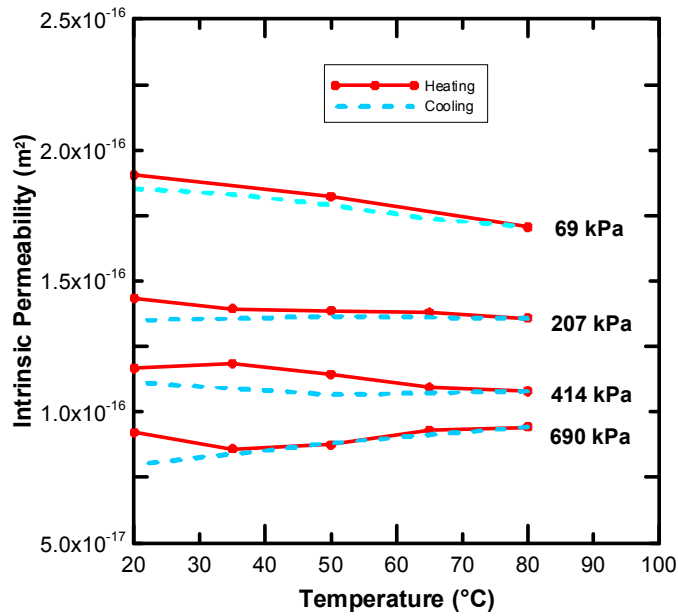


Figure 3-12 Variations of intrinsic permeability of Kaolin clay during heating and cooling at different confinement stresses

#### 3.6.4. Effect of temperature on the intrinsic permeability of Kaolin clay

Considering the dynamic viscosity and density variations of the water with temperature, the intrinsic permeability values of Kaolin clay at different temperatures were calculated. Figure 3-12 presents the changes in the intrinsic permeability of Kaolin clay with temperature. Results determine a slight reduction in the intrinsic permeability (between 3 to 10%) in most confining pressures after the temperature raised to 80 °C. This small amount of reduction in intrinsic permeability compared to a large amount of increase in hydraulic conductivity values could be because of the degeneration of a part of the adsorbed water into the free water at the elevated temperatures that is reported in the literature (Derjaguin et al. 1986; Ma and Hueckel 1993; Seiphoori 2015) which helps to increase the intrinsic permeability. Overallly, the effect of void ratio changes which casuse a reduction in intrinsic permeability overcome the absorbed water degeneration effect. In the next section, the thermal volume changes of both Ottawa sand and Kaolin clay are investigated to explore if the changes in intrinsic permeability in both materials are consistent with the void ratio changes with thermal loading.

#### 3.6.5. Discussion

Changes in void ratio with temperature were also studied in this research. Volumetric and void ratio variations with temperature were calculated by monitoring and measuring the amount of expelled water during thermal loading. Campanella and Mitchell (1968) proposed a relation (Equation 3-1) between drained (or absorbed) water ( $\Delta V_{dr}$ ) and thermal expansion of the water and solid parts to predict the thermal volume change of the specimen

$(\Delta V_m)$ . Please note, thermal volume change or consequently the changes in void ratio could also be measured by monitoring the changes in the volume of the water inside the cell considering the changes in volume of the cell by temperature.

$$(\Delta V_{dr})_{\Delta T} = \alpha_w V_w \Delta T + \alpha_s V_s \Delta T - (\Delta V_m)_{\Delta T} \quad \text{Equation 3-1}$$

In Equation 3-1,  $\alpha_w$  and  $\alpha_s$  are, respectively, the coefficient of thermal expansion of the water and soil; and  $V_w (= V_v)$  and  $V_s$  are, respectively, initial pore water volume (equal to void volume) and soil grains volume before each thermal step.

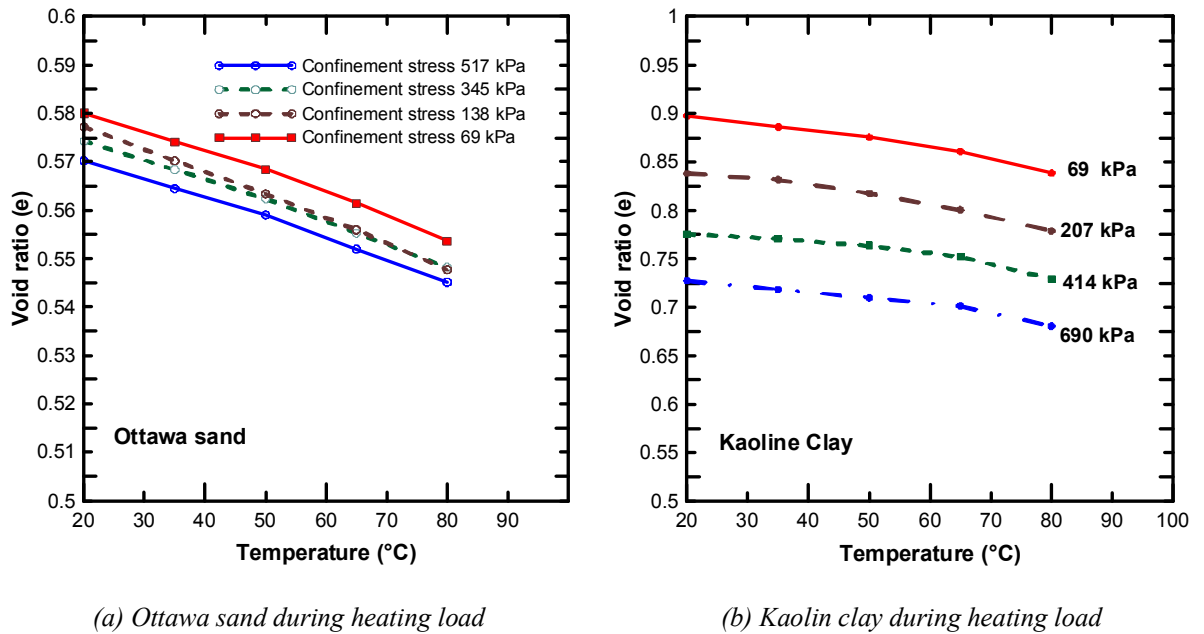


Figure 3-13 Void ratio alterations with the temperature at different confinement stresses

During thermal loading, the amount of water expelled or absorbed by the sample was

measured, and since the initial amounts for  $V_w$  and  $V_s$  were known, change in the volume of the specimen ( $\Delta V_m$ ) was calculated from Equation 3-1 at each thermal loading steps ( $\Delta T = 15^\circ\text{C}$ ) and was used to calculate the new amount for  $V_w (= V_v)$ , considering the changes in soil grains volume. Calculated values for  $V_w$  and  $V_s$ , were used as the initial pore water and solid grains volumes for the next thermal loading step. The coefficient of thermal expansion of water ( $\alpha_w$ ) was considered variable depending on the temperature of each load step ranging between  $2.07 \times 10^{-4} [1/^\circ\text{C}]$  for  $20^\circ\text{C}$  to  $6.40 \times 10^{-4} [1/^\circ\text{C}]$  for  $80^\circ\text{C}$ . Coefficient of thermal expansion for silica sand ( $\alpha_s$ ) and for Kaolin clay were considered to be equal to  $1.0 \times 10^{-5} [1/^\circ\text{C}]$ , and  $2.0 \times 10^{-4} [1/^\circ\text{C}]$ , respectively (McKinstry 1965). Void ratio values were determined using calculated (updated)  $V_w$  and  $V_s$  after each thermal load. The calculated void ratio variations with temperature during heating for Ottawa sand and Kaolin clay are presented in Figure 3-13. Comparing Figure 3-13 (a) and Figure 3-13 (b) depict that 4.5% and 6% reductions in the void ratio were recorded, respectively, for Ottawa sand and Kaolin clay when soil temperature increased from  $20^\circ\text{C}$  to  $80^\circ\text{C}$ . It is to be noted that, Delage et al. (2011) also observed almost similar thermal volume contraction in Boom clay and reported that porosity decreases from 39% ( $e=0.64$ ) to 37.2% ( $e=0.59$ ) (6 to 7% void ratio reduction) when soil temperature raised from  $20^\circ\text{C}$  to  $90^\circ\text{C}$ .

Experimental results presented in this study confirm that increase in temperature will alter soil hydraulic conductivity and intrinsic permeability. This happens not only because of fluid density and viscosity variations with temperature; thermal loading alters the pore spaces in both sand and clay and consequently could change soil fabric. It is interesting to note that, although thermal loading induces void ratio reduction in both Ottawa sand and Kaolin clay, the intrinsic permeability alterations with temperature in the studied sand and

clay were different. The intrinsic permeability of Ottawa sand reduces by approximately 50% in all confinement stresses during the heating cycle from 20 °C to 80 °C which is due to the particle rearrangement and reduction in a void ratio (volumetric change), as shown in Figure 3-13 (a). For Kaolin clay, void ratio decreases by heating to 80 °C and the intrinsic permeability reduces between 3% and 10% (5% reduction in average) for most confining pressures which is in agreement with the reduction in void ratio.

Kozeny-Carman proposed Equation 3-2 as a relation between hydraulic conductivity and void ratio.

To see if the Kozeny-Carman equation can be used to estimate the hydraulic conductivity of sandy soils at elevated temperatures the measured and calculated hydraulic conductivity using the Kozeny-Carman equation is compared. To explore the importance of considering the variations of tortuosity, specific area, and shape factor (in general soil fabric) at elevated temperatures, only the changes in void ratio with temperature were considered. As discussed above, at each thermal loading step in the experiment, void ratio, unit weight, and dynamic viscosity were measured (please see Figure 3-13, and Table 3-3). Therefore, the product of the  $C_s \times S_s \times \Gamma$  can be calculated using Kozeny-Carman equation and by utilizing the hydraulic conductivity measured at room temperature (20 °C).

$$\kappa = \frac{1}{C_s S_s \Gamma} \frac{\gamma_w}{\eta} \frac{e^3}{1+e} \quad \text{Equation 3-2}$$

- $k$  is hydraulic conductivity;
- $C_s$  is shape factor (which is a function of the shape of flow channels)
- $S_s$  is the specific surface area per unit volume of particles
- $\Gamma$  is tortuosity of flow channels
- $\gamma_w$  is the unit weight of the water

- $\eta$  is the dynamic viscosity of permeant
- $e$  is the void ratio

Then the hydraulic conductivity at any temperature could be predicted assuming the term  $C_s \times S_s \times \Gamma$  does not change by temperature and using the initial hydraulic conductivity which was measured at room temperature (20 °C) as in Equation 3-3 in which  $\kappa_2$  is the hydraulic conductivity at temperature ( $T_2$ ) and  $\kappa_1$  is the hydraulic conductivity measured at 20 °C. Equation 3-3, the hydraulic conductivity at elevated temperatures can be predicted by measuring the changes in the void ratio at two thermal steps. The comparisons between the measured and calculated hydraulic conductivity for four different confinement stresses are presented in Table 3-5. As can be seen in Table 3-5, the percentage of error increases at elevated temperatures if only thermal void ratio reduction is considered. This confirms that considering a constant value for  $C_s \times S_s \times \Gamma$  (constant values for tortuosity, shape factor, and specific area) at variable temperatures is not correct and we expect tortuosity, specific area, and shape factor to vary at elevated temperatures. Therefore, it can be concluded that the Kozeny-Carman equation can only be used if the changes in void ratio as well as tortuosity, specific area, and shape factor are accurately measured at elevated temperatures with the changes in soil fabric (arrangement of particle groups and pore spaces) or in other words, soil fabric is a function of temperature.

$$\kappa_2 = \left( \frac{1}{\frac{1}{\kappa_1} \frac{\gamma_{w_1}}{\eta_1} \frac{e_1^3}{1+e_1}} \right) \times \frac{\gamma_{w_2}}{\eta_2} \frac{e_2^3}{1+e_2} = \kappa_1 \times \frac{\frac{\gamma_{w_2}}{\eta_2} \frac{e_2^3}{1+e_2}}{\frac{\gamma_{w_1}}{\eta_1} \frac{e_1^3}{1+e_1}} \quad \text{Equation 3-3}$$

Table 3-5 Comparison of measured and calculated intrinsic permeability of Ottawa sand using Kozeny-Carman equation at different temperatures and confinement stresses

**Confinement stress = 69 kPa**

Temperature (°C)	Measured k (m/s)	Measured K (m <sup>2</sup> )	$\frac{e^3}{(1+e)}$	$\frac{\gamma_w}{(\eta)}$ (1/m.s)	Calculated $\kappa$ based on Equation 2 (m/s)	Calculated K based on Equation 2 (m <sup>2</sup> )	Differences (%)
20	3.74E-05	3.82E-12	0.1235	9786326.49	3.74E-05	4.16E-12	8.77
35	4.27E-05	3.14E-12	0.1202	13574232.79	2.62E-05	1.93E-12	-38.519779
50	4.72E-05	2.66E-12	0.1171	17753751.58	1.95E-05	1.10E-12	-58.628683
65	4.95E-05	2.22E-12	0.1133	22241449.6	1.51E-05	6.79E-13	-69.484928
80	4.97E-05	1.84E-12	0.1092	26954707.66	1.20E-05	4.46E-13	-75.817948

**Confinement stress = 138 kPa**

Temperature (°C)	Measured k (m/s)	Measured K (m <sup>2</sup> )	$\frac{e^3}{(1+e)}$	$\frac{\gamma_w}{(\eta)}$ (1/m.s)	Calculated $\kappa$ based on Equation 2 (m/s)	Calculated K based on Equation 2 (m <sup>2</sup> )	Differences (%)
20	3.64E-05	3.72E-12	0.1219	9786326.49	3.64E-05	3.72E-12	0.00
35	4.24E-05	3.12E-12	0.1180	13574232.79	2.54E-05	1.87E-12	-40.04
50	4.59E-05	2.59E-12	0.1144	17753751.58	1.88E-05	1.06E-12	-59.04
65	4.85E-05	2.18E-12	0.1104	22241449.6	1.45E-05	6.52E-13	-70.10
80	4.90E-05	1.82E-12	0.1061	26954707.66	1.15E-05	4.27E-13	-76.53

**Confinement stress = 345 kPa**

Temperature (°C)	Measured k (m/s)	Measured K (m <sup>2</sup> )	$\frac{e^3}{(1+e)}$	$\frac{\gamma_w}{(\eta)}$ (1/m.s)	Calculated $\kappa$ based on Equation 2 (m/s)	Calculated K based on Equation 2 (m <sup>2</sup> )	Differences (%)
20	3.58E-05	3.66E-12	0.1203	9786326.49	3.58E-05	3.66E-12	0.00
35	4.18E-05	3.08E-12	0.1171	13574232.79	2.51E-05	1.85E-12	-39.99
50	4.54E-05	2.56E-12	0.1138	17753751.58	1.87E-05	1.05E-12	-58.90
65	4.80E-05	2.16E-12	0.1101	22241449.6	1.44E-05	6.48E-13	-70.01
80	4.84E-05	1.80E-12	0.1064	26954707.66	1.15E-05	4.26E-13	-76.29

**Confinement stress = 517 kPa**

Temperature (°C)	Measured k (m/s)	Measured K (m <sup>2</sup> )	$\frac{e^3}{(1+e)}$	$\frac{\gamma_w}{(\eta)}$ (1/m.s)	Calculated $\kappa$ based on Equation 2 (m/s)	Calculated K based on Equation 2 (m <sup>2</sup> )	Differences (%)
20	3.51E-05	3.59E-12	0.1181	9786326.49	3.51E-05	3.59E-12	0.00
35	4.19E-05	3.09E-12	0.1149	13574232.79	2.46E-05	1.81E-12	-41.26
50	4.53E-05	2.55E-12	0.1120	17753751.58	1.84E-05	1.03E-12	-59.48
65	4.78E-05	2.15E-12	0.1083	22241449.6	1.42E-05	6.37E-13	-70.38
80	4.80E-05	1.78E-12	0.1048	26954707.66	1.13E-05	4.20E-13	-76.45

### 3.6.6. Summary

An increase in temperature changes the groundwater density and viscosity, therefore, it is expected that the soil hydraulic conductivity varies with temperature. Beyond this point, thermal loading induces volumetric changes for both sand and clay and may alter soil fabric. These variations might increase or decrease the intrinsic permeability of the soil. A modified temperature-controlled triaxial permeameter cell was used in this study to elevate soil temperature from 20 °C to 80 °C. Moreover, the setup was designed to control the temperature and pressure of the permeant water injected into the specimen. The hydraulic conductivity of both Ottawa sand and Kaolin clay under different confinement stresses (69 kPa to 690 kPa) was measured. Then, intrinsic permeability was calculated considering water property variation with temperature. The results determined that, although hydraulic conductivity increases with temperature for both Ottawa sand and Kaolin clay, the intrinsic permeability of Ottawa sand reduces by 50%, while in Kaolin clay it slightly increases when the temperature rises from 20 °C to 80 °C. Nonetheless, analyzing volumetric changes and void ratio variations for both selected soil types shows a reduction in void ratio with temperature. Reduction in the void ratio can explain the lower intrinsic permeability in Ottawa sand at the elevated temperature, however in Kaolin clay despite the void ratio reduction, another mechanism such as the degeneration of a part of the immobile water within the structure into the mobile water increases intrinsic permeability of Kaolin clay.

## CHAPTER 4

### THERMAL VOLUMETRIC CHANGES

This chapter explains the modification of the setup to accommodate a one-dimension consolidometer in a modified temperature control triaxial cell. The consolidometer in a triaxial cell provides complete and accurate control over the mechanical load (1-D vertical pressure). While the modified temperature-controlled triaxial cell explained in chapter 2 provides full control of soil temperature during thermal consolidation tests, as well as high pressure (cell pressure and back pressure) to saturate the specimen. This chapter presents data from a series of Thermal Consolidation (TC) tests on both normally consolidated and overconsolidated samples with different initial void ratios (equivalent 1-D consolidation pressures) and heating-cooling cycles using this innovative setup. In the end, a semi-analytical equation similar to the conventional consolidation equation using TC results is proposed for NC clays under different conditions (e.g., different thermal loading cycles, and 1-D consolidation pressures). The proposed equation considers thermal loading, the temperature that soil has experienced before, and 1-D consolidation pressure.

#### 4.1. Background

Thermal loading induces pore water pressure in undrained or weakly drained conditions (e.g., confined clay layers) due to the discrepancy between the thermal expansion coefficients of the pore fluid and pore volume Agar et al. (1986); (Bai et al. 2014;

Ghaaowd et al. 2015; Ghabezloo and Sulem 2009); Ghabezloo and Sulem (2010); (Morteza Zeinali and Abdelaziz 2020; Tamizdoust and Ghasemi-Fare 2020; Yao and Zhou 2013). Generation and dissipation of the thermally induced pore water pressure result in thermal volume change which is known as thermal consolidation (Campanella 1965; Ghasemi-Fare and Basu 2018; Houston and Lin 1987). Thermal consolidation can be used as one of the ground improvement techniques for both shallow and deep clay layers. Abuel-Naga et al. (2006b) introduced an innovative thermal technique for ground improvement by increasing the soil temperature and easing the consolidation through prefabricated vertical drains (Thermo-PVD).

The effects of temperature on mechanical properties of different soils have been extensively analyzed in literature (Chen et al. 2017; Ghasemi-Fare and Basu 2019; Joshaghani et al. 2018). In one of the early studies, Lewis (1950) investigated the effects of temperature on soil behavior by measuring the coefficient of compressibility and consolidation of London clay in the temperature range of 5 °C to 15 °C. He reported that the coefficient of compressibility is independent of temperature while the coefficient of consolidation highly changes with temperature. Demars and Charles (1982) observed lower thermal contraction during the heating of OC clays compared to NC clays. Delage et al. (2000) stated that temperature does not significantly affect the consolidation coefficient of Boom clay. In separate studies, Plum and Esrig (1969), Baldi et al. (1988), Sultan et al. (2002), and Abuel-Naga et al. (2007a) reported volumetric expansion instead of contraction for highly overconsolidated clays during the heating phase. Towhata et al. (1993a) heated clay samples (MC-clay which is artificial Kaolin clay and Bentonite) at several steps at the end of primary and secondary stages of consolidation. They observed

that void ratio variation during the thermal test only depends on the soil temperature changes and is independent of the absolute temperature (e.g., equal temperature increments lead to identical void ratio variations). They also expressed that cyclic thermal loading results in a quasi-overconsolidation of MC-clay and can increase the compressive strength and preconsolidation pressure. Changes in preconsolidation stress due to temperature alterations in NC and OC clays during heating and heating-cooling cycles are also reported in other researches (Abuel-Naga et al. 2006a; Abuel-Naga et al. 2007b; Cui et al. 2000; Eriksson 1989; Habibagahi 1977; Hueckel and Borsetto 1990; Laloui and Cekerevac 2003; Sultan et al. 2002; Tidfors and Sällfors 1989; Towhata et al. 1993a).

Several mechanical consolidation tests were performed in the literature at different temperatures. Experimental results showed that temperature variations may also change the preconsolidation pressure (Campanella and Mitchell 1968; Cekerevac and Laloui 2004; Finn 1952; Laloui and Cekerevac 2003; Sultan et al. 2002; Tanaka et al. 1997). In one of the recent studies, Abuel-Naga et al. (2007b) evaluated the thermal volumetric changes of soft Bangkok clay at different stress conditions (100, 200, and 300 kPa) and proposed that thermal loading can alter the mechanical behavior of Bangkok clay. In a separate study, Jarad et al. (2019), and Kaddouri et al. (2019) performed temperature-controlled 1-D consolidation and analyzed the effect of temperature on the consolidation behavior of compacted clays and concluded that temperature slightly alters the compression and swelling indices. While most researchers suggested irreversible void ratio changes for NC clays, a few observed reversible behaviors or a small volumetric expansion during the cooling phase for NC clays (Campanella and Mitchell 1968; Hueckel and Baldi 1990; Hueckel and Pellegrini 1992). Recently a few studies analyzed the effect of thermal loading

and heating rate on the thermal consolidation of different clays (Coccia and McCartney 2016; Favero et al. 2016; Joshaghani and Ghasemi-Fare 2019; Lima et al. 2013; Lotfi et al. 2014; Ma et al. 2017; Ng et al. 2019; Ye et al. 2013b), the thermal volume change of silt under cyclic heating (Vega and McCartney 2015), and the effect of thermal loading on volumetric changes of sandy soil (Liu et al. 2018). However, the volumetric changes of NC and OC clays under variable thermal loading are not fully studied. In addition, to consider thermal consolidation as a viable ground improvement method, the thermal volumetric changes of clays should be carefully evaluated with different initial conditions (e.g., initial confinement pressures). The effects of initial void ratio (initial mean effective stress) on the thermal volume change of clays have not been completely investigated. There are only limited available studies that analyzed thermal consolidation considering different normal vertical pressures (Abuel-Naga et al. 2007a; Towhata et al. 1993a). It should be noted that these studies mostly considered high consolidation pressure (more than 100 kPa) and reported almost no changes in thermal volumetric contraction with changes in vertical pressures (for 1-D thermal consolidation test). Nonetheless, thermal volumetric contraction in NC soil with a higher initial void ratio (or lower initial mean effective stress) might be different from compacted clay samples. Besides, there is still a lack of a simple and practical method to estimate thermal consolidation for field applications. Therefore, fully controlled laboratory thermal consolidation tests with different initial and thermal conditions are needed to comprehensively study the thermal volumetric changes of NC and OC clays.

## 4.2. Experimental Setup

To conduct a thermal consolidation test, we need to accommodate a consolidometer in the modified cell. A consolidometer is similar to an oedometer, with this difference that it is designed to fit in a triaxial setup so that a small amount of strain is monitored and recorded by triaxial equipment rather than conventional dial gauges. *Figure 4-1* shows the employed consolidometer assembled and disassembled. Other advantages of consolidometer are the possibility to apply backpressure which helps to speed up a saturation process, and also measuring the pore pressure at the bottom of the sample which means the possibility to do CRS (constant rate of strain) tests. In conventional consolidation tests, the load is applied in different steps with 24-hour time intervals to let the generated pore pressure dissipate, and volume change at each effective stress is recorded. This process takes several days to be completed. Measuring pore pressure at the bottom of the sample (consequently pore pressure of the sample) allows us to know effective stress at each load and enables us to do a constant rate of strain test in a much shorter time. To do the thermal consolidation test, a consolidometer was placed in the modified cell. As discussed in chapter 2, the triaxial cell provided full control of soil temperature during thermal consolidation tests, as well as confinement pressure and backpressure to saturate the specimen.



(a)



(b)

*Figure 4-1 Different parts of the triaxial insert consolidometer disassembled (a) and assembled*

*(b)*

Figure 4-2 presents the schematic shape of the consolidometer installed on the base plate of the triaxial cell and a complete setup of the test and Figure 4-3 shows the consolidometer and the sample inside it on the base plate. The base plate of the cell shown in Figure 4-3 has four valves. Two valves are connected to the tubes which are connected to the bottom of the sample. Cell pressure is adjusted and controlled by a triaxial cell pump and pore pressure inside the soil is measured using a pressure transducer connected to one of the bottom valves. The other bottom valve is connected to the cell pump during the saturation step and also stays open during the TC test (during the thermal loading) to accelerate pore pressure dissipation.

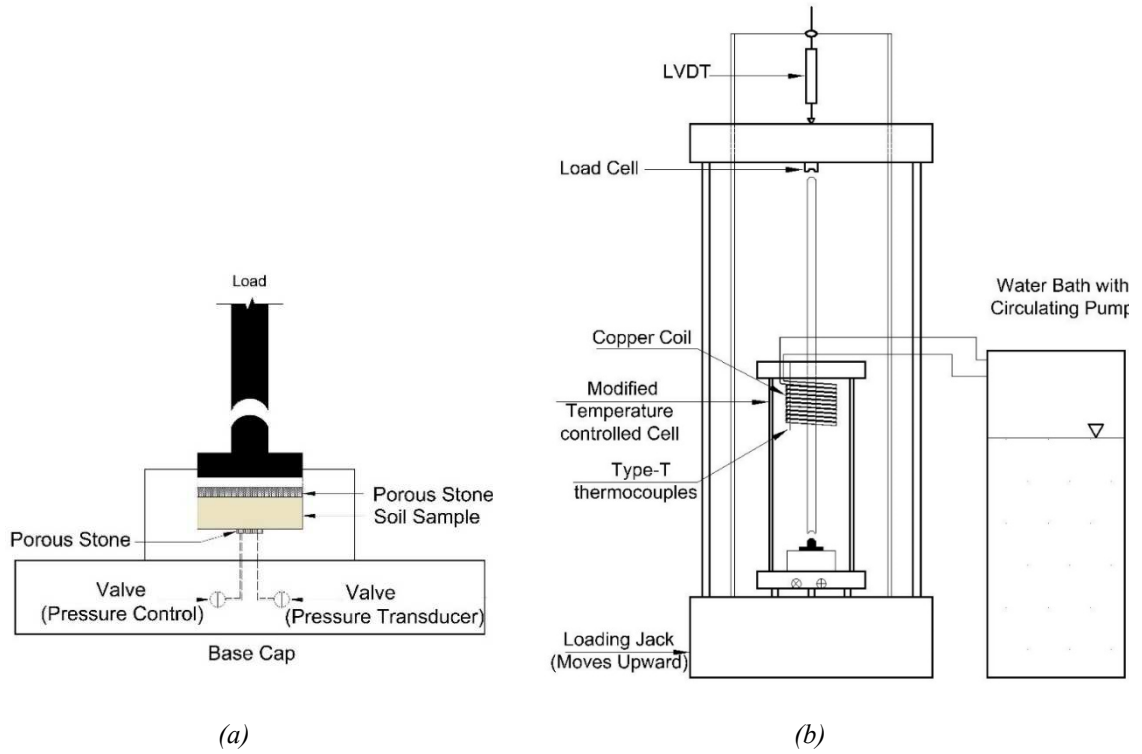


Figure 4-2 (a) Triaxial-insert consolidometer installed on the base cap of a triaxial cell (b) Complete setup of thermal consolidation test including water bath, loading frame, triaxial cell



Figure 4-3 Consolidometer and the sample inside it on the base plate

#### 4.3. Sample Preparation

Commercial Kaolin clay from Columbus Co. was selected for this study. Properties of the Kaolin clay measured in the lab are presented in Table 4-1. To perform the TC tests, samples were prepared by mixing the dried Kaolin clay with de-ionized water equal to the plastic limit. Then this mixture was used to fabricate samples in a rigid stainless-steel consolidation ring (63.5 mm diameter, 25 mm height) using the tamping method. Both bottom and top porous stones and filter papers were saturated in de-aired water for several hours before sample preparation. In the next step, the cell was filled using de-aired water and then both cell and back pressures which were connected to the same pump were gradually increased to 690 kPa to saturate the sample. For each test, to make sure that the sample was saturated, cell pressure was slightly increased and the pressure at the bottom of the sample was monitored while the other valve (used for backpressure) was kept closed. Saturation was confirmed when the Skempton B value higher than 0.95 was achieved. To make an OC Kaolin clay sample, consolidation pressure was reduced to a lower value by giving 24 hours to stabilize before thermal loading was applied to the specimen.

*Table 4-1 Columbus Kaolin Clay Geotechnical Properties*

<b>Specific Gravity</b>	<b>Plasticity Index</b>	<b>Liquid Limit</b>	<b>VCL slope (<math>\lambda</math>)</b>	<b>RCL slope (<math>\kappa</math>)</b>
2.65	21	45 %	0.228	0.08

#### 4.4. Test Procedure and Calibration Test

After sample saturation, 1-D vertical pressure was applied to consolidate the sample at the target pressure for at least 24 hours. The 1-D pressure was maintained constant during the whole thermal consolidation process. It worth mentioning that, there is an uplift

pressure proportional to the cell confining pressure which is obtained in a separate test by increasing the cell pressure and reading reaction at the load cell. For instance, when the cell pressure reached 690 kPa, the uplift force applied to the load cell was measured 79.3 N. Therefore, the amount of effective vertical stress to the specimen (1-D consolidation pressure) for each test was calculated considering the uplift pressure. The noted initial void ratio for each sample was calculated by measuring the dry mass (which is equal to the oven-dried weight of the specimen after the test) and the initial height of the sample after the consolidation step. In the next step, the thermal load was applied by changing the temperature of the cell, while the bottom valve was open and under the same constant pressure in which the cell was maintained, to avoid any pressure gradient in the sample and also to ease the dissipation of the pore pressure caused by the thermal load. During the thermal loading steps, the vertical load and cell pressure were kept constant at the mentioned values. Sample height, cell pressure, and temperature, as well as room temperature, were measured every 2 minutes during different steps of the TC test, to calculate volumetric and consequently void ratio changes. However, before analyzing the results, recorded vertical displacement measurements must carefully be calibrated considering uplift pressure, machine deflection for vertical load, and most importantly, the effect of temperature variations on the whole setup which can cause large deformation (expansion in heating and contraction in cooling) on the different parts of the test setup. To carefully calibrate the LVDT measurements, several calibration tests with the same thermal loading were performed using an aluminum dummy sample with known properties (e.g., coefficient of thermal volume expansion). Figure 4-4 shows the thermal loading and LVDT measurement of the setup for calibrations tests. Cell pressure, vertical load, and cell

temperature variations (thermal loading) were identical to the main tests to minimize the effects of the above-mentioned parameters on the results. The measurements for all TC tests were adjusted based on the calibration test outcome. Please note, almost the same results were obtained for each calibration test which confirmed the repeatability of the test procedure. The thermal diametrical strain of the specimen ring was assumed to be negligible based on the literature (Abuel-Naga et al. 2007a; Romero et al. 2003; Towhata et al. 1993a)

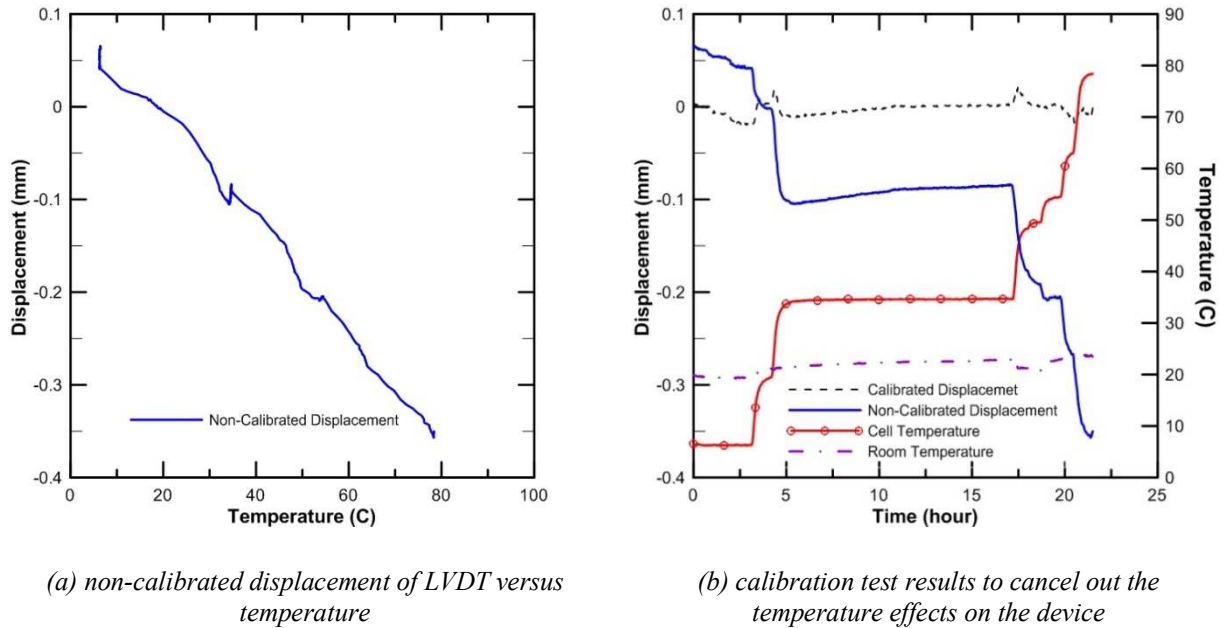


Figure 4-4 Calibration test result

#### 4.5. Test Program

In this research different series of thermal consolidation tests, were performed (Table 4-2). For the first test, while 1-D consolidation pressure was 10 kPa, soil temperature was increased from 25 °C to 50 °C and then from 50 °C to 80 °C and finally in the last step temperature was decreased from 80 °C to 25 °C. In the second series (Tests

2-4 for NC soil), with the same 1-D consolidation pressure (10 kPa), lower thermal loading steps ( $\Delta T=15$  °C) were applied to compare with test 1 with higher  $\Delta T$ . To make sure thermal consolidation was completed, cell temperature was kept constant for 24 hours at each thermal loading step which was more than the thermal loading duration in each step in Test 1. Then several tests were performed with different 1-D consolidation pressures (different initial void ratios). For these tests, soil samples were consolidated under 35 kPa, 50 kPa, 75 kPa, 125 kPa, and 200 kPa (Tests 5 to 9). On each sample, cell temperature was increased from 20 °C to 50 °C, and then to 80 °C followed by cooling down to 20 °C. The experimental results were used to determine the changes in the thermal contraction of NC Kaolin clay with variable 1-D consolidation pressures (from low mean effective stress, or high initial void ratio to higher consolidation pressure) while considering equal temperature changes (under same thermal loading). In the last step of the experiment, thermal volumetric changes of OC Kaolin clay with low and high OCR were evaluated and compared with thermal volume change in NC soil. For this comparison, the same thermal loading was applied for samples with OCRs equal to 6.5 and 1.6 (Tests 10 and 11). Table 4-2 presents the test conditions including 1-D consolidation pressure, OCR values (for OC samples), and initial void ratios as well as thermal loading, for all tests reported in this study.

Table 4-2 Test program and samples properties

Consolidation state	Test number	1-D consolidation pressure (kPa)	Heating-cooling cycles (°C)	Initial void ratio
NC	1	10	25-50-80-20	1.531
	2	10	25-35-50-65-50	1.512
	3	10	25-35-50-65-50-35-35	1.513
	4	10	20-35-50-65-50-35-20-5-20-35-50-65-80-65-50-35-20-3	1.518
	5	35	20-50-80-20	1.265
	6	50	20-50-80-20	1.195
	7	75	20-50-80-20	1.116
	8	125	20-50-80-50-20	1.060
	9	200	20-50-80-20	0.974
OCR= 6.5	10	78 to 12	20-35-50-35-20-5-20-35-50-65-80-65-50-35-20	1.103
OCR=1.6	11	70 to 44	20-35-50-65-50-35-20-5-20-35-50-65-80-68-50-35-20-5	1.008

#### 4.6. Results and Discussion

Changes in void volume and accordingly void ratio were calculated at different steps of the test (saturation, consolidation under mechanical load, and thermal load) using triaxial LVDT measurement. The experiment was repeated for different normally consolidated samples with different 1-D consolidation pressures (1-D effective stress), as well as for samples with various overconsolidation ratios (OCR). To better explain the measurement of the void ratio before, during, and after thermal loading, the different steps of the thermal consolidation test (from A to F) are shown in Figure 4-5. The figure shows the results of a TC test with 1-D consolidation pressure of 125 kPa as an example. Figure 4-5 (a) presents void ratio and temperature changes versus time before, during, and after thermal loading, and Figure 4-5 (b) shows the void ratio against the logarithm of temperature only during the heating-cooling cycle. As can be seen in Figure 4-5 (a), the

test started with saturating the sample. At this step (From point A to B on the graph) void ratio increased because of the expansion of soil during the saturation step. In the second step (from B to C) a vertical load was applied to consolidate the sample (125 kPa consolidation pressure in this test). A significant reduction in void ratio from point B to C in Figure 4-5 (a) happened due to mechanical consolidation. In the third step (heating phase) (from C to E), the cell temperature was increased from 20 °C to 50 °C (point C to D) and then from 50 °C to 80 °C (point D to E). During the heating phase (from C to E) thermal volume reduction was observed. In the cooling phase, the cell temperature was cooled down from 80 °C to 50 °C (from E to F) and then from 50 °C to 20 °C (from F to G). Experimental results during heating-cooling phases (from, C to G) show irreversible thermal contraction for NC Kaolin clay. The void ratio at different steps of the test, from the beginning of the TC test to the end of the cooling phase (From 20 °C up to 80 °C and down to 20 °C) were measured at points C to G. Figure 4-5 (b) shows void ratio variations versus temperature in the logarithmic scale (thermal consolidation curve) during the heating and cooling phases. Please note, initial void ratios reported in Table 4-2 in the test program which were also used to calculate the volumetric strain during the thermal loading, were measured right before the thermal load was started (point C).

As mentioned earlier, 9 NC samples, 1 sample with low OCR (OCR=1.6), and one with high OCR (OCR=6.5) were tested under thermal load. To explore the effect of consolidation pressure, on thermal volume change in Kaolin clay, several tests were conducted under different 1-D consolidation pressure (10kPa, 35, kPa, 50 kPa, 75 kPa, 125 kPa, 200 kPa). Plotting the void ratio against the logarithm of temperature results in a similar graph to the conventional mechanical consolidation and therefore a similar approach

is applied to propose a new relation to predicting the thermal contraction (thermal consolidation) of NC Kaolin clay.

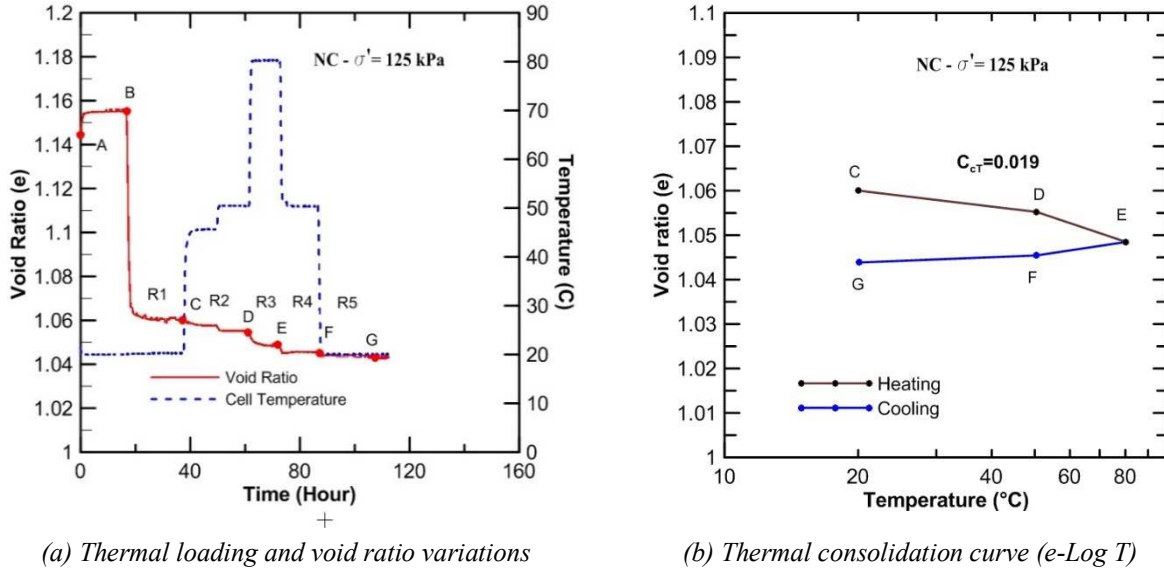


Figure 4-5 Thermal loading and void ratio variations for NC Kaolin clay

Figure 4-6 shows thermal loading steps and void ratio variations with temperature for Tests 1 to 4 (NC clay considering different thermal steps with identical 1-D consolidation pressure). As is expected, increasing the temperature results in a thermal contraction of NC clay.

Figure 4-7 presents void ratio variations (thermal contraction) observed in Tests 1 to 4 against the logarithm of temperature. Comparisons of void ratio variations shown in Figure 4-6 (a) to Figure 4-6 (d) and Figure 4-7 (a) to Figure 4-7 (d) confirm that the thermal contraction (thermal compression slope in Figure 4-7) is independent of the thermal loading steps (rate of heating). In addition, results determine irreversible volume change in NC clay.

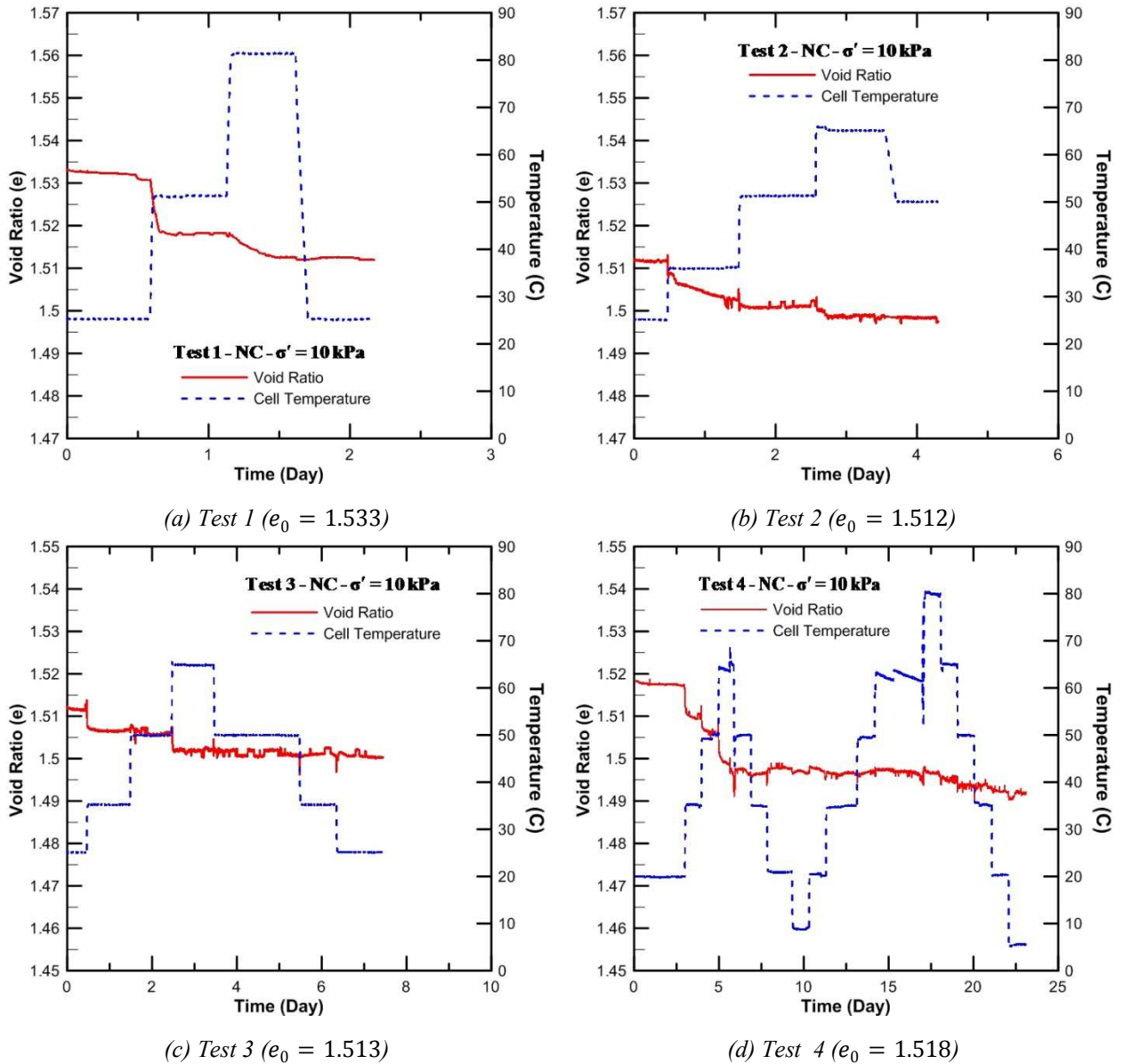
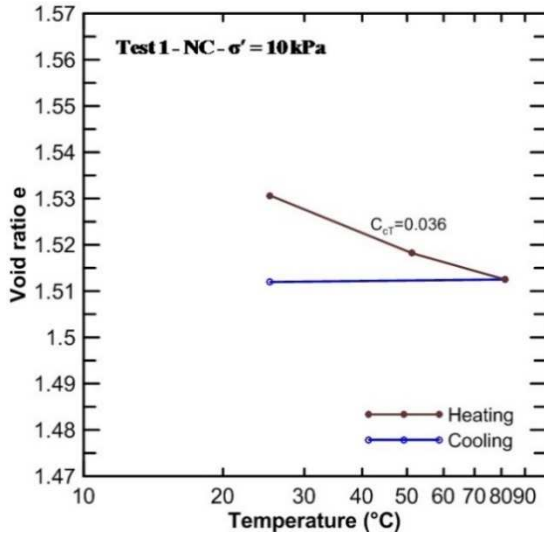


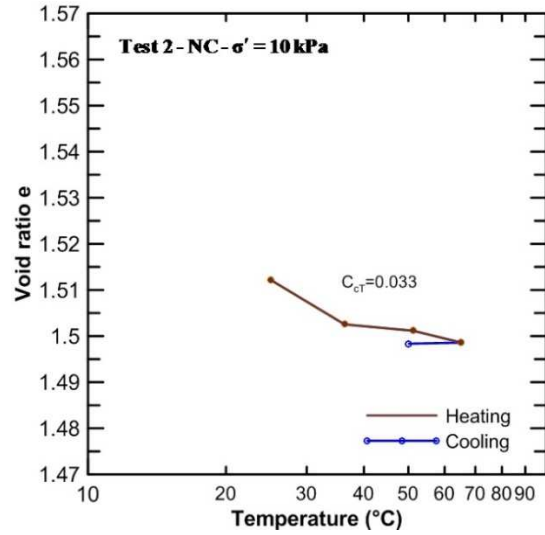
Figure 4-6 Thermal loading and void ratio variations for NC Kaolin clay (10 kPa)

Presented TC results in Figure 4-6 (d) and Figure 4-7 (d) demonstrate that heating NC clay can increase the preconsolidation pressure. As can be seen in Figure 4-7 (d), changes in void ratio during reheating the soil specimen from 20 °C to 65°C after one complete heating and cooling cycle (from 20 °C to 65 °C, and then back to 20 °C) follows

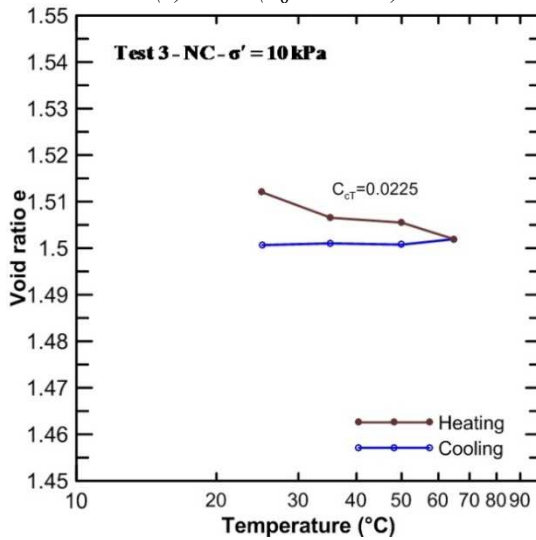
the cooling line. However, after reaching 65 °C - which is the maximum temperature soil has experienced before - the thermal consolidation slope from 65 °C to 80 °C follows back the thermal consolidation curve from its initial heating phase.



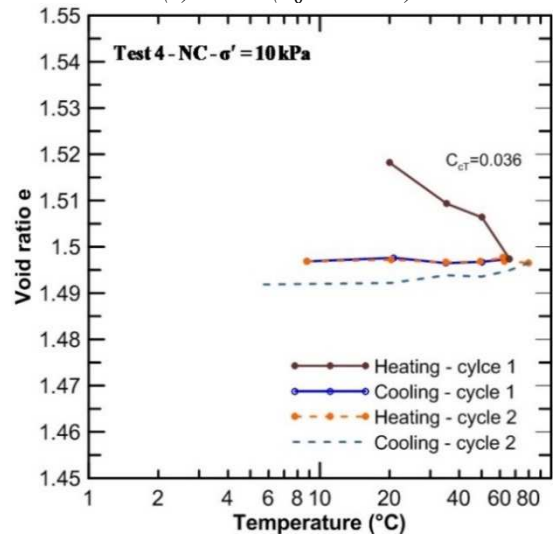
(a) Test 1 ( $e_0 = 1.533$ )



(b) Test 2 ( $e_0 = 1.512$ )



(c) Test 3 ( $e_0 = 1.513$ )



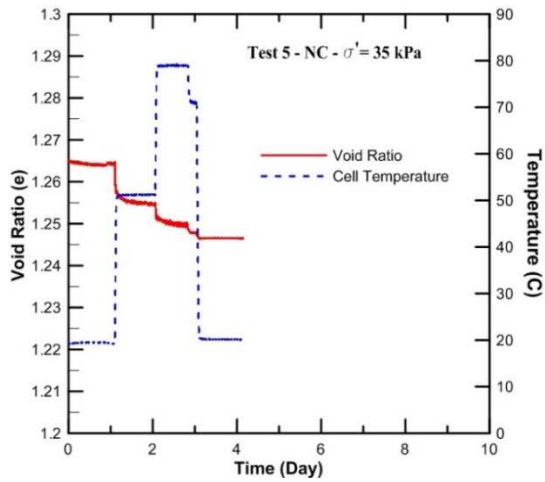
(d) Test 4 ( $e_0 = 1.518$ )

Figure 4-7 Thermal consolidations of NC Kaolin clay under different thermal loading (10 kPa)

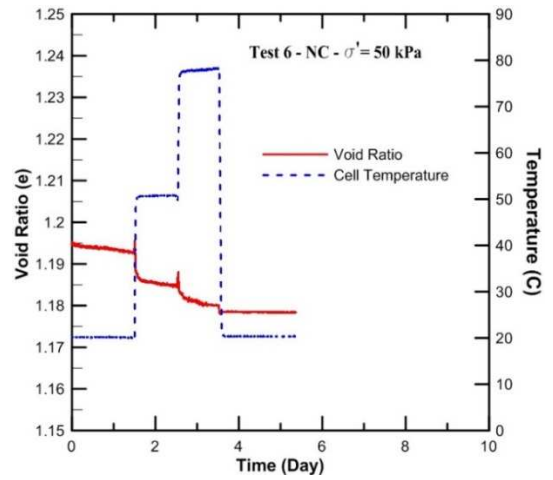
The slope of the void ratio reduction in the logarithmic temperature scale is introduced as thermal compression index ( $C_{cr}$ ). The calculated thermal compression index

for Test 1 to 4 is presented in Figure 4-7 (a) to Figure 4-7 (d). It should be also noted that the presented results in El Tawati (2010) also confirm a linear relation between the void ratio and the logarithm of temperature during the thermal consolidation test. The average  $C_{cT}$  observed in these normally consolidated samples with consolidation pressure of 10 kPa is 0.032. Please note, Tests 1 to 4 were conducted on NC clay with a high initial void ratio (low 1-D consolidation pressure). Therefore, to explore the effect of the initial void ratio on thermal contraction, more TC tests were performed with lower initial void ratios (higher 1-D consolidation pressures).

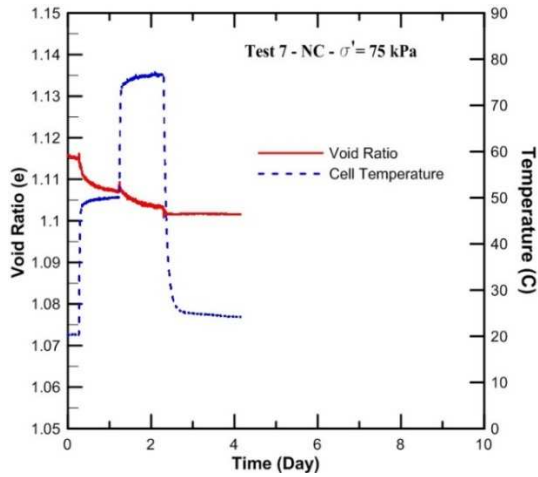
In the next series of TC tests, (Test 5 through Test 9) the effects of 1-D consolidation pressure on thermal volume change and thermal compression index were investigated. Hence, several NC samples which were consolidated under 35 kPa, 50 kPa, 75 kPa, 125 kPa, and 200 kPa vertical pressures were subjected to one heating-cooling cycle while changes in void ratios were measured. The experimental results presented in this study show lower thermal contraction for samples with a lower initial void ratio (higher 1-D consolidation pressure). Figure 4-8 presents the thermal loading steps and void ratio reduction with temperature for Tests 5 to 9. Similar to Test 1 to 4, irreversible volumetric contractions were observed for all the cases.



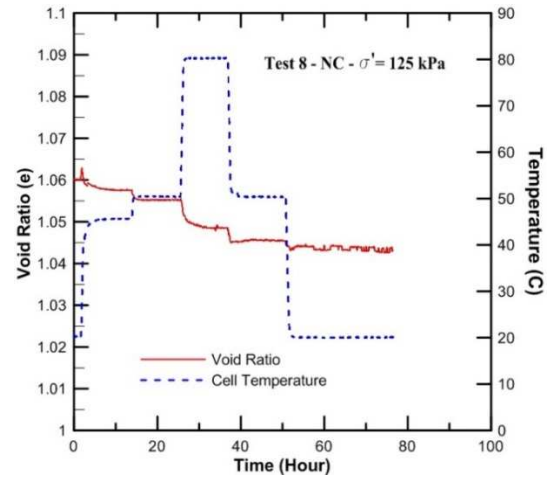
(a) Test 5, NC sample,  $e_0 = 1.265$



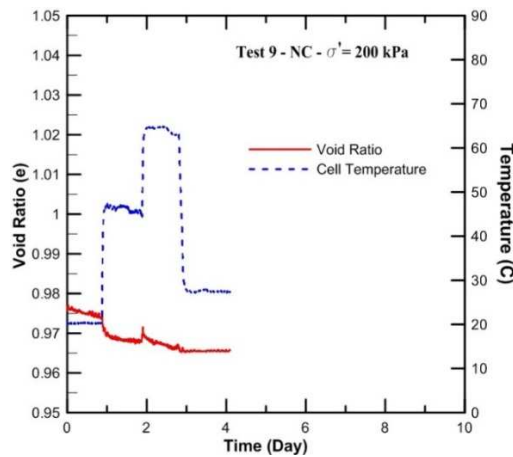
(b) Test 6, NC sample,  $e_0 = 1.195$



(c) Test 7, NC sample,  $e_0 = 1.116$

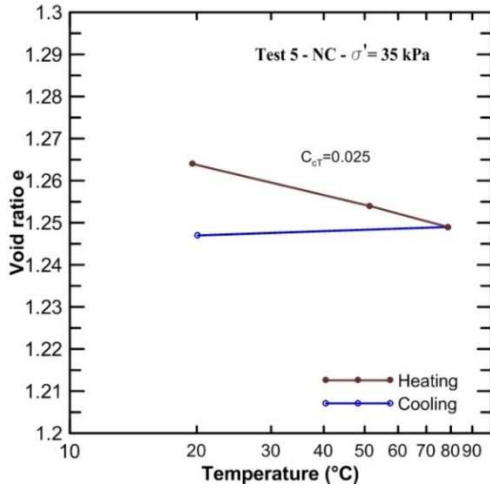


(d) Test 8, NC sample,  $e_0 = 1.060$

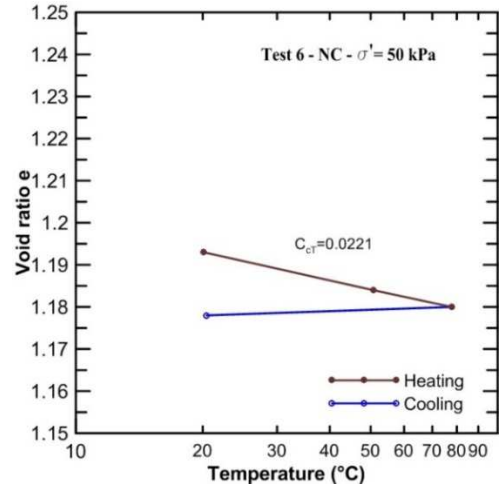


(e) Test 9, NC sample,  $e_0 = 0.974$

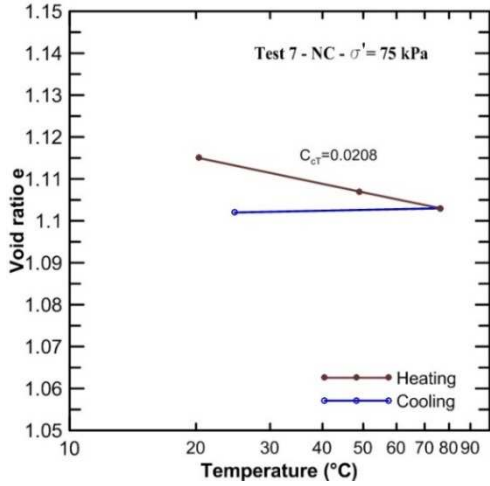
Figure 4-8 Thermal loading and void ratio variations for NC Kaolin clay



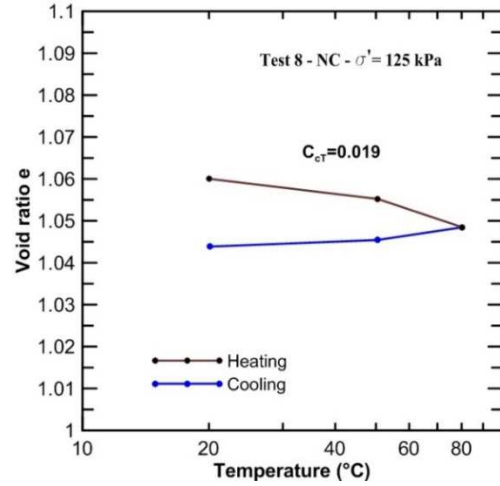
(a) Test 5, NC sample,  $e_0 = 1.265$



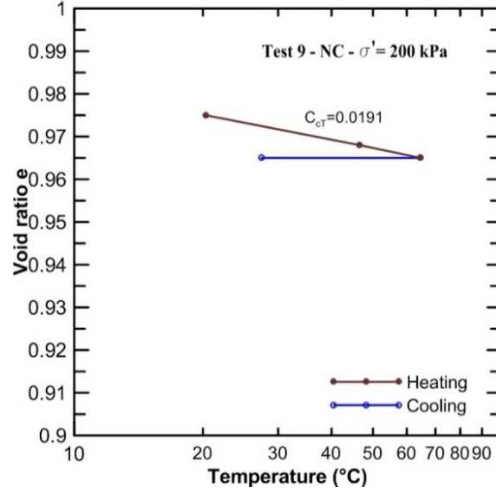
(b) Test 6, NC sample,  $e_0 = 1.195$



(c) Test 7, NC sample,  $e_0 = 1.116$



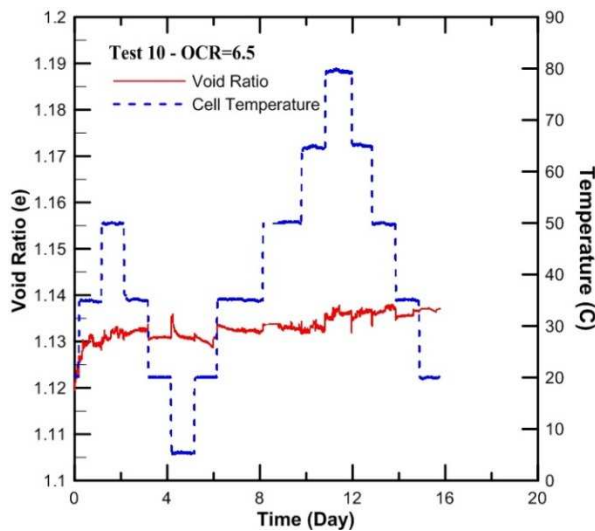
(d) Test 8, NC sample,  $e_0 = 1.060$



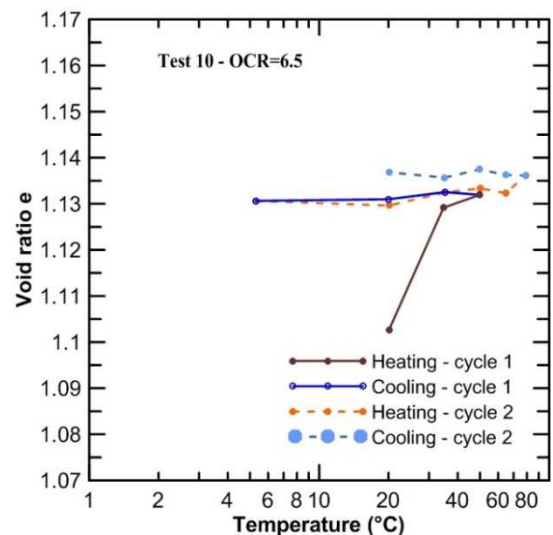
(e) Test 9, NC sample,  $e_0 = 0.974$

Figure 4-9 Thermal consolidations of NC Kaolin clay with different confinement stresses

In the next step, thermal volumetric changes of OC clay with different OCR values were explored. To prepare a test with OCR=6.5, the soil specimen was consolidated under a pressure equal to 78 kPa for 24 hours and then was unloaded to 12 kPa. The normal load (12 kPa) was kept constant for at least 24 hours. The same method was used (increasing the pressure up to 70 kPa and then unloading the pressure to 44 kPa) to have a specimen with OCR=1.6. The same thermal loading was applied for the two samples at different OCR values. Figure 4-10 shows the results for the sample with OCR=6.5. It is interesting to note that volumetric expansion was observed for the highly overconsolidated sample (OCR=6.5) with temperature increments. As can be seen in Figure 4-10, the increase in the void ratio for the first heating cycle is irreversible. However, during the second heating-cooling cycle, the expansion starts at 50 °C (from 50 °C to 80 °C) in which soil had not experienced before.



(a) Void ratio and Temperature versus Time



(b) Void ratio against the logarithm of temperature

Figure 4-10 Volumetric changes of OC sample with OCR=6.5, and  $e_0 = 1.120$  (Test 10)

Comparing observations in NC and highly overconsolidated samples, determine that there should be a threshold in which thermal volume change is insignificant. Therefore, for the next test (Test 6), a sample with a low OCR value was selected. Figure 4-11 (a) and Figure 4-11 (b) present void ratio variation with both time and temperature for the slightly overconsolidated sample (OCR=1.6). As it is expected, no significant volume change with temperature is observed for the sample with OCR =1.6.

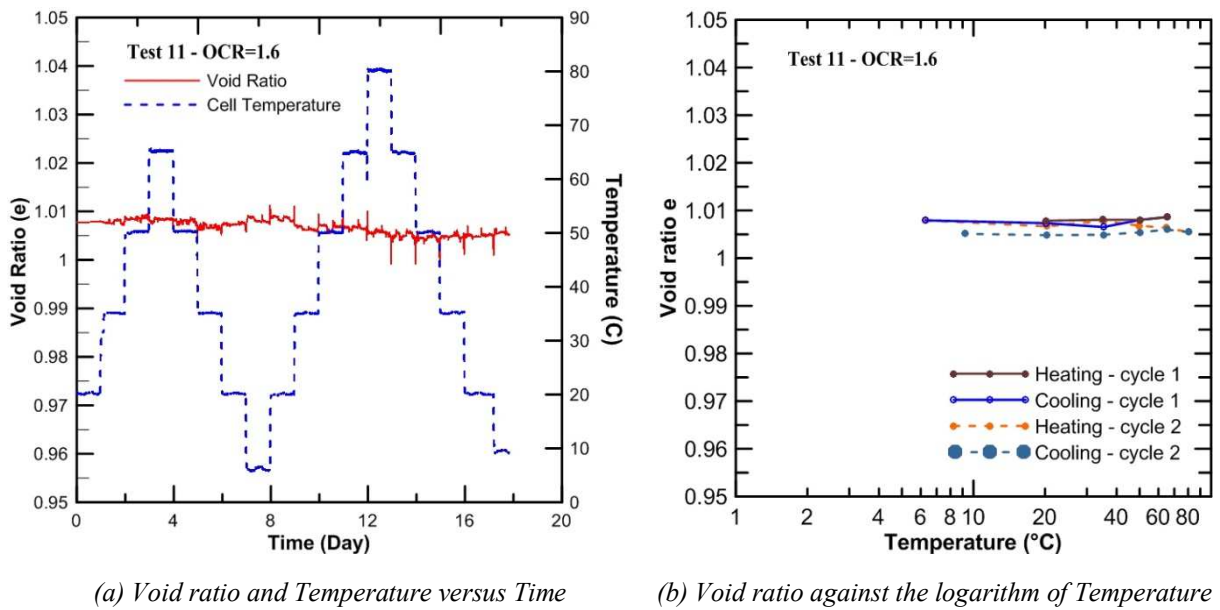


Figure 4-11 Volumetric changes of OC sample with OCR=1.6, and  $e_0 = 1.008$  (Test 11)

Cyclic thermal loadings were applied to NC and OC clays with different consolidation ratios (OCR=1.6 and 6.5). Irreversible volumetric changes during cyclic thermal loading are observed for NC and highly overconsolidated Kaolin clay. Figure 4-12 presents the volumetric strain for NC and OC samples with temperature. It shows that for NC soil, thermal load causes consolidation (about 1% volumetric strain) and for overconsolidated clay with high OCR, an increase in soil temperature results in the

volumetric expansion (about 1%), and no significant void ratio change is observed for the slightly overconsolidated sample (OCR=1.6). The results are in good agreement with previous studies (Cui and Tang 2013; Hamidi et al. 2017). Abuel-Naga et al. (2006a) showed negligible thermal volume strain for samples with OCR between 2 and 4. In another study, Baldi et al. (1988) measured thermal volume change of Pontia Clay reported thermal expansion for highly overconsolidated clay (OCR=12.5), and concluded that thermal volumetric strain is almost negligible for clays with OCR values in the range of 1.4 to 2.5. Figure 4-13 shows the results of the measured thermal volumetric expansion in MC clay by Abuel-Naga et al. (2007a).

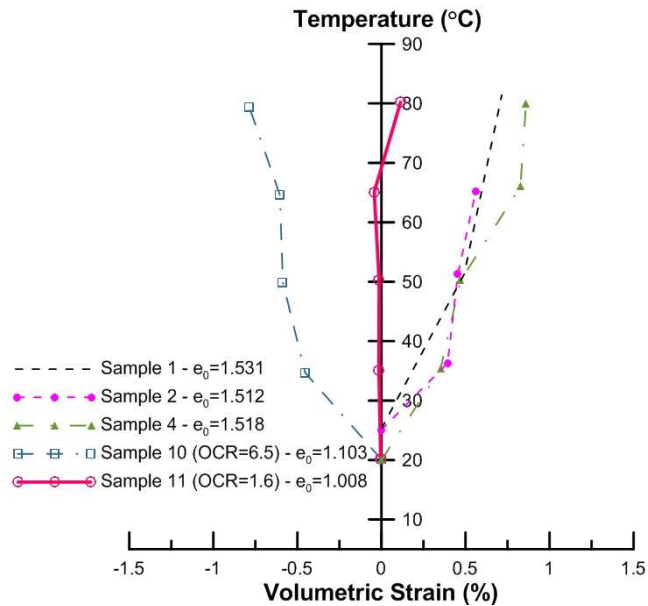


Figure 4-12 Volumetric strain for Thermal consolidation tests

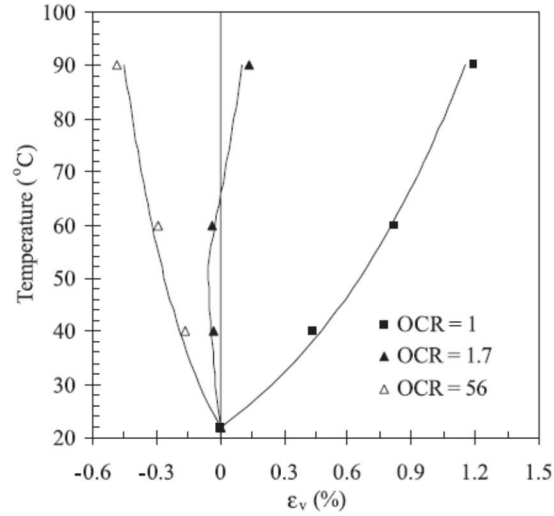


Figure 4-13 Measured thermal volumetric strains in MC clay (Abuel-Naga et al. (2007a))

#### 4.7. Semi Experimental-Analytical Relation

The thermal compression indices obtained from all the NC samples are considered to propose a simple relation that can be used to predict thermal consolidation. During mechanical consolidation, void ratio reduction for NC soil can be calculated using Equation 4-1.

$$\Delta e = C_c \log \left( \frac{\sigma_0 + \Delta \sigma}{\sigma_c} \right) \quad \text{Equation 4-1}$$

Where  $\Delta e$  is the change in void ratio,  $C_c$  is compression index,  $\sigma_0$  is initial effective stress,  $\sigma_c$  is 1-D consolidation pressure, and  $\Delta \sigma$  is stress increments.

A Constant Rate of Strain test was performed on the studied Kaolin clay to measure the compression index ( $C_c$ ) and recompression index ( $C_s$ ). Compression and recompression

indices obtained from the test were 0.228, and 0.08, respectively. Since similar behavior is observed for void ratio changes with temperature in the logarithmic scale; an equation similar to Equation 4-1 is proposed to predict the thermal consolidation of NC Kaolin clay. Equation 4-2 presents the thermal consolidation equation only for the thermal contraction that occurs in NC clay. Compression index ( $C_c$ ) is substituted with thermal compression index, ( $C_{cT}$ ) which may vary for different clays, and effective stress (mechanical loading) is substituted by the temperature gradient (thermal loading).

$$\Delta e = C_{cT} \log \left( \frac{T_0 + \Delta T}{T_c} \right) \quad \text{Equation 4-2}$$

Where  $e$  is the void ratio,  $C_{cT}$  is the thermal compression index,  $T_0$  is the initial temperature,  $T_c$  is the maximum temperature that soil has experienced before, and  $\Delta T$  is a temperature increment. Please note, this equation can only be used for NC clay which shows thermal contraction.

$C_{cT}$  for Kaolin clay is considered as the average of the thermal compression indices measured in Tests 1 to 4 with 1-D consolidation pressure of 10 kPa ( $C_{cT} = 0.032$ ). The thermal compression index at the so-called reference pressure in this study for Kaolin clay approximately equals to 15% of the mechanical compression index. The presented experimental results demonstrate that thermal volume change (thermal compression index) depends on the initial void ratio or initial state of the soil (e.g., 1-D consolidation pressure) when the 1-D consolidation pressure is less than 125 kPa. However, the thermal compression index (thermal volumetric strain) merges to a constant value for lower initial

void ratios (or higher 1-D consolidation pressures). It should be mentioned that Abuel-Naga et al. (2006a) conducted several thermal consolidation tests and concluded that the void ratio change with temperature is independent of the applied stress (preconsolidation pressure) when the stress level is more than 100 kPa (Abuel-Naga et al. 2006a). This study is a complementary analysis to the previous researches conducted by Abuel-Naga et al. (2006a) which demonstrates that void ratio change with temperature (thermal volume change) depends on the preconsolidation pressure for very low-stress level (e.g., when the 1-D consolidation pressure is less than 125 kPa). According to the presented results, it is expected that soft clays with lower confinement show higher thermal volume change.

Thermal compression indices measured in all NC tests with different 1-D consolidation pressures are shown in Figure 4-14. The results present a linear reduction in thermal compression index (void ratio reduction) with confinement in the logarithmic scale while 1-D consolidation pressure is less than 125 kPa.

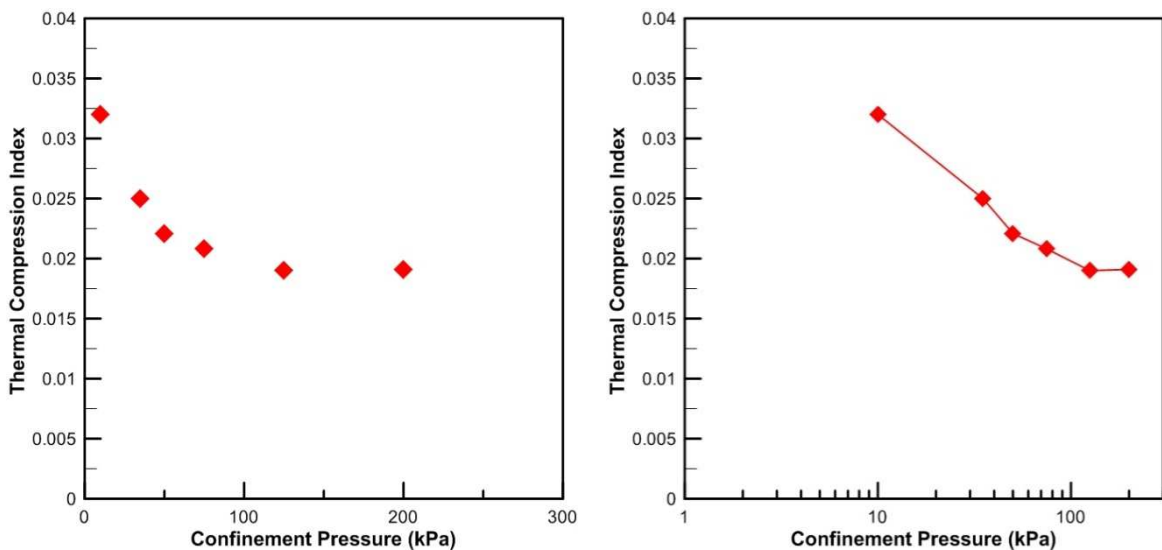


Figure 4-14 Changes in thermal compression index for different sample 1-D consolidation pressures

However, instead of changing the thermal compression index with the confinement stress, a new parameter (1-D consolidation pressure coefficient:  $\lambda_c$ ) is introduced to consider the effect of sample consolidation pressure in the thermal consolidation equation. The updated thermal consolidation equation can be expressed as:

$$\begin{cases} \Delta e = C_{cT} \lambda_c \log\left(\frac{T_0 + \Delta T}{T_c}\right) & T_0 + \Delta T > T_c \\ \Delta e = 0 & T_0 + \Delta T < T_c \end{cases} \quad \text{Equation 4-3}$$

The consolidation pressure coefficient,  $\lambda_c$  can be predicted using TC tests for different samples with different 1-D consolidation pressures. To calculate the consolidation pressure coefficient  $\lambda_c$ , the 1-D consolidation pressure of 10 kPa is considered as a reference pressure and the changes in  $\lambda_c$  are calculated using void ratio reduction and considering identical thermal compression index,  $C_{cT}$ , for all TC tests on NC clay. Table 4-3 presents the calculations for the 1-D consolidation pressure coefficient,  $\lambda_c$  for the different conditions. Figure 4-15 presents the variations of  $\lambda_c$  with 1-D consolidation pressure and accordingly Equation 4-4 is presented to consider the effect of changes in 1-D consolidation pressure (initial mean effective stress) on thermal consolidation.

$$\begin{cases} \lambda_c = -0.149 \ln(\sigma_m) + 1.29 & \sigma_m < 125 \text{ kPa} \\ \lambda_c = 0.59 & \sigma_m \geq 125 \text{ kPa} \end{cases} \quad \text{Equation 4-4}$$

Table 4-3 Calculated confinement coefficients using experimental observations

Test No	Test 1-D consolidation pressure (kPa)	$C_{cT}\lambda_c$	$\lambda_c$
1-4	10	0.0320	1.000
5	35	0.0250	0.781
6	50	0.0221	0.691
7	75	0.0208	0.650
8	125	0.0190	0.594
9	200	0.0191	0.597

Where  $\sigma_m$  is the initial mean effective stress (1-D consolidation pressure) in which soil is subjected to thermal loading.

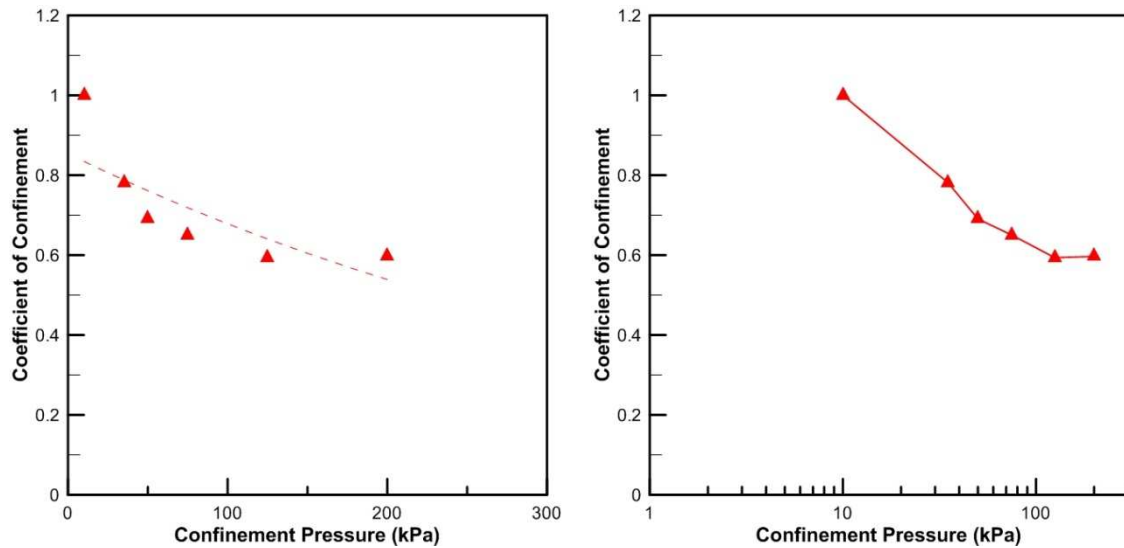


Figure 4-15 Changes in the coefficient of confinement for different 1-D consolidation pressure

Although, it is expected that the same equation with different thermal compression index at reference confinement to be replaced for different clays, further research is needed

to investigate the accuracy of the presented approach to estimate thermal consolidation in other clays.

#### 4.8. Summary

Thermal loading results in thermal volumetric contraction in normally consolidated (NC) clays while it may induce thermal volumetric expansion in overconsolidated (OC) clays. In this chapter thermal volumetric changes of Kaolin clay are carefully evaluated through 1-D Thermal Consolidation (TC) tests for both normally consolidated and overconsolidated samples. Void ratio is measured at different temperatures during heating/cooling cycles and thermal volumetric changes are calculated. Thermal consolidation curve which shows the void ratio against the logarithm of temperature is presented and the coefficient of “thermal compression index” is introduced, which is similar to the compression index in conventional mechanical consolidation. Several TC tests are conducted on samples with different initial void ratios that were consolidated under different 1D normal effective stresses. Results determine that thermal compression index (thermal volume change) depends on the initial void ratio (initial mean effective stress) when the 1-D consolidation pressure is less than 125 kPa. NC soils with a higher initial void ratio (e.g., when consolidated under lower 1-D consolidation pressure) show higher thermal volume change. However, when the 1-D consolidation pressure increases to more than 125 kPa, the thermal compression index is almost constant regardless of the consolidation pressure. Besides, experimental results show thermal volumetric expansion for highly overconsolidated clays (e.g. OCR=6.5). In the end, a new relation similar to

conventional mechanical consolidation is introduced based on the experimental measurement to predict the thermal consolidation for NC clays.

## CHAPTER 5

### HYDRAULIC CONDUCTIVITY A TIME DEPENDENT PARAMETER- A NEW PERSPECTIVE

In this Chapter, the changes of hydraulic conductivity and intrinsic permeability during the thermal loading are analyzed. As discussed in Chapter 4, the thermal consolidation (thermal volume reduction) is a time-dependent process, and therefore it is expected that the hydraulic conductivity and intrinsic permeability of the Kaolin clay have a continuous change until the volumetric change is completed. Thermal volume change or thermal consolidation takes almost 24 hours to get completed based on the sample size used in this research. It is hypothesized that the intrinsic permeability of Kaolin clay not only changes with temperature but also alters at different time steps until the thermal consolidation completely occurs at the desired temperature. Therefore hydraulic conductivity tests were performed and measurements have been recorded at different times after the temperature inside the sample stabilizes (which is 60 minutes after temperature change starts<sup>1</sup>). Based on the conclusions from chapter 3 and chapter 4, it is expected that if hydraulic conductivity measurement is repeated at a specific temperature with a long enough time interval, results would show a reduction trend, approaching a specific value at each temperature. To onfirm

---

<sup>1</sup> Refer to chapter 2

this hypothesis, a series of hydraulic conductivity (H.C) tests were conducted at different temperatures on Kaolin clay specimens using the modified cell.

### 5.1. Sample Preparation

Each sample was placed on the acrylic bottom cap and then a latex membrane was placed around it. Then, the cell was filled with water followed by increasing to the related confining pressure. In the next step, the sample was saturated under 138 kPa pressure at the top and bottom of the sample for 24 hours. After verifying the sample saturation by measuring the Skempton's coefficient  $B$ , the test was started by applying a hydraulic gradient of 138 ( $i=138$ ). The first series of tests are conducted under 345 kPa confinement pressure, on a sample of Kaolin clay with 101.6 mm diameter and 25.4 mm height. The second and third series are, respectively, conducted under 448 kPa and 690 kPa confinement pressures with similar sizes of samples. Figure 0-1 shows one of the samples on the base plate of the cell, before placing the chamber.



*Figure 0-1 Kalin sample placed on the base plate and covered by a latex membrane*

## 5.2. Test procedure

The test setup and procedure were similar to Chapter 3 and similarly, fluid movement through the sample was measured with the digitally controlled flow pump during the test and between every two tests to track void volume changes. H.C was measured at room temperature and then, the sample temperature increased to 50 °C. At this temperature, H.C was measured after 1 hour, 12 hours, 24 hours, and 48 hours. As mentioned earlier, the volume of the water passed through the sample was also measured between tests to calculate the void ratio according to Equation 3-1 in chapter 3. The same process was repeated at 80 °C. Figure 0-2 shows different parts of the test setup that has been used for hydraulic conductivity tests.

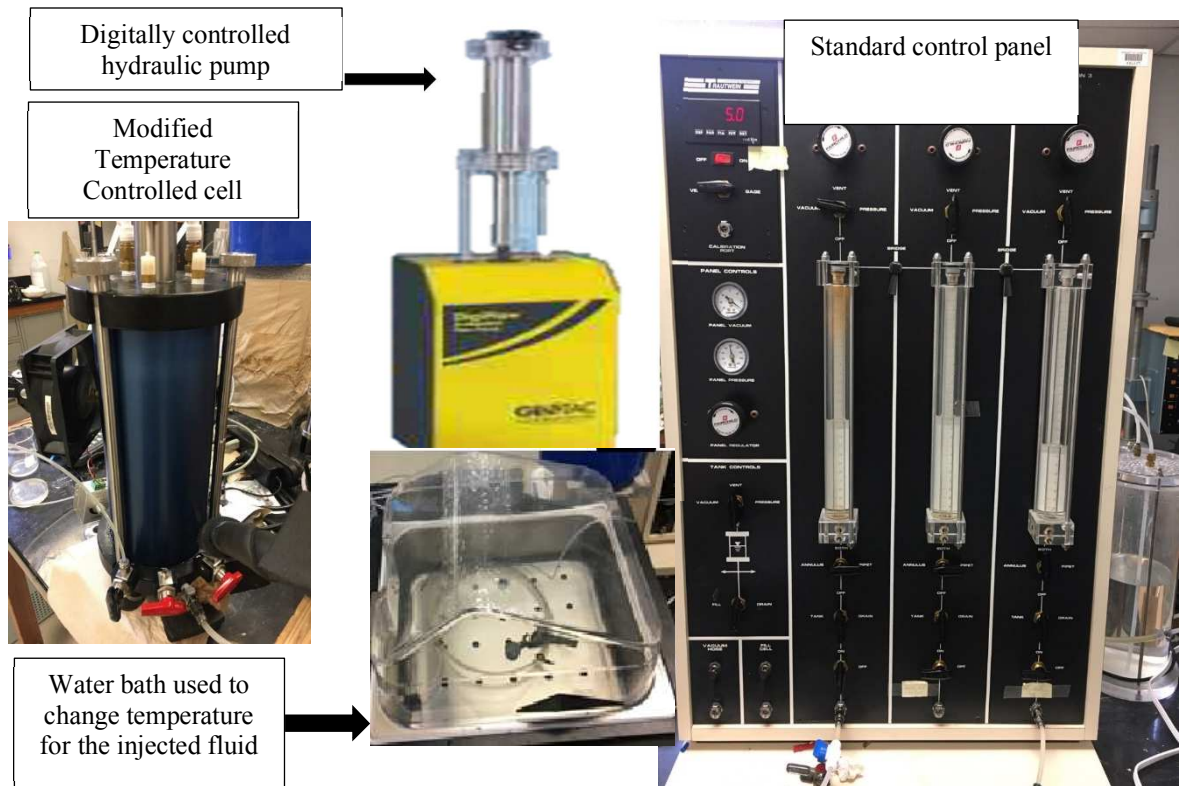


*Figure 0-2 View of the setup test for the hydraulic conductivity test*

### 5.3. Test Results

#### 5.3.1. Hydraulic Conductivity

Figure 0-3 presents the hydraulic conductivity values of the test with 345 kPa confining pressure. As it is shown, there is a considerable increase in the values of H.C when temperature increases from 20 °C to 50 °C and then 50 °C to 80 °C. As discussed in Chapter 3, the reason is because of the reduction in the dynamic viscosity of water in higher temperatures that makes water moves through flow channels easier. The symbols at 50 °C and 80 °C represent several measurements at different time intervals from the start of heating. As it was mentioned earlier, and based on the conclusions from Chapter 3 and Chapter 4, measured H.C values show a reduction when we repeat measurement after 12 hours, 24 hours, and 48 hours. The same behavior is shown for the test at different confining pressures (Figure 0-4). As presented earlier in Chapter 4, the reduction of H.C. in time is due to the thermal consolidation in the soil (thermal volume reduction) at higher temperatures which is a slow process. However, the effect of time on H.C. values was not attainable from tests and the results in Chapter 4 since test repeating was performed at a short time interval and it changes with time was neglected. It is interesting to note that by comparing Figure 0-3 and Figure 0-4 it can be concluded that the reduction in permeability of Kaolin clay with thermal loading (at T= 50 °C and 80 °C) is lower when the confinement increases. As was shown in Chapter 4, the thermal consolidation is dependent on the confining pressure (less consolidation happens in samples with higher confinements) ), therefore it is expected that lower thermal void ratio reduction (thermal volume reduction) results in fewer changes in H.C. and consequently on intrinsic permeability of Kaolin clay

during the thermal consolidation process. It is interesting to report that the measurement in this chapter also confirms the hypothesis and equation provided in Chapter 4 for the effect of confinement on thermal volume reduction. The reduction in the H.C values in time is more limited in a test with higher confining pressure (i.e. in Figure 0-4 is less than in Figure 0-3).

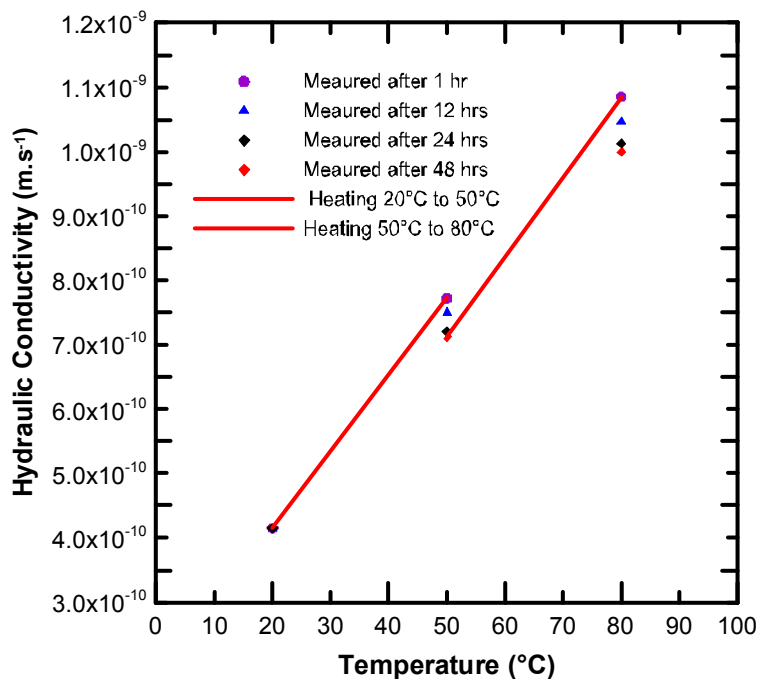


Figure 0-3 Hydraulic Conductivity versus Temp at different measurement time-345 kPa Confining Pressure

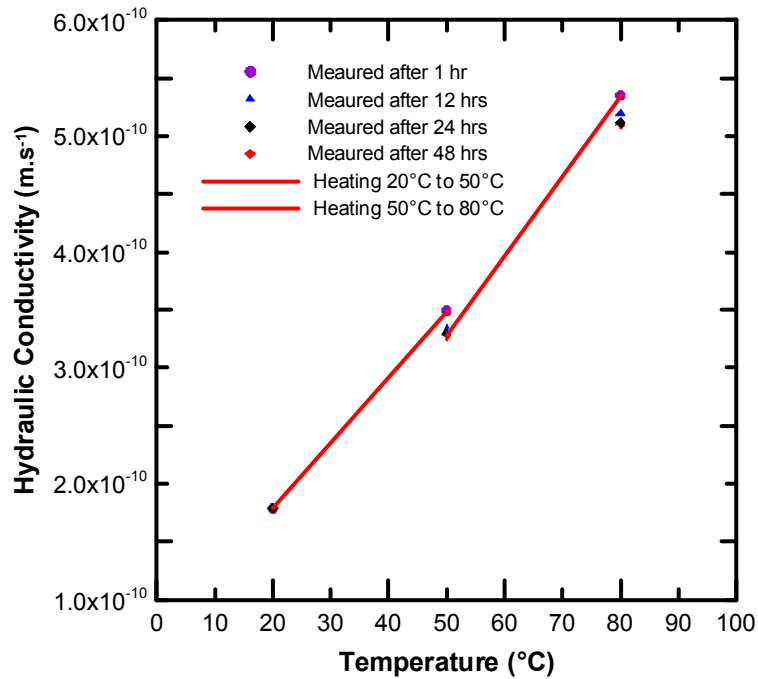


Figure 0-4 Hydraulic Conductivity versus Temp at different measurement time, 690 kPa Confining Pressure

### 5.3.2. Intrinsic Permeability

Figure 0-5 presents the changes of intrinsic permeability of Kaolin clay under 345 kPa confining pressure with thermal loading. For intrinsic permeability, since the effect of water viscosity changes is excluded from the calculations, the results directly reflect the changes in the soil fabric. When the soil temperature increases, it shows an increase in the values of intrinsic permeability. This early behavior can be related to the soil particle rearrangement, which causes a release of water, and also as discussed in Chapter 3, due to the degenerations of double-layer water into bulk water and increasing the number of flow channels. However, it is interesting to note that after the temperature stabilizes at the desired temperature (e.g.,  $T = 50\text{ }^{\circ}\text{C}$  or  $T = 80\text{ }^{\circ}\text{C}$ ), the intrinsic permeability starts to drop due to void ratio reduction. During this step, thermal volume reduction and the initial

changes in some flow channels are canceling out their effects. As it can be seen in Figure 0-5 and Figure 0-6, the counter effect of volume reduction on soil intrinsic permeability variations gets stronger in time which is because the thermal consolidation is happening over time. Therefore, we observe a reduction in intrinsic permeability over time.

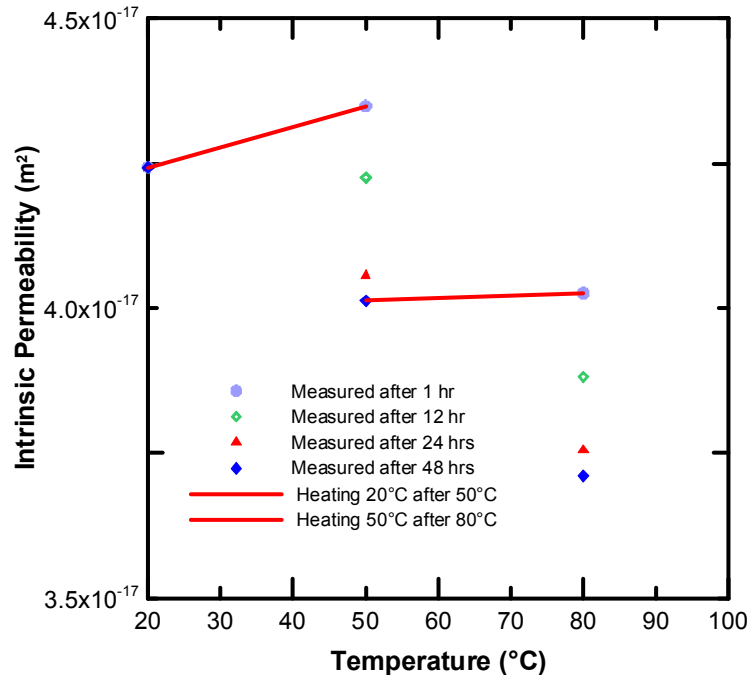


Figure 0-5 Intrinsic Permeability versus Temp. at different measurement time, 345 kPa Confining Pressure

Similar to the confining pressure effect that was observed in H.C tests, intrinsic permeability values reduction over time is also showing a reduction trend by confining pressure increase. In another word, the soil intrinsic permeability reduction is lower for higher confinement pressures. Figure 0-6 (690 kPa) shows limited variations in intrinsic permeability over time compared to Figure 0-5 (345 kPa).

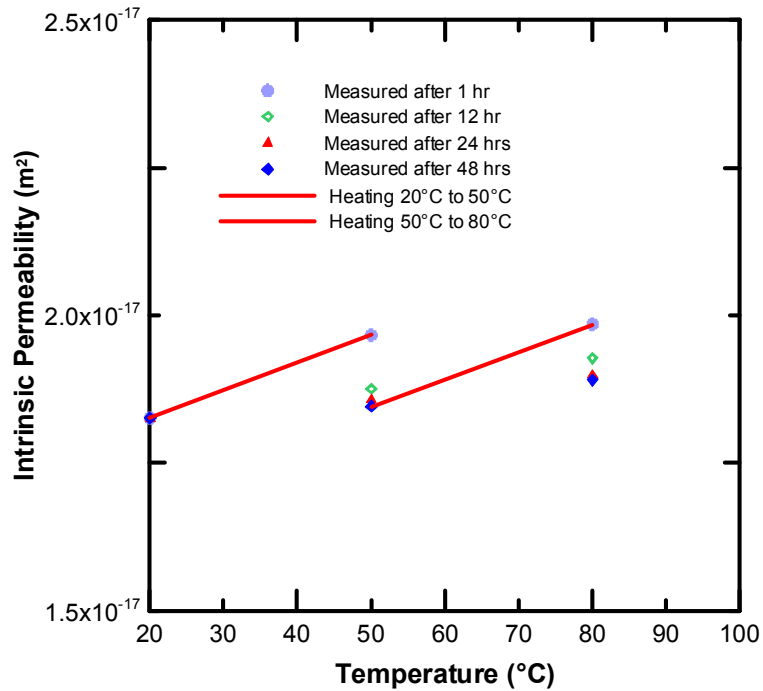


Figure 0-6 Intrinsic Permeability versus Temp at different measurement time, 690 kPa Confining Pressure

Figure 0-7 and Figure 0-8 present the changes in hydraulic conductivity measurements versus time at 50 °C and 80 °C, respectively. Similarly, the intrinsic permeability values versus time of measurement are presented in Figure 0-9 and Figure 0-10. It is obvious that when the measurements are made after a longer period, both hydraulic conductivity and intrinsic permeability are reduced. The figures also show the H.C. and soil intrinsic permeability merge to a constant value after a thermal consolidation has fully occurred.

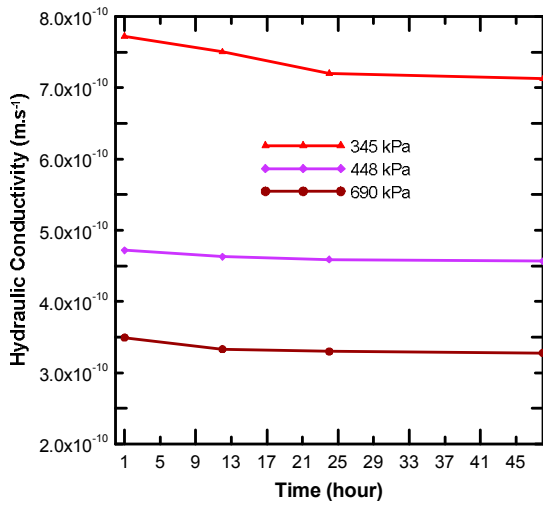


Figure 0-7 Hydraulic Conductivity changes versus measurement time, heating at 50°C, different Confining Pressure

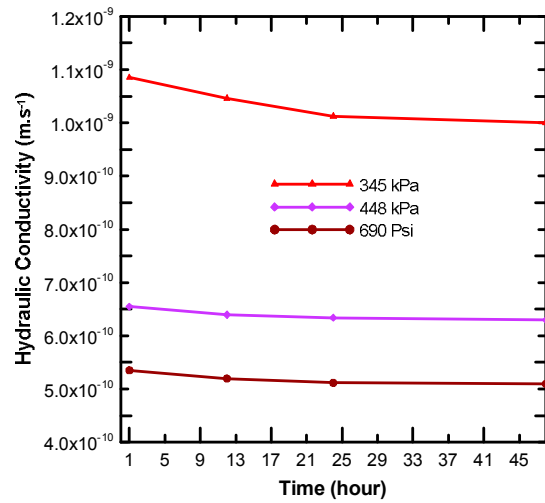


Figure 0-8 Hydraulic Conductivity changes versus measurement time, heating at 80°C, different Confining Pressure

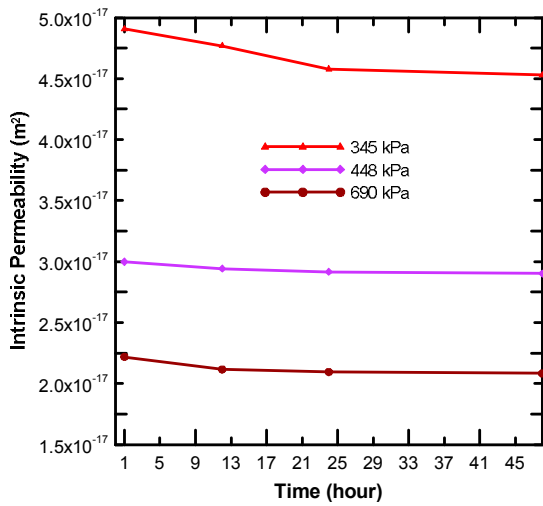


Figure 0-9 Intrinsic Permeability changes versus measurement time, heating at 50°C, different Confining Pressure

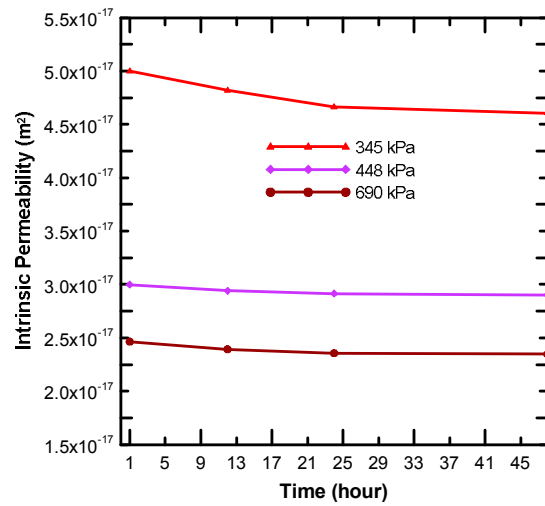


Figure 0-10 Intrinsic Permeability changes versus measurement time, heating at 80°C, different Confining Pressure

### 5.3.3. Cyclic tests

In all the conducted tests in this chapter, the thermal load was followed by a cooling step to study the effect of one heating-cooling cycle on the soil hydraulic properties. Figure 0-11 and Figure 0-12 show the hydraulic conductivity changes in a cyclic test with measurement time at 48 hours of temperature changes to make sure the volume reduction due to thermal loading has stabilized. These figures clearly show the changes in soil fabric after a complete heating-cooling cycle. Since during the thermal load, thermal consolidation (results in a more compacted soil) causes soil fabric change and void ratio reduction, the permeability of the soil is reduced after one heating-cooling cycle. Please note that the amount of residual reduction is more at 20 °C compared to 50 °C, because the soil at 20 °C has experienced a higher amount of thermal load (60 °C temperature increase, compared to 30 °C for the soil at 50 °C). It is interesting to note that the changes in void ratio and consequently in changes of soil hydraulic properties at room temperature before and after a complete heating-cooling cycle depends on the soil confining pressure. The results show that H.C. and consequently Kaolin clay intrinsic permeability reduction under 345 kPa at both 20 °C and 50 °C are more than those in test with 690 kPa confining pressure.

Similar graphs are plotted for intrinsic permeability for the cyclic load. The measurements are again based on 48 hours readings after temperature change is started. Results show how intrinsic permeability is reduced after a heating-cooling cycle when measurements are based on long-term readings. This confirms that the void ratio and soil fabric changes due to the thermal consolidation that was discussed in Chapter 4. Similar to hydraulic conductivity results, in intrinsic permeability, the confining pressure has an

important effect on the results. As it was described in Chapter 4, the consolidation pressure coefficient ( $\lambda_c$ ) can be used to predict the effect of confining pressure.

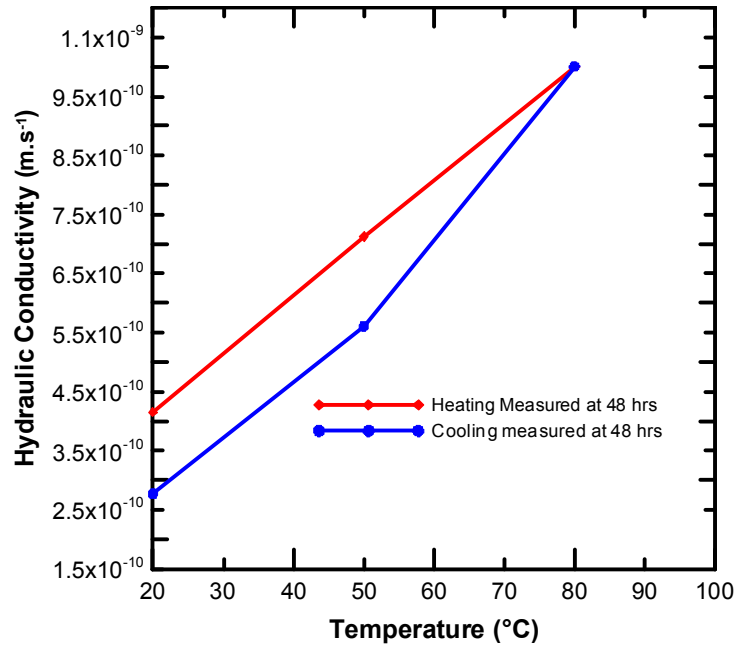


Figure 0-11 Cyclic Hydraulic Conductivity test at 345kPa

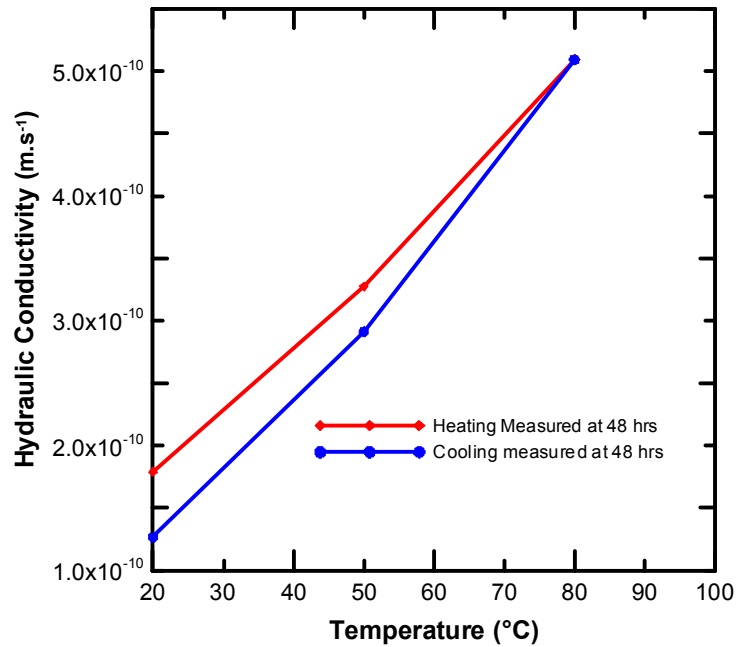


Figure 0-12 Cyclic Hydraulic Conductivity test at 690kPa

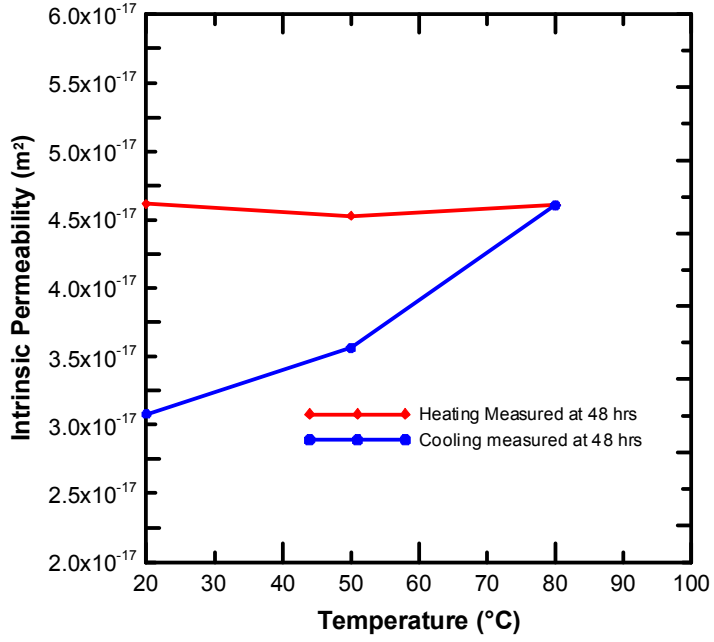


Figure 0-13 Cyclic Intrinsic Permeability test at 345kPa

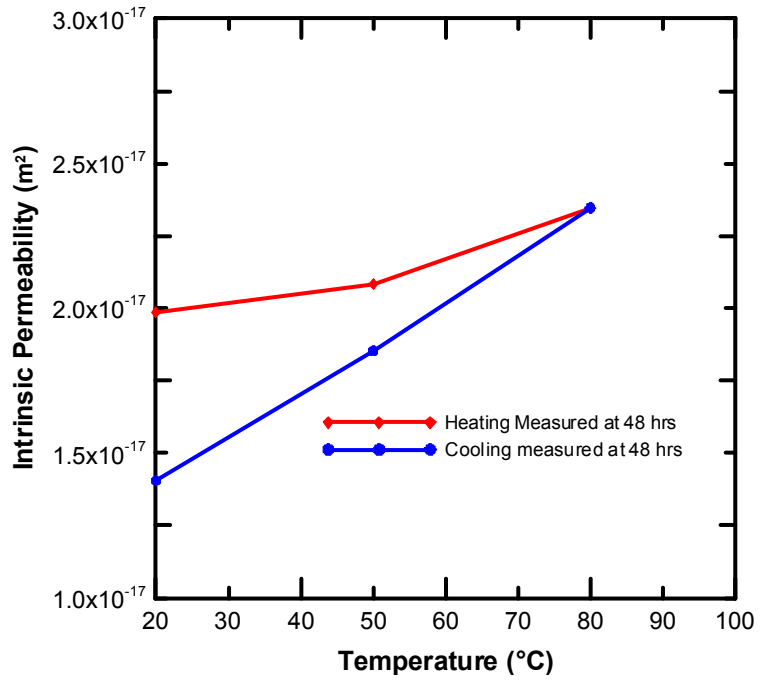


Figure 0-14 Cyclic Intrinsic Permeability test at 690 kPa

#### 5.3.4. Void ratio change

Void ratio changes in thermal load is calculated at different elapsed time in a separate test (different sample) with 345 kPa confining pressure. The reason is to avoid the possible effects of H.C test and soil particle rearrangement that can affect void ratio change. The measurements are again repeated at 1 hr, 12 hours, 24 hours and 48 hours and results are presented in Figure 0-15. Again the significant difference is observed between measurements after 1 hour and 12 hours. The results of 12 hours, 24 hours and 48 hours are very closed to each other and are overlapped in the plot. Results show that the void ratio is time dependant and at each temperature, void volume is reducing, which is in agreement with the H.C and I.P changes in time as mentioned earlier in this Chapter, as well as with thermal consolidation results in Chapter 4.

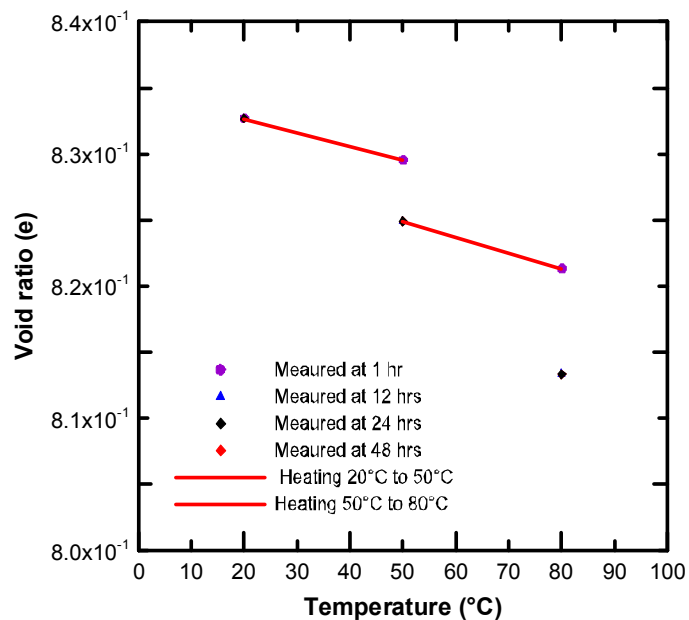


Figure 0-15 Void ratio changes at different measurement time in heating

#### 5.4. Summary

Based on the findings in chapter 3 and chapter 4, it is expected that not only the temperature change affects the hydraulic conductivity and intrinsic permeability values, the gradual changes in the void ratio (soil fabric) will cause a progressive change in hydraulic conductivity and intrinsic permeability values during thermal loading. Therefore, in this chapter, a series of tests were conducted to analyze these progressive changes, by reading those parameters at different time frames of 1 hr, 12 hours, 24 hours, and 48 hours under variable confining pressures. Results of hydraulic conductivity, intrinsic permeability, and void ratio are plotted versus time and also versus temperature for a better insight. Results confirm that thermal loads cause soil fabric changes and as a result both hydraulic conductivity and intrinsic permeability change over time. The progressive changes are depicted in figures by tracking measurements at different time frames, and also the effects of confining pressure are presented in both hydraulic conductivity and intrinsic permeability changes by temperature.

## CHAPTER 6

### DISCUSSION, CONCLUSION AND RECOMMENDATIONS

#### 6.1. Discussion and Conclusion

In this research, to better understand the soil thermo-hydro-mechanical behavior, a series of tests were conducted under different temperature loadings and different initial mechanical loads (initial confinement or initial void ratio). Volumetric changes, hydraulic conductivity, and intrinsic permeability of Ottawa sand and Kaolin clay which are common standard soil in geotechnics, were the focus in this research.

To investigate the changes in the mentioned parameters the most common test equipment is to modify a triaxial cell to change the temperature of the confining fluid and as a result, soil temperature. The temperature in the soil sample will finally reach the confining fluid temperature. To change the temperature of the fluid inside the cell, two different ways may be employed. In the first method, a heat source is accommodated inside the cell and the cell fluid temperature is directly changed. Immersion heaters and metal heat exchangers are the most common heating sources. The temperature-controlled cell which is used in this study is a modified triaxial cell with an internal heat exchanger. A spiral copper coil is mounted under the top cap of the cell as the heat exchanger (heating/cooling source) with both ends extruded out of the cell top cap. A water bath pumps the heat carrier fluid to the copper coil while the temperature of the fluid can be adjusted and maintained at the water bath control panel. The temperature can easily be

changed at the control panel at a desired rate of change. Two thermocouples are placed inside the cell to measure the temperature at different depths of the cell and the results are continuously recorded using a data logger with an adjustable rate of recording. To keep the temperature in the cell uniform, an innovative method of circulation water inside the cell was designed and employed.

To conduct the thermal consolidation in soil, a specific consolidometer is inserted in an innovative temperature-controlled triaxial cell to analyze the thermal volume change of Kaolin clay under different conditions. Four series of TC tests are performed to: 1) analyze the effect of thermal loading steps on void ratio changes with temperature, 2) investigate the volume change in NC and OC clays with thermal loading, and 3) study the effect of initial mean effective stress (initial 1-D consolidation pressure) on the thermal contraction of NC clay. Experimental observations demonstrate that void ratio reduction (volumetric changes) is independent of thermal loading steps but highly depends on OCR value. The results also indicate a linear relationship between the void ratio and the logarithm of temperature. While irreversible contraction is observed after one heating-cooling cycle of NC clays, highly overconsolidated soil shows irreversible expansion. Results determine no significant volumetric changes with temperature for the sample with OCR equals 1.6. Besides, the volumetric changes of Kaolin clay under different 1-D consolidation pressures (initial mean effective stresses) are studied. Results demonstrate samples under lower consolidation pressure (higher initial void ratio), show higher thermal volume contraction. While samples with higher 1-D consolidation pressure (lower initial void ratio) experience lower thermal volume reduction. The experimental observations show a 40% reduction in thermal volumetric strain when the initial mean effective stress increases from 10 kPa to

125 kPa. As a result, a new relation is proposed to estimate the thermal consolidation of normally consolidated Kaolin clay using conventional consolidation equation and TC tests under different consolidation pressures. However, further research is required to investigate the accuracy of the proposed equation to estimate thermal consolidation in different clayey soils.

To analyze the variations of hydraulic conductivity, intrinsic permeability, and the volumetric changes of sandy and clayey soils with temperature under different confinement stresses, the modified temperature-controlled cell is used as a permeameter cell. In addition to the modified cell, the main required parts of the test setup are a water bath to change the temperature of the injected water to the cell, two digitally controlled hydraulic pumps to measure the volume of the water that flows through the sample, and the second pump to provide cell pressure, standard control panel to control the pressure of the sample at its top, and the data acquisition of the triaxial device to record the volume of the flowed water. Several calibration tests were conducted to prepare the final setup. Results confirm that changes in the temperature alter not only the soil hydraulic conductivity but also the intrinsic permeability. This happens because thermal loading changes the soil fabric (e.g., soil particle rearrangements and void ratio changes) and porosity in both sand and clay. Experimental observations confirm a 35% increase in hydraulic conductivity of the saturated sandy soil. However, considering fluid properties (e.g., density and dynamic viscosity) variation with temperature, a 50% reduction in intrinsic permeability is observed for the saturated sand. This reduction in intrinsic permeability happens due to a decrease in void ratio and volume contraction of the soil specimen during the thermal loading. The void ratio variations with temperature during the thermal loading cycles are measured

based on the volume of the expelled and absorbed water, and the estimated amount of volume expansion and contraction according to the initial water content. As a result, thermal loading in the ground results in different behaviors for sand and clay. In sandy soil, void ratio reduction with temperature increase causes lower intrinsic permeability. However, for clayey soil, intrinsic permeability slightly increased with temperature despite the void ratio reduction. This happened because, at elevated temperatures, a part of the immobile water within the structure could move into the mobile water to increase the flow channels.

In the third part of the research, a series of tests are performed to study the effect of time in measurements of hydraulic conductivity values after the temperature change. Based on the findings in the thermal consolidation and permeability section, it was concluded that soil fabric (consequently void ratio) is changing over time. Therefore, the hydraulic conductivity test after the thermal load is repeated at each temperature, it is expected to see a progressive trend that will finally merge to a constant value after thermal consolidation is achieved. To verify this prediction, 2 samples of Kaolin clay with 101.8 mm diameter and 25.4 mm height are tested under different confining pressures of 345 kPa and 690 kPa. Results of the hydraulic conductivity and related intrinsic permeability confirm that soil fabric and void volume are changing gradually, by reflecting a reduction in the measured values over time. Besides, a heating-cooling cyclic test is conducted for each sample, and the long-term (reading after 48 hours) parameters at 20 °C and 50 °C (residue changes) are compared. In addition, confining pressure (initial condition of the soil) affects the amount of this reduction (amount of soil volume change), which is in good agreement with the findings in chapter 4. As it was shown in chapter 4, higher confining pressure results in a

lower amount of volume change and this means a limited range of the change in the hydraulic conductivity and related intrinsic permeability over time and also in the values of the residue changes. It is observed that hydraulic conductivity and soil intrinsic permeability drop by 8% under 345 kPa confining pressure from 1 hour to 48 hours after the soil temperature is stabilized at the  $T=80$  °C. However, a lower reduction is observed for higher confining pressures which is 4.7 % for test under confining pressure of 690 kPa. This reduction in soil H.C. and intrinsic permeability confirm the irreversible changes in soil fabric (thermal consolidation) during the thermal loading.

## 6.2. Recommendations

Based on the obtained experiences and the results of the tests, there are some areas and directions to elaborate the current study and to increase the accuracy of the results:

- Exploring the effect of confining pressures with a broader range on soil thermal volume reduction and hydraulic properties variations by performing more tests on the selected soils in different confining pressures
- Analyze the Thermo-hydro-mechanical response of different soil types by performing separate tests to study void ratio changes and other parameters for other soil types
- Study the mechanistic process of frozen soils and freeze-thaw cycles. Since the modified cell can be used in temperatures lower than the freezing point, (by having

a mix of water and glycol, as cell fluid and heat/cool carrier fluid in the water bath), the temperature range of the tests can be extended to study frozen soil.

- Analyze the Thermo-hydro-mechanical response of unsaturated soil. Installing proper sensors to measure suction in the soil, will give the opportunity to study unsaturated soils
- Repeating the permeability tests with another modification to the setup. In the permeability test, instead of passing the tube through a water bath, a length of the tube can be placed in the cell, before connecting to the sample, this will give a more accurate change in the temperature of the injecting water to the sample.

## REFERENCES

- Abuel-Naga, H., Bergado, D., Ramana, G., Grino, L. & Rujivipat, P. 2006a. Experimental evaluation of engineering behavior of soft Bangkok clay under elevated temperature. *Journal of geotechnical and geoenvironmental engineering*, 132, 902-910.
- Abuel-Naga, H.M., Bergado, D., Bouazza, A. & Ramana, G. 2007a. Volume change behaviour of saturated clays under drained heating conditions: experimental results and constitutive modeling. *Canadian Geotechnical Journal*, 44, 942-956.
- Abuel-Naga, H.M., Bergado, D. & Chaiprakaikeow, S. 2006b. Innovative thermal technique for enhancing the performance of prefabricated vertical drain during the preloading process. *Geotextiles and Geomembranes*, 24, 359-370.
- Abuel-Naga, H.M., Bergado, D.T. & Bouazza, A. 2007b. Thermally induced volume change and excess pore water pressure of soft Bangkok clay. *Engineering Geology*, 89, 144-154.
- Agar, J., Morgenstern, N. & Scott, J. 1986. Thermal expansion and pore pressure generation in oil sands. *Canadian Geotechnical Journal*, 23, 327-333.
- Aktan, T. & Ali, S. 1975. Effect of cyclic and in situ heating on the absolute permeabilities, elastic constants, and electrical resistivities of rocks. Fall Meeting of the Society of Petroleum Engineers of AIME. Society of Petroleum Engineers.

- Alsherif, N. & McCartney, J. 2015. Thermal behaviour of unsaturated silt at high suction magnitudes. *Géotechnique*, 65, 703-716.
- Alsherif, N., McCartney, J. & Caicedo, B. 2013. Triaxial cell for nonisothermal shear strength of compacted silt under high suction magnitudes. *Advances in unsaturated soils*. Proceedings of the First PanAmerican Conference on Unsaturated Soils, Cartagena de los Indias, Colombia. 20–22 Feb. 2013. CRC Press Boca Raton, FL, 147-152.
- Arihara, N. 1974. A study of non-isothermal single and two-phase flow through consolidated sandstones. Stanford Univ., CA (USA). Stanford Geothermal Program.
- Aruna, M. 1977. THE EFFECTS OF TEMPERATURE AND PRESSURE ON ABSOLUTE PERMEABILITY OF SANDSTONES. American Nuclear Society Topical Meeting Golden.
- Bai, B., Guo, L. & Han, S. 2014. Pore pressure and consolidation of saturated silty clay induced by progressively heating/cooling. *Mechanics of Materials*, 75, 84-94.
- Baldi, G., Hueckel, T. & Pellegrini, R. 1988. Thermal volume changes of the mineral–water system in low-porosity clay soils. *Canadian Geotechnical Journal*, 25, 807-825.
- Campanella, R.G. 1965. Effect of temperature and stress on the time-deformation behavior of saturated clay. University of California, Berkeley.
- Campanella, R.G. & Mitchell, J.K. 1968. Influence of temperature variations on soil behavior. *Journal of Soil Mechanics & Foundations Div.*

- Cekerevac, C. & Laloui, L. 2004. Experimental study of thermal effects on the mechanical behaviour of a clay. *International journal for numerical analytical methods in geomechanics*, 28, 209-228.
- Cekerevac, C., Laloui, L.J.I.j.f.n. & geomechanics, a.m.i. 2004. Experimental study of thermal effects on the mechanical behaviour of a clay. 28, 209-228.
- Chen, W., Ma, Y., Yu, H., Li, F., Li, X. & Sillen, X. 2017. Effects of temperature and thermally-induced microstructure change on hydraulic conductivity of Boom Clay. *Journal of Rock Mechanics and Geotechnical Engineering*, 9, 383-395.
- Cho, W., Lee, J. & Chun, K. 1999. The temperature effects on hydraulic conductivity of compacted bentonite. *Applied clay science*, 14, 47-58.
- Coccia, C.J.R. & McCartney, J.S. 2016. Thermal volume change of poorly draining soils II: model development and experimental validation. *Computers Geotechnics*, 80, 16-25.
- Cui, Y.-J. & Tang, A.M. 2013. On the chemo-thermo-hydro-mechanical behavior of geological and engineered barriers *Journal of Rock Mechanics and Geotechnical Engineering*, 5, 169-178.
- Cui, Y.J., Sultan, N. & Delage, P. 2000. A thermomechanical model for saturated clays. *Canadian Geotechnical Journal*, 37, 607-620.
- Damiano, E., Greco, R., Guida, A., Olivares, L. & Picarelli, L. 2017. Investigation on rainwater infiltration into layered shallow covers in pyroclastic soils and its effect on slope stability. *Engineering Geology*, 220.

- Darbari, Z., Jaradat, K.A. & Abdelaziz, S.L. 2017. Heating–freezing effects on the pore size distribution of a kaolinite clay. *Environmental Earth Sciences*, 76, 713.
- Delage, P., Sultan, N., Cui, Y.-J. & Ling, L.X. 2011. Permeability changes in Boom clay with temperature. arXiv preprint arXiv:1112.6396.
- Delage, P., Sultan, N. & Cui, Y.J. 2000. On the thermal consolidation of Boom clay. *Canadian Geotechnical Journal*, 37, 343-354.
- Demars, K. & Charles, R. 1982. Soil volume changes induced by temperature cycling. *Canadian Geotechnical Journal*, 19, 188-194.
- Derjaguin, B., Karasev, V., Khromova, E.J.J.o.c. & science, i. 1986. Thermal expansion of water in fine pores. 109, 586-587.
- Derjaguin, B.J.F.i.p. 1986. Properties of water layers adjacent to interfaces. 663-738.
- Dou, H.-q., Han, T.-c., Gong, X.-n. & Zhang, J. 2014. Probabilistic slope stability analysis considering the variability of hydraulic conductivity under rainfall infiltration–redistribution conditions. *Engineering Geology*, 183, 1-13.
- El Tawati, A. 2010. Impact of the rate of heating on the thermal consolidation of compacted silt. *Masters Abstracts International*.
- Eriksson, L. 1989. Temperature effects on consolidation properties of sulphide clays. *International Conference on Soil Mechanics and Foundation Engineering: 13/08/1989-18/08/1989*. Balkema Publishers, AA/Taylor & Francis The Netherlands, 2087-2090.

- Favero, V., Ferrari, A. & Laloui, L. 2016. Thermo-mechanical volume change behaviour of Opalinus Clay. *International Journal of Rock Mechanics Mining Sciences*, 90, 15-25.
- Finn, F. 1952. The effect of temperature on the consolidation characteristics of remolded clay. *Symposium on Consolidation Testing of Soils*. ASTM International.
- François, B., Laloui, L. & Laurent, C. 2009. Thermo-hydro-mechanical simulation of ATLAS in situ large scale test in Boom Clay. *Computers and Geotechnics*, 36, 626-640.
- Gao, H. & Shao, M. 2015. Effects of temperature changes on soil hydraulic properties. *Soil and Tillage Research*, 153, 145-154.
- Garakani, A.A., Haeri, S.M., Khosravi, A. & Habibagahi, G. 2015. Hydro-mechanical behavior of undisturbed collapsible loessial soils under different stress state conditions. *Engineering Geology*, 195, 28-41.
- Ghaaowd, I., Takai, A., Katsumi, T. & McCartney, J.S. 2015. Pore water pressure prediction for undrained heating of soils. *Environmental Geotechnics*, 4, 70-78.
- Ghabezloo, S. & Sulem, J. 2009. Stress dependent thermal pressurization of a fluid-saturated rock. *Rock Mechanics and Rock Engineering*, 42, 1.
- Ghabezloo, S. & Sulem, J. 2010. Temperature induced pore fluid pressurization in geomaterials. *arXiv preprint arXiv:1011.6501*.
- Ghasemi-Fare, O. & Basu, P. 2018. Influences of ground saturation and thermal boundary condition on energy harvesting using geothermal piles. *Energy and Buildings*, 165, 340-351.

- Ghasemi-Fare, O. & Basu, P. 2019. Coupling heat and buoyant fluid flow for thermal performance assessment of geothermal piles. *Computers Geotechnics*, 116, 103211.
- Gobran, B., Brigham, W. & Ramey Jr, H. 1987. Absolute permeability as a function of confining pressure, pore pressure, and temperature. *SPE Formation Evaluation*, 2, 77-84.
- Greenberg, D.B., Cresap, R.S. & Malone, T.A. 1968. Intrinsic permeability of hydrological porous mediums: Variation with temperature. *Water Resources Research*, 4, 791-800.
- Habibagahi, K. 1977. Temperature effect and the concept of effective void ratio. *Indian Geotechnical Journal*, 7, 14-34.
- Hamidi, A., Tourchi, S. & Kardooni, F. 2017. Thermo-mechanical constitutive modeling of unsaturated clays based on the critical state concepts. *Journal of Rock Mechanics and Geotechnical Engineering*, 30, 1e10.
- Hillel, D. 2013. *Fundamentals of soil physics*. Academic Press.
- Houston, S.L. & Lin, H.D. 1987. A thermal consolidation model for pelagic clays. *Marine Georesources & Geotechnology*, 7, 79-98.
- Hueckel, T. & Baldi, G. 1990. Thermoplasticity of saturated clays: experimental constitutive study. *Journal of geotechnical engineering*, 116, 1778-1796.
- Hueckel, T. & Borsetto, M. 1990. Thermoplasticity of saturated soils and shales: constitutive equations. *Journal of geotechnical engineering*, 116, 1765-1777.

- Hueckel, T. & Pellegrini, R. 1992. Effective stress and water pressure in saturated clays during heating–cooling cycles. *Canadian Geotechnical Journal*, 29, 1095-1102.
- Jarad, N., Cuisinier, O. & Masrouri, F. 2019. Effect of temperature and strain rate on the consolidation behaviour of compacted clayey soils. *European Journal of Environmental and Civil Engineering*, 23, 789-806, doi: 10.1080/19648189.2017.1311806.
- Jefferson, I. & Rogers, C.D.F. 1998. Liquid limit and the temperature sensitivity of clays. *Engineering Geology*, 49, 95-109.
- Joshaghani, M. & Ghasemi-Fare, O. 2019. A Study on thermal consolidation of fine grained soils using modified triaxial cell. *Eighth International Conference on Case Histories in Geotechnical Engineering ASCE*, Philadelphia, Pennsylvania 148 - 156.
- Joshaghani, M., Ghasemi-Fare, O. & Ghavami, M. 2018. Experimental Investigation on the effects of temperature on physical properties of sandy soils. *IFCEE 2018*, 675-685.
- Kaddouri, Z., Cuisinier, O. & Masrouri, F. 2019. Influence of effective stress and temperature on the creep behavior of a saturated compacted clayey soil. *Geomechanics for Energy and the Environment*, 17, 106-114.
- Laloui, L. & Cekerevac, C. 2003. Thermo-plasticity of clays: an isotropic yield mechanism. *Computers Geotechnics*, 30, 649-660.
- Lewis, W. 1950. Effect of Temperature on the Consolidation of Soils. *Nature*, 166, 614-615.

- Lima, A., Romero, E., Gens, A., Li, X. & Vaunat, J. 2013. Thermo-hydraulic behaviour of Boom clay using a heating cell: an experimental study. *Multiphysical Testing of Soils and Shales*. Springer, 163-168.
- Liu, H., Liu, H., Xiao, Y. & McCartney, J.S. 2018. Influence of temperature on the volume change behavior of saturated sand. *Geotechnical Testing Journal*, 41, 747-758.
- Lotfi, E., Delfan, S., Hamidi, A., Shahir, H. & Fardi, G. 2014. A numerical approach for one dimensional thermal consolidation of clays. *International Journal of Civil Engineering*, 12, 80-87.
- Ma, C. & Hueckel, T. 1993. Thermomechanical effects on adsorbed water in clays around a heat source. *International journal for numerical analytical methods in geomechanics*, 17, 175-196.
- Ma, Q., Ng, C.W.W., Mašín, D. & Zhou, C. 2017. An approach for modelling volume change of fine-grained soil subjected to thermal cycles. *Canadian Geotechnical Journal*, 54, 896-901.
- McKay, W.I. & Brigham, W. 1984. Effects of temperature on the absolute permeability of consolidated sandstone. Stanford Univ., CA (USA). Petroleum Research Inst.
- McKinstry, H.A. 1965. Thermal expansion of clay minerals. *American Mineralogist: Journal of Earth Planetary Materials*, 50, 212-222.
- Monfared, M., Sulem, J., Delage, P. & Mohajerani, M. 2014. Temperature and damage impact on the permeability of Opalinus clay. *Rock mechanics and rock engineering*, 47, 101-110.

- Morin, R. & Silva, A. 1984. The effects of high pressure and high temperature on some physical properties of ocean sediments. *Journal of Geophysical Research: Solid Earth*, 89, 511-526.
- Morteza Zeinali, S. & Abdelaziz, S.L. 2020. Thermal Consolidation Theory. *Journal of geotechnical and geoenvironmental engineering*, 147, 04020147.
- Ng, C.W.W. & Leung, A.K. 2012. In-situ and laboratory investigations of stress-dependent permeability function and SDSWCC from an unsaturated soil slope. *Geotech Eng*, 43, 26-39.
- Ng, C.W.W., Mu, Q.Y. & Zhou, C. 2019. Effects of specimen preparation method on the volume change of clay under cyclic thermal loads. *Geotechnique*, doi: 10.1680/jgeot.16.P.293.
- Plum, R. & Esrig, M. 1969. SOME TEMPERATURE EFFECTS ON SOIL COMPRESSIBILITY AND PORE WATER PRESSURE. Highway Research Board Special Report.
- Potter, J., Dibble, W. and Nur, A. 1981. Effects of temperature and solution composition on the permeability of St. Peters sandstone-Role of iron (III). *Jo. Pet. Tech*, 33, 905-907.
- Pusch, R. 1992. Use of bentonite for isolation of radioactive waste products. *Clay Minerals*, 27, 353-361.
- Pusch, R. & Güven, N. 1990. Electron microscopic examination of hydrothermally treated bentonite clay. *Engineering Geology*, 28, 303-314.

- Ren, J., Shen, Z.-z., Yang, J., Zhao, J. & Yin, J.-n. 2014. Effects of temperature and dry density on hydraulic conductivity of silty clay under infiltration of low-temperature water. *Arabian Journal for Science Engineering Geology*, 39, 461-466.
- Romero, E., Gens, A. & Lloret, A. 2001. Temperature effects on the hydraulic behaviour of an unsaturated clay. *Unsaturated Soil Concepts and Their Application in Geotechnical Practice*. Springer, 311-332.
- Romero, E., Gens, A. & Lloret, A. 2003. Suction effects on a compacted clay under non-isothermal conditions. *Géotechnique*, 53, 65-81.
- Sadeghi, H. & AliPanahi, P. 2020. Saturated hydraulic conductivity of problematic soils measured by a newly developed low-compliance triaxial permeameter. *Engineering Geology*, 105827.
- Sageev, A. 1980. The Design and Construction of an Absolute Permeameter to Measure the Effect of Elevated Temperature on the Absolute Permeability to Distilled Water of Unconsolidated Sand Cores. Stanford Geothermal Program.
- Savvidou, C., Britto, A.J.S. & foundations. 1995. Numerical and experimental investigation of thermally induced effects in saturated clay. 35, 37-44.
- Seiphoori, A. 2015. Thermo-hydro-mechanical characterisation and modelling of Wyoming granular bentonite. Nagra.
- Somerton, W. & Gupta, V. 1965. Role of fluxing agents in thermal alteration of sandstones. *Journal of Petroleum Technology*, 17, 585-588.
- Sultan, N., Delage, P. & Cui, Y. 2002. Temperature effects on the volume change behaviour of Boom clay. *Engineering Geology*, 64, 135-145.

- Sydansk, R. 1980. Discussion of the effect of temperature and confining pressure on single-phase flow in consolidated rocks. *J. Pet. Technol.*, 32.
- Tamizdoust, M.M. & Ghasemi-Fare, O. 2020. A fully coupled thermo-poro-mechanical finite element analysis to predict the thermal pressurization and thermally induced pore fluid flow in soil media. *Computers and Geotechnics*, 117, 103250.
- Tanaka, N., Graham, J. & Crilly, T. 1997. Stress-strain behaviour of reconstituted illitic clay at different temperatures. *Engineering Geology*, 47, 339-350.
- Tidfors, M. & Sällfors, G. 1989. Temperature effect on preconsolidation pressure. *Geotechnical Testing Journal*, 12, 93-97.
- Towhata, I., Kuntiwattanaku, P., Seko, I. & Ohishi, K. 1993a. Volume change of clays induced by heating as observed in consolidation tests. *Soils and Foundations*, 33, 170-183.
- Towhata, I., Kuntiwattanaku, P., Seko, I. & Ohishi, K. 1993b. Volume change of clays induced by heating as observed in consolidation tests. *Soils and Foundations*, 33, 170-183.
- Vega, A. & McCartney, J.S. 2015. Cyclic heating effects on thermal volume change of silt. *Environmental Geotechnics*, doi: 10.1680/envgeo.13.00022.
- Villar, M.V. & Lloret, A.J.A.C.S. 2004. Influence of temperature on the hydro-mechanical behaviour of a compacted bentonite. 26, 337-350.
- Weinbrandt, R., Ramey Jr, H. & Casse, F. 1975. The effect of temperature on relative and absolute permeability of sandstones. *Society of Petroleum Engineers Journal*, 15, 376-384.

- Yao, Y. & Zhou, A. 2013. Non-isothermal unified hardening model: a thermo-elasto-plastic model for clays. *Géotechnique*, 63, 1328-1345.
- Ye, W.-M., Wan, M., Chen, B., Chen, Y.-G., Cui, Y.-J. & Wang, J. 2012. Temperature effects on the unsaturated permeability of the densely compacted GMZ01 bentonite under confined conditions. *Engineering Geology*, 126, 1-7.
- Ye, W.-M., Wan, M., Chen, B., Chen, Y., Cui, Y. & Wang, J. 2013a. Temperature effects on the swelling pressure and saturated hydraulic conductivity of the compacted GMZ01 bentonite. *Environmental Earth Sciences*, 68, 281-288.
- Ye, W., Zhang, Y., Chen, Y., Chen, B. & Cui, Y.-J. 2013b. Experimental investigation on the thermal volumetric behavior of highly compacted GMZ01 Bent. *Applied Clay Science*, 83, 210-216.

## CURRICULUM VITA

Mohammad Joshaghani

Address: University of Louisville, W.S. Speed Room 100

Tel: (502) 550 - 3730

Email: [mo.joshaghani@gmail.com](mailto:mo.joshaghani@gmail.com)

Website: <https://www.linkedin.com/in/mjoshaghani-geotechniques/>

### Education

---

*April 2021*

UNIVERSITY OF LOUISVILLE

Doctoral Degree in Civil Engineering

- Dissertation: Thermo-Hydro-Mechanical characterization of Ottawa sand and Kaolin clay through experimental Models

*2013*

SHARIF UNIVERSITY OF TECHNOLOGY

Master's Degree in Civil Engineering

- Thesis: Physical Modeling of Seismic Slope Stability on Shaking Table
- Advisor: Fardin Jafarzade, Associate Professor

*2010*

SHARIF UNIVERSITY OF TECHNOLOGY

Bachelor's Degree in civil engineering

### Research Experience

---

*8/2016~ 4/2021*

UNIVERSITY OF LOUISVILLE, J.B SPEED SCHOOL OF ENGINEERING

PhD Research and Teaching Assistant

- Involving in Kentucky Transportation Cabinet project entitled 'Automatic heated bridge decks using active geothermal energy'. (since 2019).
- Actively involving in National Science Foundation (NFS) project entitled 'Fundamental Investigation of Interactions of Temperature, Pore Water Pressure, and Pore Fluid Flow in Soil Media'. (Grant No. CMMI-1804822) (since 2017)
- TA of Geomechanics lab (Fall 2019) and Statics Course (Summer 2019)
- Modifying Standard Test Devices (Permeameter, Consolidometer, and Triaxial) in Geotechnics lab, in order to have the tests at different temperatures
- Performing statistical analysis and developing Analytical models
- Analyzing laboratory test results for selection, prediction and estimation of engineering design parameters
- Performing numerical modeling and simulation of pore water behavior in the ground
- Research associate at ongoing KYTC and NSF projects

*2010~ 2013*

SHARIF UNIVERSITY OF TECHNOLOGY, TEHRAN, IRAN

- Physical modeling of a sandy slope in a rigid box and slope stability assesment and deformation estimation under seismic load on shaking table
- Instrumentation installment and seismic data validation and analyses